

VIRGINIA ELECTRIC AND POWER COMPANY
RICHMOND, VIRGINIA 23261

June 8, 1979

Mr. Victor Stello, Jr., Director
Division of Operating Reactors
U. S. Nuclear Regulatory Commission
Washington, D. C. 20555

Serial No. 457
PSE&C:CMRjr/cwh

Docket Nos.: 50-280-
50-281

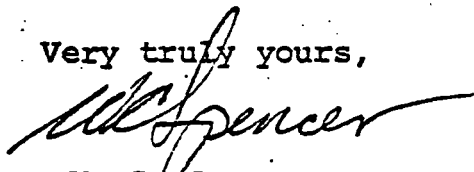
License Nos.: DPR-32
DPR-37

Dear Mr. Stello:

SOIL STRUCTURE INTERACTION REPORT
SURRY POWER STATION - UNITS 1 AND 2

The staff has required that documentation be provided to explain in detail the methodology used in soil structure interaction (SSI) techniques in the pipe stress reanalysis effort for Surry Power Station Units 1 and 2. Accordingly, we are forwarding to you the attached document entitled "Soil Structure Interaction in the Development of Amplified Response Spectra for Surry Power Station Units 1 and 2." We believe this document fully satisfies the staff's requirements for completing the documentation effort.

Very truly yours,



W. C. Spencer
Vice President - Power Station
Engineering and Construction
Services

Attachment

ADD: LTR ENCL
40/40
R MATTSON
J KNIGHT
V NOONAN
W RUSSELL

7906110194

SURRY POWER STATION, UNITS 1 AND 2

SOIL-STRUCTURE INTERACTION IN THE
DEVELOPMENT OF AMPLIFIED RESPONSE SPECTRA

FOR

SURRY POWER STATION, UNITS 1 AND 2

VIRGINIA ELECTRIC AND POWER COMPANY

June 8, 1979

50-280/281

Ltr 6-8-79

7906110194

50-280/281

Ltr 6-8-79

7906110194

RETURN TO REACTOR DOCKET
FILES

STONE & WEBSTER ENGINEERING CORPORATION

SURRY POWER STATION, UNITS 1 AND 2

TABLE OF CONTENTS

<u>Section</u>	<u>Title</u>	<u>Page</u>
1.0	INTRODUCTION	1-1
2.0	SOIL PROPERTIES.	2-1
2.1	SUBSURFACE DATA.	2-1
2.2	SUBSURFACE PROFILE	2-2
2.3	SOIL PARAMETERS.	2-4
2.3.1	Static Parameters.	2-5
2.3.1.1	Pleistocene Sands.	2-5
2.3.1.2	Pleistocene Clays.	2-6
2.3.1.3	Miocene Clays.	2-7
2.3.2	Geophysical Data	2-8
2.4	MODULUS AND DAMPING PROFILES	2-10
2.4.1	Small Strain Shear Modulus	2-10
2.4.2	Strain-Dependent Modulus and Damping	2-13
2.4.2.1	Summary of SHAKE Analysis.	2-13
2.4.2.2	Earthquake Accelerograms	2-14
2.4.2.3	Soil Profile	2-15
2.4.2.4	Strain Dependency Relationships.	2-17
2.4.2.5	Strain Compatible Shear Moduli and Damping	2-19
2.4.2.6	Variation of Shear Modulus	2-20
2.5	SUMMARY ON SOIL PROPERTIES	2-23
2.6	REFERENCES	2-25
3.0	GROUND RESPONSE.	3-1
3.1	DESIGN BASIS EARTHQUAKE (DBE) AND OPERATING BASIS EARTHQUAKE (OBE)	3-1
3.2	GROUND RESPONSE SPECTRA.	3-1
3.3	ARTIFICIAL TIME HISTORY.	3-2
3.4	GROUND RESPONSE SPECTRA AT BASE OF CONTAINMENT	3-3
3.5	REFERENCES	3-4
4.0	AMPLIFIED RESPONSE ANALYSIS.	4-1
4.1	DESCRIPTION OF THE THREE-STEP ANALYSIS	4-2

SURRY POWER STATION; UNITS 1 AND 2

TABLE OF CONTENTS (Cont)

<u>Section</u>	<u>Title</u>	<u>Page</u>
4.1.1	Frequency-Dependent Soil Stiffness	4-2
4.1.2	Embedment Correction	4-7
4.1.3	Kinematic Interaction.	4-8
4.1.4	Interaction Analysis	4-10
4.2	STRUCTURAL MODELING.	4-15
4.3	RESULTS.	4-17
4.4	REFERENCES	4-18
5.0	COMPARISON OF RESULTS.	5-1
5.1	REFUND/FRIDAY VS PLAXLY.	5-1
5.2	FSAR EARTHQUAKE VS REGULATORY GUIDE 1.60 EARTHQUAKE.	5-2
5.3	VARIATION OF SOIL PROPERTIES	5-3
5.4	SAMPLE PIPE STRESS PROBLEMS.	5-4
6.0	APPLICATION OF SEISMIC INPUT TO PIPE STRESS ANALYSIS	6-1
6.1	AMPLIFIED RESPONSE SPECTRA	6-1
6.2	BUILDING DISPLACEMENTS	6-2
7.0	INVESTIGATION OF THE EFFECTS OF EARTHQUAKES SMALLER THAN THE DBE .	7-1
8.0	CONCLUSIONS.	8-1
8.1	USE OF SOIL-STRUCTURE INTRACTION	8-1
8.2	SOIL PROPERTIES.	8-1
8.3	GROUND RESPONSE.	8-2
8.4	AMPLIFIED RESPONSE ANALYSIS.	8-2
8.5	COMPARISON OF RESULTS.	8-3
8.6	APPLICATION OF ARS TO PIPE STRESS ANALYSIS	8-6
8.7	EFFECTS OF GROUND ACCELERATION ON ARS.	8-6
8.8	COMPUTER PROGRAM VERIFICATION.	8-6

SURRY POWER STATION, UNITS 1 AND 2

TABLE OF CONTENTS (Cont)

<u>Section</u>	<u>Title</u>	<u>Page</u>
9.0	APPENDICES	9.1-1
9.1	SHAKE.	9.1-1
9.2	PLAXLY	9.2-1
9.3	REFUND AND EMBED	9.3-1
9.4	KINACT	9.4-1
9.5	FRIDAY	9.5-1
9.6	CONSOLIDATION TEST DATA CONDENSATE POLISHING DEMINERALIZER	9.6-1

SURRY POWER STATION, UNITS 1 AND 2

LIST OF TABLES

<u>Table</u>	<u>Title</u>
2-1	Summary of Geophysical Data
2-2	Poisson's Ratio - Free Field
2-3	Shear Modulus Determinations, Hardin and Black Equations
2-4	Strain Compatible Soil Properties - Free Field
2-5	Strain Compatible Soil Properties - Reactor Containment
2-6	Strain Compatible Soil Properties - Auxiliary Building
2-7	Strain Compatible Soil Properties - Turbine/Service Building E-W Component
2-8	Strain Compatible Soil Properties - Main Steam Valve House N-S Component
2-9	Strain Compatible Soil Properties - Containment Spray Pumphouse
2-10	Strain Compatible Soil Properties - Safeguards Building N-S Component
2-11	Strain Compatible Soil Properties - Fuel Building E-W Component
2-12	Strain Compatible Soil Properties - Reactor Containment, First Iteration Values
2-13	Strain Compatible Soil Properties - Free Field, Gmax $\pm 50\%$
2-14	Strain Compatible Soil properties - Reactor Containment, Gmax $\pm 50\%$
5-1	Sample Problem 706 - Pipe Stress Summary, Psi
5-2	Sample Problem 1020 - Pipe Stress Summary, Psi
5-3	Sample Problem 1555 - Pipe Stress Summary, Psi

SURRY POWER STATION, UNITS 1 AND 2

LIST OF FIGURES

<u>Figure</u>	<u>Title</u>
2-1	Plan Location of Borings and Piezometers
2-2	Site Plot Plan
2-3	Subsurface Profiles, Section A-A'
2-4	Subsurface Profiles, Section B-B'
2-5	Subsurface Profiles, Section C-C'
2-6	Density vs. Elevation for Pleistocene Sands
2-7	Water Contents and Atterberg Limits vs. Elevation
2-8	Preconsolidation Stresses in Clays
2-9	Summary of Consolidation Test Data in Miocene Clays
2-10	Total Unit Weight vs. Elevation for Miocene Clays
2-11	Summary of Gmax vs. Elevation
2-12	Shear Modulus Factor for Sands
2-13	Shear Modulus Factor for Clays
2-14	Damping Ratio for Sands
2-15	Damping Ratio for Clays
2-16	Comparison of Field and Laboratory Modulus Determination
3-1	Response Spectra-Operational Basis Earthquake
3-2	Response Spectra-Design Basis Earthquake
3-3	Spectrum of Artificial Time History at 2 Percent Damping
3-4	Ground Response Spectra Gmax
3-5	Ground Response Spectra Gmax +50%

SURRY POWER STATION, UNITS 1 AND 2

LIST OF FIGURES (Cont)

<u>Figure</u>	<u>Title</u>
3-6	Ground Response Spectra Gmax -50%
4-1	The Three-Step Solution
4-2	The Boussinesq and Cerruti Problems
4-3	Idealization of the Basic REFUND Solution for Concentrated Loads
4-4	REFUND Coordinate System
4-5	Kinematic Interaction
4-6	Generalized Dynamic Model of a Category I Structure
4-7	Typical Displacement Profiles
4-8	Typical Acceleration Profiles
5-1	Comparison of REFUND/FRIDAY and PLAXLY Results - ARS at Mat
5-2	Comparison of REFUND/FRIDAY and PLAXLY - ARS at Operating Floor
5-3	Comparison of REFUND/FRIDAY and PLAXLY - ARS at Springline
5-4	Comparison of the FSAR and Regulatory Guide 1.60 Earthquakes - ARS at Mat
5-5	Comparison of the FSAR and Regulatory Guide 1.60 Earthquakes - ARS at Operating Floor
5-6	Comparison of the FSAR and Regulatory Guide 1.60 Earthquakes - ARS at Springline
5-7	Comparison of ARS for Soil Parameter Variations - Horizontal Response Spectrum at Mat - Damp = 0.5%
5-8	Comparison of ARS for Soil Parameter Variations - Horizontal Response Spectrum at Mat - Damp = 1.0%
5-9	Comparison of ARS for Soil Parameter Variations - Horizontal Response Spectrum at Mat - Damp = 3.0%
5-10	Comparison of ARS for Soil Parameter Variations - Horizontal Response Spectrum at Operating Floor - Damp = 0.5%

SURRY POWER STATION, UNITS 1 AND 2

LIST OF FIGURES (Cont)

<u>Figure</u>	<u>Title</u>
5-11	Comparison of ARS for Soil Parameter Variations - Horizontal Response Spectrum at Operating Floor - Damp = 1.0%
5-12	Comparison of ARS for Soil Parameter Variations - Horizontal Response Spectrum at Operating Floor - Damp = 3.0%
5-13	Comparison of ARS for Soil Parameter Variations - Horizontal Response Spectrum at Springline - Damp = 0.5%
5-14	Comparison of ARS for Soil Parameter Variations - Horizontal Response Spectrum at Springline - Damp = 1.0%
5-15	Comparison of ARS for Soil Parameter Variations - Horizontal Response Spectrum at Springline - Damp = 3.0%
5-16	Comparison of ARS for Soil Parameter Variations - Horizontal Response Spectrum at Mat
5-17	Comparison of ARS for Soil Parameter Variations - Horizontal Response Spectrum at Mat
5-18	Comparison of ARS for Soil Parameter Variations - Horizontal Response Spectrum at Mat
5-19	Comparison of ARS for Soil Parameter Variations - Horizontal Response Spectrum at Operating Floor
5-20	Comparison of ARS for Soil Parameter Variations - Horizontal Response Spectrum at Operating Floor
5-21	Comparison of ARS for Soil Parameter Variations - Horizontal Response Spectrum at Operating Floor
5-22	Comparison of ARS for Soil Parameter Variations - Horizontal Response Spectrum at Springline
5-23	Comparison of ARS for Soil Parameter Variations - Horizontal Response Spectrum at Springline
5-24	Comparison of ARS for Soil Parameter Variations - Horizontal Response Spectrum at Springline
9.1-1	Amplification Function of Soil
9.1-2	Soils Profile

SURRY POWER STATION, UNITS 1 AND 2

LIST OF FIGURES (Cont)

<u>Figure</u>	<u>Title</u>
9.2-1	Comparison of ARS by PLAXLY and FLUSH at Operating Floor
9.2-2	PLAXLY Flow Diagram (3 sheets)
9.3-1	Luco's Two-Layer Problem
9.3-2	Rocking Stiffness Comparison - Real Part
9.3-3	Rocking Stiffness Comparison - Imaginary Part
9.3-4	Horizontal Stiffness Comparison - Real Part
9.3-5	Horizontal Stiffness Comparison - Imaginary Part
9.3-6	Vertical Stiffness Comparison - Real Part
9.3-7	Vertical Stiffness Comparison - Imaginary Part
9.3-8	REFUND and EMBED Flow Diagrams (2 sheets)
9.4-1	Translational Response Spectra at Base of Rigid, Massless Foundation
9.4-2	Rotational Response Spectrum at Base of Rigid, Massless Foundation
9.4-3	KINACT Flow Diagram
9.5-1	Comparison of FRIDAY and STARDYNE ARS at the Roof
9.5-2	STARDYNE Model
9.5-3	FRIDAY Flow Diagram (2 sheets)

SURRY POWER STATION, UNITS 1 AND 2

1.0 INTRODUCTION

On March 13, 1979 the Nuclear Regulatory Commission (NRC) issued an Order to Show Cause to the Virginia Electric and Power Company (VEPCO). The order required shutdown of the Surry Power Station Units 1 and 2 within 48 hours after receipt of the order.

The order required all piping systems originally seismically analyzed using algebraic summation of intramodal responses to be reanalyzed using methodology currently acceptable to the NRC staff. In carrying out this reanalysis, amplified response spectra developed using soil-structure interaction (SSI) techniques have been used.

Soil-structure interaction has been the subject of much dialogue between the Staff, VEPCO, and Stone & Webster since the Order, the fundamental purpose of which was to agree on the details of the SSI methodology for use in developing suitable amplified response spectra and their use in subsequent pipe stress analysis.

Over the course of numerous discussions, the NRC staff asked for documentation in a number of areas, and it is the purpose of this report to reply in detail to the NRC staff's requests. This report includes and supplements information on SSI previously submitted by letters dated May 2, 1979 and May 24, 1979.

SURRY POWER STATION, UNITS 1 AND 2

This report describes the basis for performing soil-structure interaction analyses to develop amplified response spectra for use in reevaluating the pipe stress and support loads. The soil properties are developed from subsurface data into a soil profile, in which each stratum has its own soil parameters. The required dynamic properties in each layer are described first by the small strain values of shear modulus, and then site response analysis is used to develop values of damping and shear modulus that are compatible with the strains to be expected during an earthquake. The design basis earthquake (DBE) and the operating basis earthquake (OBE) are described by ground response spectra and by artificial time histories that give response spectra enveloping the ground response spectra. The analysis of soil-structure interaction is performed by two methods: a one-step, finite element method, and a three-step, analytically based method. This report describes how these methods, including the structural representation, are derived and how they are used to develop amplified response spectra.

Results for different methods and for different input are compared, and their application to pipe stress analysis is discussed.

The results show that the three-step (REFUND/FRIDAY) method gives conservative results that are consistent with the present state-of-the-art of soil-structure interaction.

SURRY POWER STATION, UNITS 1 AND 2

2.0 SOIL PROPERTIES

The soil properties developed for use in the soil-structure interaction analyses are presented in this section of the report. The computer program SHAKE developed by Schnabel, Lysmer, and Seed⁽¹⁾ and discussed in Section 9.1 was used to calculate strain compatible shear moduli and damping from low strain values determined from field testing and empirical formulae based on laboratory test data. Although most of the data are included in reports that have been previously submitted to the NRC for completeness, the data are summarized below.

2.1 SUBSURFACE DATA

Soil properties used in the SHAKE analyses were obtained from previous geotechnical studies at the site for Units 1 and 2 in 1966⁽¹⁾ and 1969⁽²⁾ and Units 3 and 4 in 1973.⁽³⁾ Additional data, included in Appendix 9.6, were obtained in 1978 from previously unpublished studies related to construction of a new condensate polishing demineralizer adjacent to the Unit 2 turbine building. Subsurface profiles for use in this analysis were developed from data compiled from each of these studies. The correlation of soil properties over the entire Surry site is discussed in detail in Section 2.3.

SURRY POWER STATION, UNITS 1 AND 2

Investigations conducted prior to the construction of Units 1 and 2⁽¹⁾ included 65 test borings to a maximum depth of 200 feet, laboratory tests on soil samples to determine shear strength, compressibility, permeability, and density, and seismic refraction surveys to measure compressional and shear wave velocities of near surface soils. Further testing reported in the Surry 1 and 2 FSAR⁽²⁾ included determinations of relative density of the upper sands, consolidation testing of upper and lower clays, and pile load tests. Resonant column tests were run on two samples of Pleistocene clay and one of Miocene clay.⁽³⁾ The boring location plan for Units 1 and 2 is shown on Figure 2-1.

More extensive geotechnical investigations were conducted for the Units 3 and 4 site study, and are presented in the Surry 3 and 4 Geotechnical Report.⁽³⁾ These studies included 67 borings varying in depth from 91.5 to 175 feet, piezometer installations, laboratory testing on split-spoon and thin wall tube samples, borehole permeability tests, and seismic cross-hole surveys. The boring location plan for Units 3 and 4 is shown on Figure 2-2.

2.2 SUBSURFACE PROFILE

Generalized soil profiles through the containments of Units 1 and 2 are presented in Figures 2-3 and 2-4. A profile through the Units 3 and 4 containments, presented as Figure 2-5, is an extension of Section A-A in

SURRY POWER STATION, UNITS 1 AND 2

Figure 2-3. These sections were interpreted from borehole data and are representative of subsurface conditions underlying the Surry site.

In general, the upper 65 to 85 feet consists of a complex deposit of Pleistocene age fluvial and estuarine sediments overlain by occasional, thin, recent alluvial deposits. In the vicinity of Units 1 and 2, the Pleistocene deposits are characterized by alternating layers of dense sands and over consolidated, plastic clays down to approximately El -40 feet, the top of the Miocene clay sediments. Groundwater levels, measured in piezometers installed in the upper and lower Pleistocene sands at Units 1 and 2, indicate an average water level at approximately El +5 feet.

The surface of the Miocene clay represents an erosional plain from which the overlying Pliocene and early Pleistocene deposits have been removed. This surface is very regular, smooth, and at times capped by a thin, gravelly sand layer. The Miocene clay at the site consists of moderately to highly plastic, stiff to medium, grayish green silty clay. The Miocene clay is the deepest stratum penetrated by borings at the site. Regionally, the upper 150 to 200 feet of the Miocene sediments are considered to be of the Yorktown formation. The Yorktown is underlain by the St. Mary's and Calvert formations, also of Miocene age. These three formations comprise the Chesapeake Group and are estimated to be about 240 feet thick in the site area. (3)

SURRY POWER STATION, UNITS 1 AND 2

Underlying the Miocene formation at an estimated El -280 feet are older Eocene and Paleocene sediments, consisting mainly of marls and quartz sands. These soils are represented in the SHAKE analyses as dense sands, with a layer thickness of 100 feet. For purposes of analyses, the bottom of the Paleocene sands has been established as the base layer, resulting in a total soil column depth of 406 feet.

Cretaceous sediments, consisting of clay and sand beds to bedrock, underlie the Paleocene marls for a thickness of about 900 feet. Bedrock at the site is estimated at 1,300 feet below the ground surface based upon deep drill holes in the region.

2.3 SOIL PARAMETERS

A comparison was made between soil properties obtained from investigations of Units 1 and 2^(1,2) and those obtained from Units 3 and 4⁽³⁾ to determine the feasibility of using the cross-hole data from the latter units to obtain small strain shear modulus values. Composite plots of various soil properties were compiled from available data to verify the similarity of the soils, and to determine parameters for use in an empirical determination of shear modulus using the Hardin and Black formulas.⁽³⁾

SURRY POWER STATION, UNITS 1 AND 2

Properties directly input into SHAKE to define the soil profile include total unit weight, small strain shear modulus, and small strain damping. Shear moduli calculated from Hardin and Black formulas were based on static parameters such as plasticity index, overconsolidation ratio, void ratio, and effective overburden pressure. The derivation of these properties is discussed in detail in Section 2.3.1. Geophysical data used to obtain low strain shear moduli and Poisson's ratio are discussed in Section 2.3.2.

2.3.1 Static Parameters

Static parameters used to define the soil profile input into SHAKE and to correlate properties of the soil units at the site are discussed below.

2.3.1.1 Pleistocene Sands

Pleistocene sands and Pleistocene clay occur in alternating layers above E1 -40 feet. The sands are dense and generally high in silt content. A comparison of blow counts from borings taken in the main plant area for Units 1 and 2 with blow counts from Surry 3 and 4 indicates that the average relative density for the Pleistocene sands is about 70 percent and that the Units 1 and 2 data agree with the Units 3 and 4 data. The dry unit weight of the sand is plotted against elevation on Figure 2-6. An average value of dry unit weight of 98 pcf was used in the analyses.

SURRY POWER STATION, UNITS 1 AND 2

2.3.1.2 Pleistocene Clays

Pleistocene clays at the site are dark olive to dark gray, with low to medium plasticity. Atterberg limits plot along or slightly above Casagrande's A-line. Liquid limits range from about 50 to 70 percent and natural water contents vary from about 30 to 60 percent. Atterberg limits for Units 1 and 2 are plotted with data from Units 3 and 4 on Figure 2-7.

Consolidation tests conducted on the Pleistocene clays indicate that the overconsolidation ratio (OCR) of the Pleistocene clays is approximately 3. The maximum past pressure of the clays at Surry increases linearly with depth, verifying that the site has been subject to significant erosion of overlying sediments. Preconsolidation pressures, obtained by Schmertman's method, (b) from recent unpublished studies at Units 1 and 2 (Appendix 9.6) are plotted on Figure 2-8. The preconsolidation pressures from Surry 3 and 4 data have been recomputed, using Schmertmann's technique, (b) and are replotted on Figure 2-8. The replotted points agree closely with the estimated past vertical effective stress line developed for the site and used in the SHAKE analyses.

SURRY POWER STATION, UNITS 1 AND 2

2.3.1.3 Miocene Clays

The Miocene clay is a stiff, olive green, overconsolidated clay with a liquid limit varying from about 45 to about 75 percent and a natural water content varying from 30 to 40 percent. Sporadic thin lenses of sand are found within the clay zone. Atterberg limits and water contents for samples from Units 1 and 2 are plotted with Units 3 and 4 data on Figure 2-7. An average water content of 38 percent and plasticity index of 46 percent were used for the upper 50 feet of the Miocene clay in the analyses. Between elevations -90 and -190 feet, an average PI of 36 percent was used. Preconsolidation pressures are plotted on Figure 2-8 and OCR is plotted on Figure 2-9. As with the Pleistocene clay, the maximum past pressure increases linearly with depth, indicating previous erosion at the site. The OCR for the Miocene clay decreases with depth, from approximately 3.3 at the top to an extrapolated value of 1.3 toward the bottom of the layer.

Total unit weight for the Miocene clay is plotted on Figure 2-10. Agreement between Units 1 and 2 data and Units 3 and 4 data is good, further indicating the uniformity of the Miocene clay at the site. An average total unit weight of 120 pcf was used in the SHAKE analyses.

SURRY POWER STATION, UNITS 1 AND 2

2.3.2 Geophysical Data

Cross-hole and up-hole seismic surveys were performed for the site study at Units 3 and 4. The cross-hole survey was conducted along a line connecting the proposed location of the Unit 3 containment with the Unit 4 containment, in Borings B201 through B206 (see Figure 2-2). Up-hole tests were performed in boreholes B339 and B340 to verify the cross-hole data. P and S wave velocities were measured in each hole at 10 foot intervals down to El -140. A summary of seismic wave velocities is presented in Table 2-1. Shear wave velocity remains fairly constant with depth, exhibiting only a slight increase toward the lower depths. Below the ground water table, measured compression wave velocities in actuality represent the P wave velocity through the groundwater, and a value of 5000 fps has been used in computations for Poisson's ratio.

Dynamic Poisson's ratios were calculated from P and S wave velocities, using the following equation:

$$\mu = \frac{1-2R}{2-2R}$$

where μ = Dynamic Poisson's ratio

$$R = \left(\frac{V_S}{V_P} \right)^2$$

SURRY POWER STATION, UNITS 1 AND 2

V_s = shear wave velocity

V_p = compression wave velocity

Above the groundwater table, the measured compressional wave velocity was obtained from Table B-5 of Reference 1, based on a seismic refraction test performed at Units 1 and 2. An average value of $V_p = 2008$ fps was used with the measured shear wave velocity to calculate the dynamic Poisson's ratio for soil above the groundwater table.

Shear wave velocities used to calculate dynamic Poisson's ratio below the water table were calculated from strain compatible values of shear modulus obtained from the SHAKE analyses in the free field and presented in Table 2-4 for the DBE and OBE cases, according to the following equation:

$$V_s = \sqrt{\frac{G}{P}}$$

where V_s = strain compatible shear wave velocity

G = strain compatible shear modulus

P = mass density of soil

Poisson's ratios for each layer, for DBE and OBE conditions, are listed in Table 2-2.

SURRY POWER STATION, UNITS 1 AND 2

2.4 MODULUS AND DAMPING PROFILES

Soil profiles were developed for the free-field case and under each Category I structure. These profiles are based on the generalized soil profiles described in Section 2.2 and are tabulated in Tables 2-4 through 2-12. Soil parameters associated with each layer have been developed from laboratory and field testing at Units 1 and 2 and Units 3 and 4. Values of low strain shear modulus were obtained primarily from cross-hole tests at Units 3 and 4⁽³⁾ and checked using empirical formulas from Hardin and Black⁽⁵⁾ and laboratory data reported by Hardin.⁽⁴⁾ Comparisons between soil data from Units 1 and 2 and Units 3 and 4, discussed in Section 2.3.1, show excellent agreement.

2.4.1 Small Strain Shear Modulus

Small strain shear modulus values input into SHAKE were obtained predominately from the cross-hole data from Units 3 and 4 discussed in Section 2.3.2 because shear wave velocity data from Units 1 and 2⁽¹⁾ were incomplete. Shear modulus values from tests at Units 3 and 4 are plotted on Figure 2-11. Values of shear modulus obtained from geophysical testing represent the maximum or small strain values. The solid line on Figure 2-11 represents the average value for G_{max} input into SHAKE.

SURRY POWER STATION, UNITS 1 AND 2

Shear modulus values from cross-hole data were checked using the Hardin and Black empirical formulas. (3) For sands:

$$G_{\max} = 1230 \frac{(2.973-e)^2}{1+e} (\bar{\sigma}_{\text{oct}})^{0.5}$$

where:

G_{\max} = small strain shear modulus in psi

e = void ratio

$\bar{\sigma}_{\text{oct}}$ = effective octahedral normal stress in psi

For clays:

$$G_{\max} = 1230 \frac{(2.973-e)^2}{1+e} (\text{OCR})^K (\bar{\sigma}_{\text{oct}})^{0.5}$$

where:

OCR = overconsolidation ratio

K = factor dependent upon plasticity index (PI)

SURRY POWER STATION, UNITS 1 AND 2

For sands, K_s was calculated using Hendron's plot of OCR vs. K_s .⁽⁸⁾ The OCR was considered to be similar to that for the underlying clays, in that the preconsolidation loads are attributable to eroded sediments. For clays, K_s was calculated from a plot of K_s vs PI for various OCR from Brooker and Ireland.⁽⁹⁾ Data used to obtain shear modulus from Hardin and Black formulas are presented in Table 2-3. The values of G_{max} are plotted with shear modulus values obtained from cross-hole tests on Figure 2-11. Agreement between the two methods is excellent, with the empirically derived shear moduli slightly less than the seismic values.

Resonant column tests were performed by Hardin⁽⁴⁾ on two block samples taken in the Pleistocene clay and a tube sample driven into the Miocene clay using a Dames & Moore sampler. Hardin tested each sample at the end of primary consolidation, after approximately 2 to 3 hours, and overnight to determine the effects of secondary consolidation. The shear wave velocities corresponding to these shear moduli were plotted with time for each sample water content, and the shear wave velocity and shear modulus at 20 years were extrapolated to determine the long-term effect of secondary consolidation. Anderson and Woods⁽¹³⁾ have shown that laboratory determinations of shear modulus on clay soils agree with field determinations when the laboratory data are extrapolated to a time of 20 years. Figure 2-16 shows that the laboratory obtained shear moduli and damping agree well with the cross hole obtained

SURRY POWER STATION, UNITS 1 AND 2

shear moduli for a wide range of effective confining stresses and natural water contents.

2.4.2 Strain Dependent Modulus and Damping

The calculation of strain dependent modulus and damping profiles is discussed in detail in the following sections.

2.4.2.1 Summary of SHAKE Analysis

The computer program SHAKE⁽¹⁾ was used to obtain values of shear modulus and damping at strain levels compatible with those induced during DBE and OBE conditions. The time histories from the El Centro 1940 (North-South component) and Kern County (Taft S69E) earthquakes were normalized to a peak acceleration of .15g and .07g for the DBE and OBE, respectively. These motions were input at the ground surface and deconvolved in the free field to El -380 feet, which was established as the base layer for SHAKE. The deconvolved time history was then amplified up through the soil profile to the base of the structure. Iterations of shear modulus and damping with strain were performed internally by SHAKE in both the free field and under the structures. The values obtained from the final iteration were tabulated for each layer in the soil profile, and the average values of shear modulus and damping using El Centro and Taft accelerograms as input were used in soil-

SURRY POWER STATION, UNITS 1 AND 2

structure interaction calculations. Strain compatible shear modulus and damping values for the DBE and OBE are included in Tables 2-4 to 2-11.

2.4.2.2 Earthquake Accelerograms

Two strong motion time-history accelerograms were used in the SHAKE analyses to determine strain compatible soil properties: the 1940 El Centro earthquake (North-South component) and the 1952 Kern County earthquake (S69E component of the Taft record). The El Centro earthquake record was chosen because it is representative of the strongest motions available from deep soil sites, whereas Taft was chosen because of its wide frequency range and strong motion characteristics.

The Taft S69E record, from the 1952 Kern County earthquake, has a maximum acceleration of .179g at a time of 3.70 sec and a mean square frequency of 2.95 Hz. Each value of the accelerogram was multiplied by a factor of .836 to scale the record to a peak acceleration of .15g for the DBE at Surry. A similar scaling technique was used to obtain the Taft record for the OBE. Frequencies over 20 Hz were excluded from the time history input at ground surface in order to allow convergence of the iterations when deconvoluting in the free field and to maintain deconvoluted time histories with mean square frequencies close to the original Taft record in each of the layers of the soil profile. The time history at the base layer, El -380 feet in this

SURRY POWER STATION, UNITS 1 AND 2

analysis, was stored for later use in amplification analyses under each of the structures. The peak acceleration of the Taft record at the base layer after deconvolution to El -380 feet was .215g.

The 1940 El Centro earthquake, North-South record, was also used in the SHAKE analyses. The maximum recorded acceleration at El Centro was .349g at a time of 2.12 sec, with a mean square frequency of 3.18 Hz. Each value of the accelerogram was multiplied by a factor of .43 to scale the El Centro record to the Surry DBE. Frequencies above 15 Hz were cut off the El Centro record. The peak acceleration of the El Centro record at the base layer after deconvolution to El -380 feet was .324g.

2.4.2.3 Soil Profile

A horizontally layered, idealized soil profile was established for the SHAKE analysis based on previous studies discussed in Section 2.2. A description of the profile and relevant soil properties for each layer are included in Tables 2-4 to 2-11 for the free field case and for each structure. In the free field, the profile consists of three layers of Pleistocene soils, from the ground surface at El +26 feet to the top of the Miocene clay at El -40 feet. The Miocene clay extends from -40 to -280 feet, overlying a 100 foot layer of Eocene and Paleocene sands. The base layer has been set at El -380 feet.

SURRY POWER STATION, UNITS 1 AND 2

The soil profiles under each structure are identical to the free field case below El -40 feet. The soil profiles shown in Figures 2-3 and 2-4 have been used to define the soil layering under each structure in the Pleistocene sediments. The containment is founded on the Miocene clay, at El -40 feet, but the other structures are founded at higher elevations, either on the Pleistocene clay or sand.

The structures themselves have been represented as "pseudosoils" in the SHAKE analysis. These soils are described by unit weights and shear wave velocities that are compatible with the structure. For unit weight, the total weight of the structure was divided by the thickness of the pseudosoil layer. The shear wave velocity was computed from the first harmonic natural period of the structure, using the following equation:

$$V_s = \frac{4H}{T}$$

where:

V_s = equivalent shear wave velocity for structure

H = thickness of pseudosoil layer

T = natural period of the structure

SURRY POWER STATION, UNITS 1 AND 2

2.4.2.4 Strain Dependency Relationships

The variation of shear modulus with strain is input into SHAKE using the shear modulus factor K varying with strain. K is an empirical factor relating shear modulus to confining stress for sands and undrained shear strength for clays. The shear modulus is calculated from the shear modulus factor K by the following equations:

For sands:

$$G = 1000K_s (\bar{\sigma}_n)^{0.5} F$$

where:

G = shear modulus in psf

K_s = shear modulus factor for sands

$\bar{\sigma}_n$ = effective octahedral stress in psf

F_s = scaling factor of low strain shear modulus value

For clays:

$$G = K_c F_c$$

SURRY POWER STATION, UNITS 1 AND 2

where:

F_c = scaling factor for low strain shear modulus value

K_c = shear modulus factor for clays

The decrease of shear modulus with increasing shear strain is presented in terms of K to conform with the input format required in the SHAKE program. The strain dependency relationships of K_s and K_c , plotted with shear strain, are presented in Figures 2-12 and 2-13, respectively. These curves are based on empirical data plotted by Seed and Idriss and reported in the Shannon and Wilson report. (11) The factor F is calculated internally by the program, using the small strain values of shear modulus and K_s or K_c input into the program. This calculated value of F is used in subsequent iterations to compute the new shear modulus based on a K vs shear strain curve that has been shifted from the empirical curve by the factor F to account for site conditions as defined by G_{max} .

The increase of damping ratio for sands and clays with increasing shear strain is plotted on Figures 2-14 and 2-15, respectively. These curves are based on data plotted by Seed and Idriss. (11) The curves were modified by the use of a damping correction factor, (12) which accounts for the variability of damping with depth:

SURRY POWER STATION, UNITS 1 AND 2

$$F_D = 2.53 - 0.45 \log \bar{\sigma}_v$$

where:

F_D = factor modifying damping curves

$\bar{\sigma}_v$ = vertical effective overburden stress in psf

2.4.2.5 Strain Compatible Shear Moduli and Damping

The shear moduli and damping values corresponding to the shear strain induced by the DBE and OBE are presented in tabular form for each structure analyzed and for the free field case in Tables 2-4 through 2-11. The results represent values obtained from the last iteration of shear moduli and damping. Criteria for convergence of iterations were established at plus or minus 5 percent of the previously iterated value. The data include strain-compatible moduli and damping ratios calculated from the two earthquake accelerograms described in Section 2.4.2.2, i.e., El Centro North-South and Taft S69E. An average value was calculated for each soil layer and used to model the soil in subsequent soil-structure interaction analyses.

For the reactor containments, values of shear modulus and damping from the first iteration of SHAKE are listed for DBE and OBE conditions in Table 2-12. These values represent SHAKE's first estimate of the shear strain level

SURRY POWER STATION, UNITS 1 AND 2

induced by the earthquake and, therefore, result in shear moduli values that are too high, and damping values that are too low in the upper portion of the profile, and too high at depth. The differences between the low strain values of shear modulus (Gmax) and the first iteration values vary by as much as 450 percent, but subsequent iterations converge quite rapidly. Typical variations between first and second iteration values are only 10 to 20 percent, which is close to the final iteration convergence criterion of 5 percent difference.

2.4.2.6 Variation of Shear Modulus

The effect of increasing and decreasing the low strain shear moduli (Gmax) by 50 percent was evaluated using SHAKE. The El Centro and Taft earthquake records, normalized for the DBE, were input at the ground surface in the free field, deconvoluted to the base layer and then amplified up through the soil to the containment structure. All soil parameters other than the low strain shear moduli remained unchanged.

The depth of the soil profile for the analysis using Gmax minus 50 percent was reduced from 406 to 261 feet. The use of such low values of shear moduli with a deep soil profile causes the iterations for strain dependent properties to diverge. Convergence was attained by eliminating the frequency content of the time histories above 10 Hz and by establishing the half space at a higher

SURRY POWER STATION, UNITS 1 AND 2

elevation. The full profile was used in the soil-structure interaction analysis, using extrapolated values of strain compatible modulus and damping for the bottom layers of the profile.

The strain compatible soil properties for G_{max} plus 50 percent and G_{max} minus 50 percent are listed on Tables 2-13 and 2-14, for the free field and under the reactor containment, respectively. Poisson's ratio, calculated for these cases using small strain values and strain compatible values from the DBE, are listed on Table 2-2. Strain compatible soil properties for G_{max} are included in Tables 2-4 and 2-5 for the free field and containment, respectively.

The expected variation of shear modulus at low strain levels and at strain levels associated with strong motion earthquakes was evaluated using cross-hole data from the site⁽⁷⁾ and laboratory data used to obtain the shear modulus factor for clays curve in Figure 2-13, as reported in Reference 11.

In this analysis, the shear modulus factors G/S_u were normalized with the low strain value of G_{max}/S_u from the same curve, resulting in a G/G_{max} versus shear strain relationship. To determine the variation of G , which is a function of the product of G_{max} and G/G_{max} , it is assumed that G_{max} and G/G_{max} are uncorrelated. Thus

SURRY POWER STATION, UNITS 1 AND 2

$$V_G^2 = V_{Gmax}^2 + V_{G/Gmax}^2 + V_{Gmax}^2 V_{G/Gmax}^2$$

where

V_{Gmax} = coefficient of variation of in situ G_{max} values from shear wave velocities determined from cross-hole data (Figure 2-11)

$V_{G/Gmax}$ = coefficient of variation of G/G_{max} from SW-AJA curves (Ref. 11)

V_G = coefficient of variation of G values at various shear strain levels

From V_G , the expected variation as a percentage of the average G value for a particular shear strain level can be estimated. This variation was ± 8.4 percent at low shear strains and ranged from ± 46.1 to ± 77.8 percent of the average shear modulus at a shear strain level of 2×10^{-3} to 6×10^{-1} percent, the range of shear strain levels generated by the DBE and OBE at the site. Although the percentage variation of the average G value is higher at higher shear strain levels, the actual range of moduli values is approximately the same as at low strain levels.

SURRY POWER STATION, UNITS 1 AND 2

2.5 SUMMARY ON SOIL PROPERTIES

Procedures followed to obtain soil properties for the soil-structure interaction analyses and their use in developing amplified response spectra are summarized as follows.

First, a small strain soil profile was developed from the best available soil data, including cross hole seismic shear wave velocity measurements, as well as data from borings and samples.

Second, the effect of an earthquake in the free field was evaluated using the SHAKE computer program. The control motion was specified at the surface of the free field; two real records were used - El Centro and Taft - normalized to the acceleration level of the specified design earthquake (OBE or DBE). The program iterated to obtain values of shear modulus and damping compatible with the levels of strain developed during the earthquake. The average of the results from the two records was used in further analyses and is here called the strain compatible, free field profile.

Third, the moduli and material damping for the strain compatible, free field profile were used for the REFUND/FRIDAY analyses.

SURRY POWER STATION, UNITS 1 AND 2

Fourth, the motion at the base of the profile obtained in the SHAKE analysis of the free field was input to several profiles representing the soil column under the Category I buildings. The top layers of these profiles had masses and fundamental periods equivalent to those of the corresponding buildings. The small strain values of soil shear moduli were adjusted to account for the additional static stresses imposed by the buildings. The computer program SHAKE was run to obtain strain compatible moduli and damping values for each building profile. The average of results for the two time histories established each profile.

Fifth, the strain compatible properties under each building were used in the finite element dynamic analyses as soil properties directly under the corresponding buildings. The strain compatible, free field soil properties were used for the elements representing the free field. Strain compatible soil properties were interpolated between these values for two columns of elements adjacent to the building.

Sixth, no further iteration on soil properties was performed in either the REFUND/FRIDAY or the finite element analysis.

SURRY POWER STATION, UNITS 1 AND 2

2.6. REFERENCES

1. Dames & Moore Report, Environmental Studies Proposed Nuclear Power Plant. Surry, Virginia, December 1966.
2. Virginia Electric & Power Company, Final Safety Analysis Report. Surry Power Station, Units 1 and 2, Part B, Volume 1, December 1969.
3. Virginia Electric & Power Company, Geotechnical Report. Surry Power Station, Units 3 and 4, June, 1973.
4. Virginia Electric & Power Company, Preliminary Safety Analysis Report, Surry Power Station, Units 1 and 2, Appendix 59.9A, October 1967.
5. Hardin, B.O. and Black, W.L., Closure to Vibration Modulus of Normally Consolidated Clays. Journal of Soil Mechanics and Foundations Division, ASCE Volume 95, SM 6, November 1969.
6. Schmertmann, J.M., The Undisturbed Consolidation of Clay. Trans. ASCE, Vol 120, p 1201, 1955.
7. Virginia Electric & Power Company. Preliminary Safety Analysis Report. Surry Power Station, Units 3 and 4, Comment 2.62, Amendment 7 and Comment 2.5.4.4, enclosure 3, Amendment 1.

SURRY POWER STATION, UNITS 1 AND 2

8. Lambe, T.W. and Whitman, R.V. Soil Mechanics, Fig. 10.12. p 128, John Wiley, New York, 1969, after Hendron, 1963.
9. Lambe, T.W. and Whitman, R.V. Soil Mechanics. Fig. 20.8, p 300, John Wiley, New York, 1969, after Brooker and Ireland, 1965.
10. Schnabel, P.B., Lysmer, J., and Seed, H.B. SHAKE, A Computer Program for Earthquake Response Analysis of Horizontally Layered Sites. Earthquake Engineering Research Center, Report No. EERC72-12 December 1972 (as modified for SWEC Computer System in Program ST211 Version 2 Level 0).
11. Shannon & Wilson - Agbabian-Jacobson - Soil Behavior Under Earthquake Loading Conditions. Report prepared for U.S. Atomic Energy Commission, Contract No. W-705-eng-26, January 1972.
12. Newmark, N.U., and Hall, W.J., Seismic Design Criteria for Nuclear Reactor Facilities. May 25, 1967.
13. Anderson, D.G. and Woods, R.D., Comparison of Field and Laboratory Shear Moduli, in In Situ Measurement of Soil Properties, ASCE Specialty Conference, No. Carolina State University, June 1975.

SURRY POWER STATION, UNITS 1 AND 2

TABLE 2-1

SUMMARY OF GEOPHYSICAL DATA

<u>Elevation (ft)</u>	<u>Shear Wave Velocity (fps)</u>	<u>Compression Wave Velocity (fps)</u>
+10	900	5200
0	900-950	5800
-10	900	5600
-20	900	5700
-30	900	5500
-40	950	5500
-50	1000	5400
-60	980	5400
-70	970	5400
-80	1000	5200
-90	950	5500
-100	970	5000
-110	1000	5400
-120	950	5600
-130	1000	5500
-140	1000	5500

SURRY POWER STATION, UNITS 1 AND 2

TABLE 2-2
POISSON'S RATIO
FREE FIELD

Layer	Top of Layer Elev.	Average Gmax		Gmax +50%		Gmax -50%	
		DBE	OBE	Low Strain	DBE	Low Strain	DBE
1	+26	.442	.442	.406	.406	.473	.473
2	+5	.491	.487	.477	.482	.493	.497
3	-20	.496	.494	.477	.493	.493	.499
4	-40	.496	.494	.475	.493	.492	.498
5	-65	.495	.493	.475	.493	.492	.499
6	-90	.495	.493	.476	.491	.492	.499
7	-123	.496	.493	.476	.492	.492	.499
8	-157	.496	.493	.476	.492	.492	.499
9	-190	.496	.493	.476	.492	.492	.499
10	-235	.496	.493	.476	.493	.492	.499*
11	-280	.477	.468	.446	.457	.484	.493*
12	-330	.481	.471	.446	.463	.484	.494*

NOTE:

* Extrapolated Data used in SS1.

SURRY POWER STATION, UNITS 1 AND 2

TABLE 2-3
SHEAR MODULUS DETERMINATIONS
HARDIN AND BLACK EQUATIONS

<u>Elevation of Layer</u>	<u>Soil Unit</u>	<u>Plastic Index (Percent)</u>	<u>OCR</u>	<u>K_n</u>	<u>Total Unit Weight (ksf)</u>	<u>e</u>	<u>G from Hardin -Black (ksf)</u>	<u>Gmax used in SHAKE (ksf)</u>
+26 to +5	Pleistocene Clay	44	3.5	1.00	.120	1.26	1011	1585
+5 to -20	Pleistocene Sand	-	3.0	0.55	.120	0.70	2229	3310
-20 to -40	Pleistocene Clay	32	3.0	0.90	.120	0.84	3091	3310
-40 to -90	Miocene Clay	46	3.3	1.00	.110	1.05	3160	3310
-90 to -190	Miocene Clay	36	2.3	0.80	.120	1.05	3211	3530
-190 to -280	Miocene Clay	30	1.3	0.60	.120	0.96	3487	3530
-280 to -380	Eocene and Paleocene Sands	-	1.3	0.50	.135	0.40	8448	8225

SURRY POWER STATION, UNITS 1 AND 2

TABLE 2-4

STRAIN COMPATIBLE SOIL PROPERTIES

Free Field
Average Gmax

Layer No.	Thick- ness (ft)	Top of Layer Elev.	Low Strain Values		Total Unit Wt (kcf)	Soil Unit	DBE = 0.15g									OBE = 0.07g								
			Gmax (ksf)	Cs (fps)			Shear Modulus (ksf)			Damping			Shear Modulus (ksf)			Damping								
							Taft S69E	ElCentro N-S	Aver- age	Taft S69E	ElCentro N-S	Aver- age	Taft S69E	ElCentro N-S	Aver- age	Taft S69E	ElCentro N-S	Aver- age						
			1	21			+26	1585	.120	Pleistocene Clay	581	547	564	.069	.072	.071	840	823	832	.051	.051	.051		
2	25	+5	3310	.120	Pleistocene Sand	1859	1746	1802	.071	.076	.074	2468	2380	2424	.044	.048	.046							
3	20	-20	3310	.120	Pleistocene Clay	793	766	780	.070	.071	.071	1255	1201	1228	.052	.054	.053							
4	25	-40	3310	.110	Miocene Clay	760	797	778	.068	.067	.068	1149	1155	1152	.053	.053	.053							
5	25	-65	3310	.110	Miocene Clay	881	895	888	.060	.060	.060	1190	1261	1226	.050	.047	.049							
6	33	-90	3530	.120	Miocene Clay	976	909	943	.056	.058	.057	1476	1405	1441	.041	.043	.042							
7	33	-123	3530	.120	Miocene Clay	916	879	898	.055	.056	.056	1425	1323	1374	.041	.043	.042							
8	34	-157	3530	.120	Miocene Clay	908	890	899	.053	.053	.053	1368	1304	1336	.040	.042	.041							
9	45	-190	3530	.120	Miocene Clay	871	843	857	.051	.052	.052	1349	1344	1347	.039	.039	.039							
10	45	-235	3530	.120	Miocene Clay	854	742	798	.049	.053	.051	1298	1301	1300	.038	.038	.038							
11	50	-280	8225	.135	Eocene Sands	5497	4018	4758	.034	.051	.043	6459	6195	6327	.024	.027	.026							
12	50	-330	8225	.135	Paleocene Sands	4696	3309	4003	.041	.059	.050	6105	5654	5880	.026	.031	.029							

SURRY POWER STATION, UNITS 1 & 2

TABLE 2-5

STRAIN COMPATIBLE SOIL PROPERTIES

Reactor Containment
Average Gmax

Layer No.	Thick-ness (ft)	Top of Layer Elev.	Low Strain Values		Total Unit Wt (kef)	Soil Unit	DBE = 0.15g						OBE = 0.07g						
			Gmax (ksf)	Cs (fps)			Shear Modulus (ksf)			Damping			Shear Modulus (ksf)			Damping			
							Taft S69E	ElCentro N-S	Aver-age	Taft S69E	ElCentro N-S	Aver-age	Taft S69E	ElCentro N-S	Aver-age	Taft S69E	ElCentro N-S	Aver-age	
1	21	+26		1073	.1106	Structure													
2	45	+5		1073	.1106	Structure													
3	25	-40	3310		.110	Miocene Clay	720	728	724	.072	.071	.072	1175	1138	1157	.054	.055	.055	
4	25	-65	3310		.110	Miocene Clay	728	861	795	.068	.062	.065	1121	1196	1159	.053	.051	.052	
5	33	-90	3530		.120	Miocene Clay	959	845	902	.058	.062	.060	1423	1405	1414	.044	.044	.044	
6	33	-123	3530		.120	Miocene Clay	935	881	908	.055	.057	.056	1396	1299	1348	.042	.045	.044	
7	34	-157	3530		.120	Miocene Clay	900	878	889	.054	.055	.055	1325	1343	1334	.042	.041	.042	
8	45	-190	3530		.120	Miocene Clay	853	799	826	.053	.054	.054	1318	1325	1322	.040	.040	.040	
9	45	-235	3530		.120	Miocene Clay	838	751	795	.050	.053	.052	1284	1269	1277	.039	.039	.039	
10	50	-280	8225		.135	Eocene Sands	5430	3937	4684	.035	.053	.044	6509	6239	6374	.024	.027	.026	
11	50	-330	8225		.135	Paleocene Sands	4518	3225	3872	.043	.061	.052	6117	5721	5919	.026	.030	.029	

SURRY POWER STATION, UNITS 1 AND 2

TABLE 2-9

STRAIN COMPATIBLE SOIL PROPERTIES

Containment Spray Pumphouse

Layer No.	Thick-ness (ft)	Top of Layer Elev.	Low Strain Values		Total Unit Wt (kcf)	Soil Unit	DBE = 0.15g						OBE = 0.07g					
			Gmax (ksf)	Cs (fps)			Shear Modulus (ksf)			Damping			Shear Modulus (ksf)			Damping		
							Taft S69E	ElCentro N-S	Aver-age	Taft S69E	ElCentro N-S	Aver-age	Taft S69E	ElCentro N-S	Aver-age	Taft S69E	ElCentro N-S	Aver-age
1	17	+26		1838	.064	Structure												
2	4	+9	3310		.120	Pleistocene Clay	1771	1654	1713	.050	.052	.051	2352	2297	2325	.038	.039	.039
3	25	+5	3310		.120	Pleistocene Sand	2087	1948	2018	.065	.072	.069	2609	2533	2571	.041	.044	.043
4	20	-20	3310		.120	Pleistocene Clay	838	804	821	.072	.073	.073	1347	1271	1309	.052	.055	.054
5	25	-40	3310		.110	Miocene Clay	744	787	766	.072	.070	.071	1175	1165	1170	.055	.055	.055
6	25	-65	3310		.110	Miocene Clay	829	863	846	.065	.063	.064	1156	1220	1188	.053	.050	.052
7	33	-90	3530		.120	Miocene Clay	991	873	932	.057	.061	.059	1451	1420	1436	.043	.044	.044
8	33	-123	3530		.120	Miocene Clay	935	895	915	.056	.057	.057	1426	1343	1385	.042	.044	.043
9	34	-157	3530		.120	Miocene Clay	898	878	888	.054	.055	.055	1319	1362	1341	.042	.041	.042
10	45	-190	3530		.120	Miocene Clay	855	834	845	.053	.054	.054	1341	1354	1348	.040	.039	.040
11	45	-235	3530		.120	Miocene Clay	818	751	785	.051	.053	.052	1282	1300	1291	.039	.039	.039
12	50	-280	8225		.135	Eocene Sands	5533	3985	4759	.034	.052	.043	6415	6256	6336	.025	.027	.026
13	50	-330	8225		.135	Paleocene Sands	4762	3242	4002	.041	.061	.051	6117	5705	5911	.027	.031	.029

SURRY POWER STATION, UNITS 1 AND 2

TABLE 2-10

STRAIN COMPATIBLE SOIL PROPERTIES

Safeguards Building
N-S Component

Layer No.	Thick-ness (ft)	Top of Layer Elev.	Low Strain Values		Total Unit Wt (kcf)	Soil Unit	DBE = 0.15g						OBE = 0.07g					
			G _{max} (ksf)	Cs (fps)			Shear Modulus (ksf)			Damping			Shear Modulus (ksf)			Damping		
							Taft S69E	ElCentro N-S	Aver-age	Taft S69E	ElCentro N-S	Aver-age	Taft S69E	ElCentro N-S	Aver-age	Taft S69E	ElCentro N-S	Aver-age
1	16.5	+26		2444	.076	Structure												
2	4.5	+95	3310		.120	Pleisto-cene Clay	1671	1549	1610	.051	.053	.052	2242	2172	2207	.039	.040	.040
3	25	+5	3310		.120	Pleisto-cene Sand	2027	1882	1955	.067	.074	.071	2575	2490	2533	.042	.045	.044
4	20	-20	3310		.120	Pleisto-cene Clay	827	794	811	.071	.073	.072	1328	1275	1302	.052	.054	.053
5	25	-40	3310		.110	Miocene Clay	744	790	767	.071	.069	.070	1167	1183	1175	.054	.054	.054
6	25	-65	3310		.110	Miocene Clay	837	864	851	.064	.063	.064	1162	1225	1194	.052	.050	.051
7	33	-90	3530		.120	Miocene Clay	987	886	937	.057	.060	.059	1456	1410	1433	.043	.044	.044
8	33	-123	3530		.120	Miocene Clay	930	889	910	.056	.057	.057	1425	1335	1380	.041	.044	.043
9	34	-157	3530		.120	Miocene Clay	897	882	890	.054	.055	.055	1326	1343	1335	.042	.042	.042
10	45	-190	3530		.120	Miocene Clay	856	835	846	.053	.053	.053	1341	1333	1337	.040	.040	.040
11	45	-235	3530		.120	Miocene Clay	826	749	788	.051	.053	.052	1284	1289	1287	.039	.039	.039
12	50	-280	8225		.135	Eocene Sands	5526	3971	4749	.034	.052	.043	6420	6220	6320	.025	.027	.026
13	50	-330	8225		.135	Paleocene Sands	4764	3242	4003	.041	.061	.051	6138	5680	5909	.026	.031	.029

SURRY POWER STATION, UNITS 1 AND 2

TABLE 2-11

STRAIN COMPATIBLE SOIL PROPERTIES

Fuel Building
E-W Component

Layer No.	Thick-ness (ft)	Top of Layer Elev.	Low Strain Values		Total Unit Wt (kcf)	Soil Unit	DBE = 0.15g						OBE = 0.07g						
			G _{max} (ksf)	Cs (fps)			Shear Modulus (ksf)			Damping			Shear Modulus (ksf)			Damping			
							Taft S69E	ElCentro N-S	Aver-age	Taft S69E	ElCentro N-S	Aver-age	Taft S69E	ElCentro N-S	Aver-age	Taft S69E	ElCentro N-S	Aver-age	
1	21	+26		2397	.173	Structure													
2	4	+5		2397	.173	Structure													
3	21	+1	3310		.120	Pleistocene Sand	1648	1456	1552	.074	.082	.078	2298	2259	2279	.047	.049	.048	
4	20	-20	3310		.120	Pleistocene Clay	781	748	765	.067	.068	.068	1180	1187	1184	.052	.052	.052	
5	25	-40	3310		.110	Miocene Clay	774	826	800	.064	.062	.063	1099	1163	1131	.052	.050	.051	
6	25	-65	3310		.110	Miocene Clay	903	866	885	.057	.058	.058	1166	1275	1221	.048	.045	.047	
7	33	-90	3530		.120	Miocene Clay	950	898	924	.055	.057	.056	1458	1331	1395	.040	.044	.042	
8	33	-123	3530		.120	Miocene Clay	832	910	871	.056	.053	.055	1410	1240	1325	.040	.044	.042	
9	34	-157	3530		.120	Miocene Clay	895	848	872	.052	.053	.053	1397	1255	1326	.038	.042	.040	
10	45	-190	3530		.120	Miocene Clay	863	821	842	.050	.052	.051	1341	1299	1320	.038	.039	.039	
11	45	-235	3530		.120	Miocene Clay	885	705	795	.047	.052	.050	1317	1180	1249	.037	.040	.039	
12	50	-280	8225		.135	Eocene Sands	5369	3890	4630	.035	.051	.043	6501	5936	6219	.023	.029	.026	
13	50	-330	8225		.135	Paleocene Sands	4681	3234	3958	.040	.059	.050	5904	5566	5735	.028	.031	.030	

SURRY POWER STATION, UNITS 1 AND 2

TABLE 2-13

STRAIN COMPATIBLE SOIL PROPERTIES

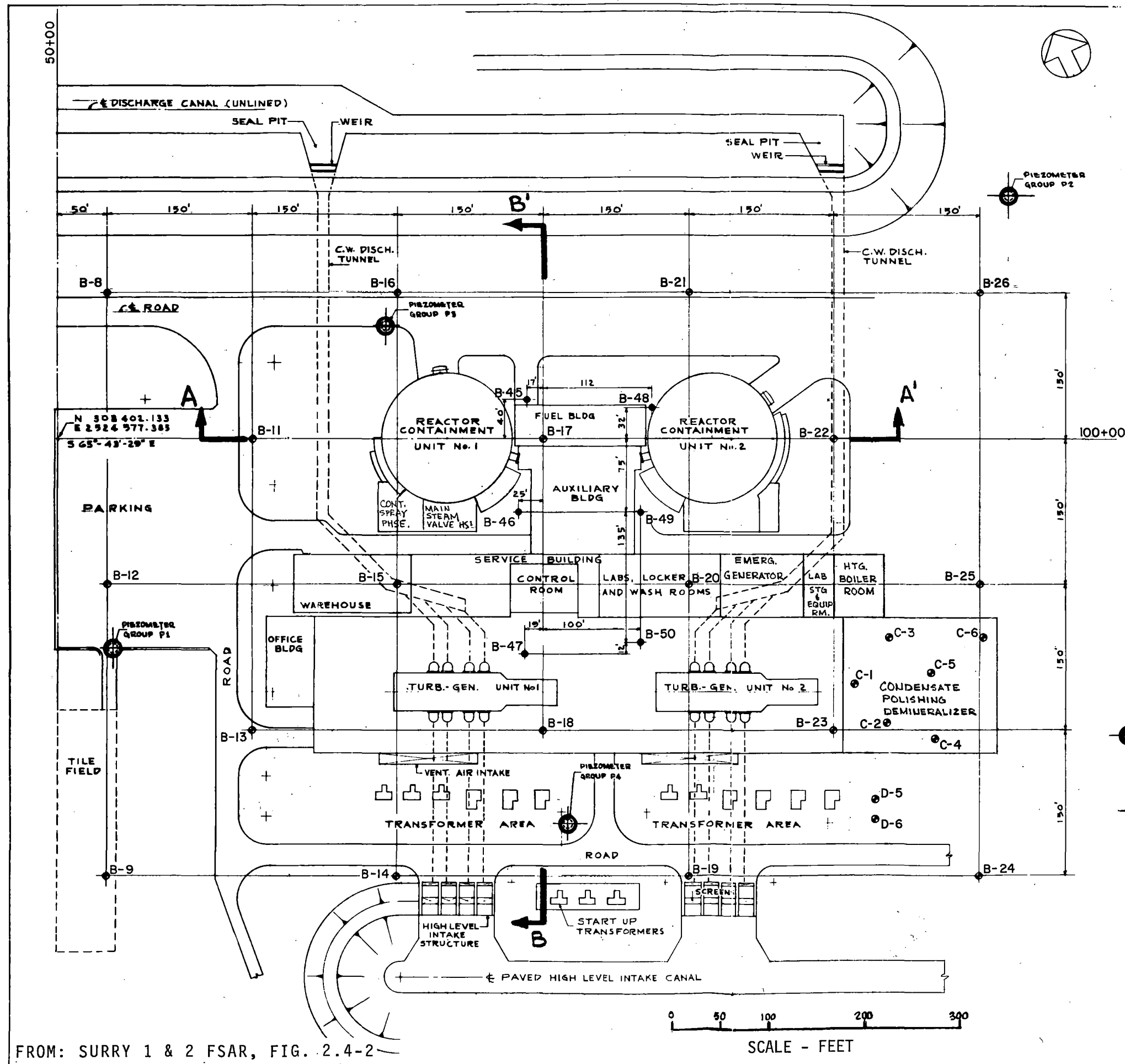
Gmax ± 50%

Free Field

Layer No.	Thick-ness (ft)	Top of Layer Elev.	Low Strain Values		Total Unit Wt (kcf)	Soil Unit	Average Gmax + 50% (DBE)						Average Gmax - 50% (DBE)					
			Gmax (ksf)	Cs (fps)			Shear Modulus (ksf)			Damping			Shear Modulus (ksf)			Damping		
							Taft S69E	ElCentro N-S	Aver-age	Taft S69E	ElCentro N-S	Aver-age	Taft S69E	ElCentro N-S	Aver-age	Taft S69E	ElCentro N-S	Aver-age
1	21	+26	1585	.120	Pleisto-cene Clay	1058	1038	1048	.058	.059	.059	192	172	182	.090	.094	.092	
2	25	+5	3310	.120	Pleisto-cene Sand	3351	3149	3250	.054	.060	.057	672	674	673	.099	.098	.099	
3	20	-20	3310	.120	Pleisto-cene Clay	1463	1367	1415	.062	.065	.064	334	359	347	.076	.074	.075	
4	25	-40	3310	.110	Miocene Clay	1290	1263	1277	.064	.065	.065	351	334	343	.070	.072	.071	
5	25	-65	3310	.110	Miocene Clay	1287	1330	1309	.061	.060	.061	323	329	326	.070	.069	.070	
6	33	-90	3530	.120	Miocene Clay	1665	1656	1661	.052	.052	.052	340	358	349	.066	.065	.066	
7	33	-123	3530	.120	Miocene Clay	1629	1475	1552	.050	.053	.052	328	316	322	.064	.065	.065	
8	34	-157	3530	.120	Miocene Clay	1568	1435	1502	.048	.051	.050	327	271	299	.061	.071	.066	
9	45	-190	3530	.120	Miocene Clay	1531	1426	1479	.047	.049	.048	316	219	268	.059	.080	.070	
10	45	-235	3530	.120	Miocene Clay	1455	1412	1433	.046	.047	.047	-	-	256*	-	-	.070*	
11	50	-280	8225	.135	Eocene Sands	8723	7903	8313	.031	.037	.035	-	-	1413*	-	-	.064*	
12	50	-330	8225	.135	Paleocene Sands	7953	6831	7392	.034	.043	.039	-	-	1183*	-	-	.065*	

NOTE:

* Extrapolated data used in SSI.



PIEZOMETER LEVELS 11-2-67

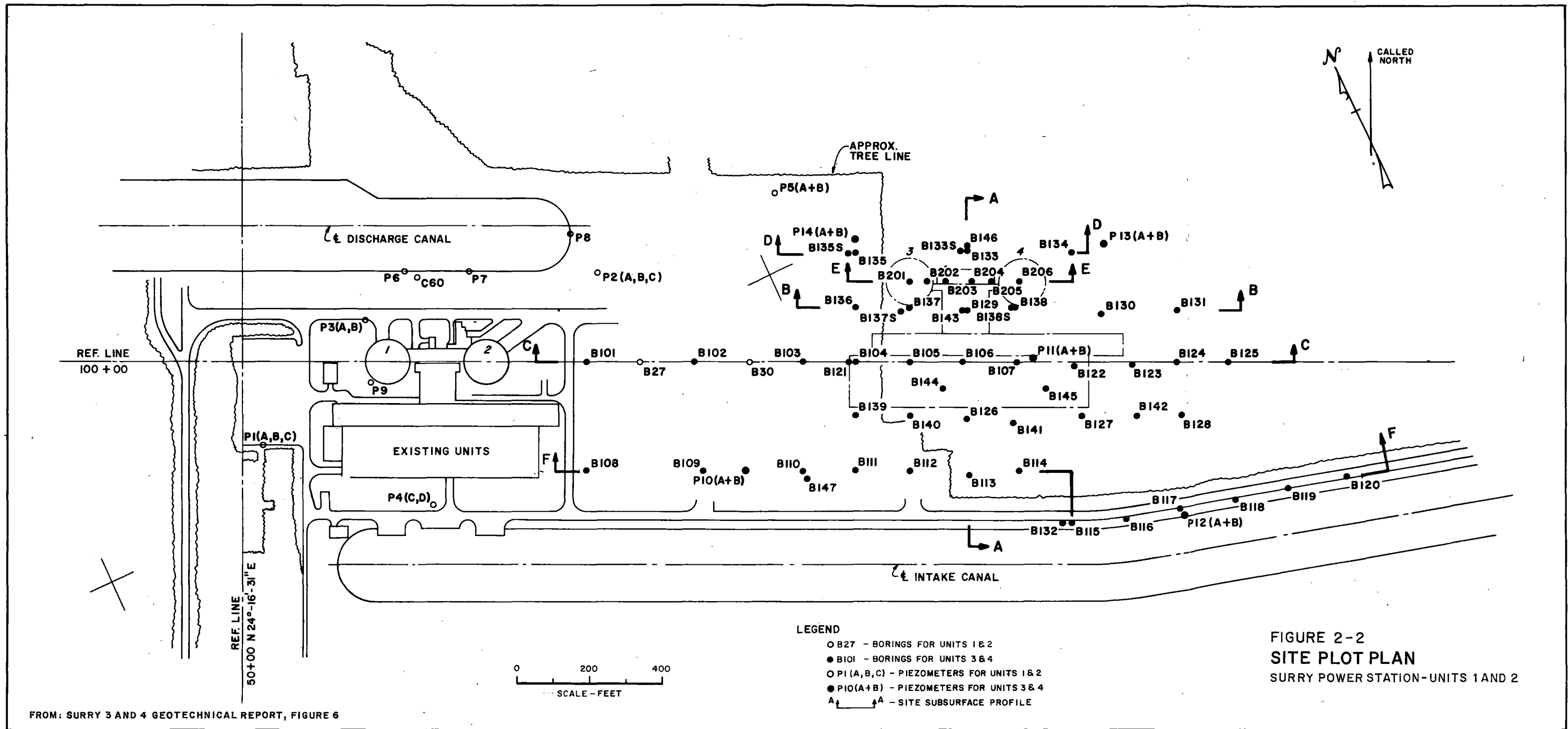
NO.	TIP	ELEV.
P1A	-10.0	+1.1
P1B	-19.0	+1.3
P1C	-31.2	+1.9
P2A	-8.1	+3.7
P2B	-33.5	+3.5
P2C	-38.2	+3.2
P3A	-31.0	-17.8
P3B	-51.0	-12.2
P4C	-31.0	+2.2
P4D	-55.0	-3.3
P5A	-7.0	+5.0
P5B	-37.0	+5.3
COFFERDAM NO. 1		
SAND N. WALL S. WALL		
A	-7.0	-9.0
B	-22.0	-24.0

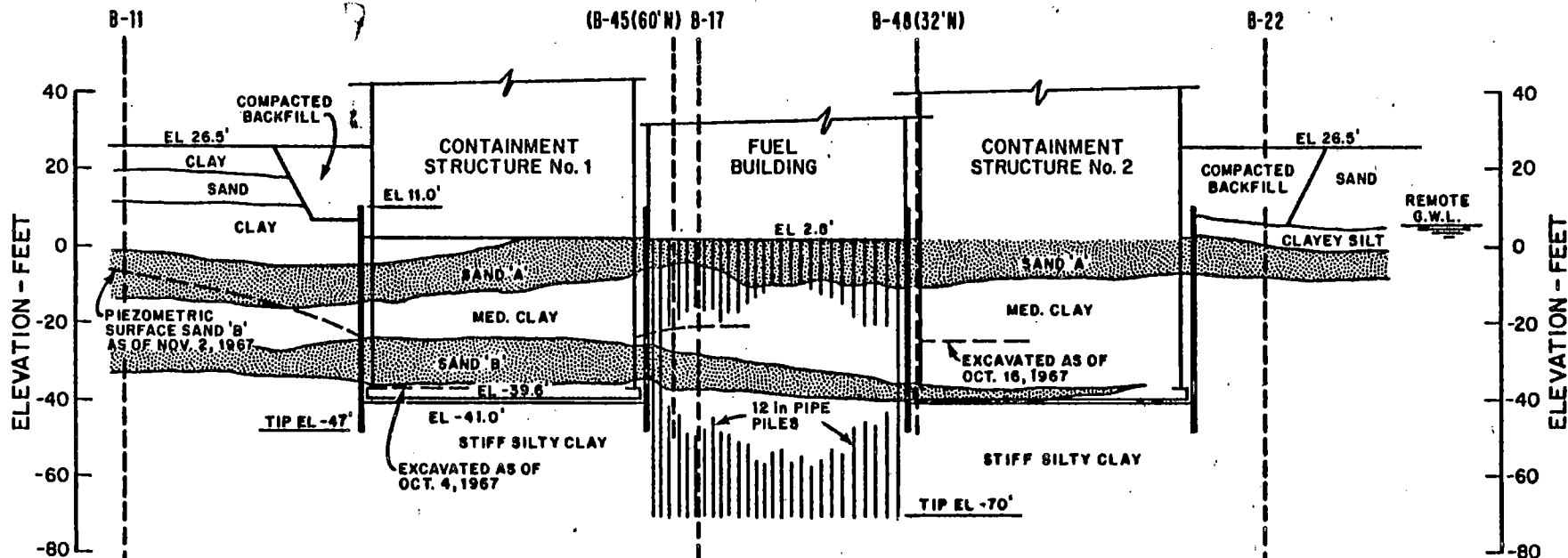
 DENOTES LOCATION OF PIEZOMETER GROUP
 DENOTES BORINGS

FIGURE 2-1
 PLAN LOCATION OF
 BORINGS AND PIEZOMETERS
 SURRY POWER STATION
 UNITS 1 AND 2

FROM: SURRY 1 & 2 FSAR, FIG. 2.4-2

0 50 100 200 300
SCALE - FEET





NOTES:

1. SAND "A" AND SAND "B" CORRESPOND TO PLEISTOCENE SANDS IN TEXT.
2. MED. CLAY CORRESPONDS TO PLEISTOCENE CLAY IN TEXT.
3. STIFF SILTY CLAY CORRESPONDS TO MIOCENE CLAY IN TEXT.

SECTION A-A'

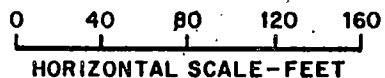


FIGURE 2-3
SUBSURFACE PROFILES
SURRY POWER STATION-UNITS 1 AND 2

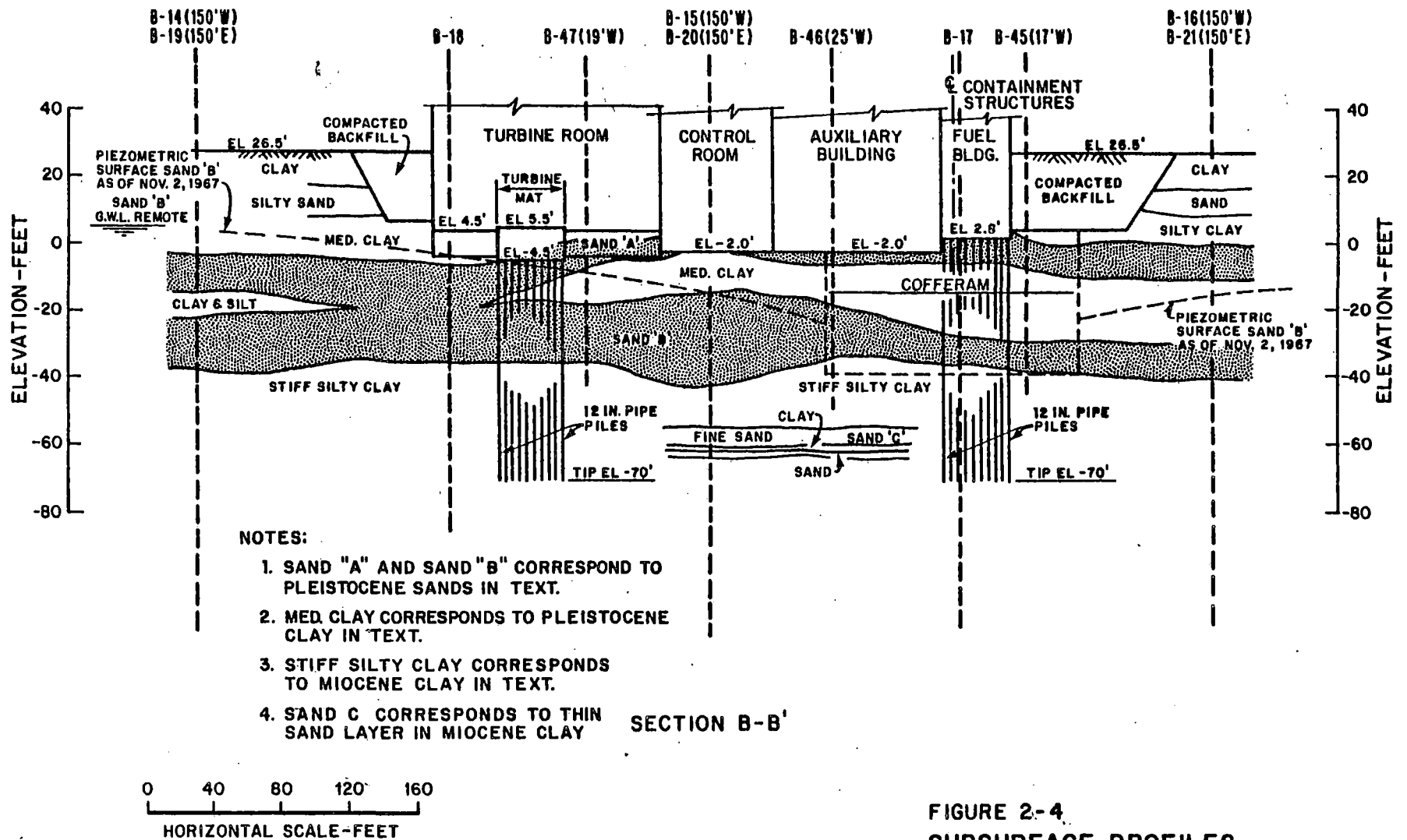
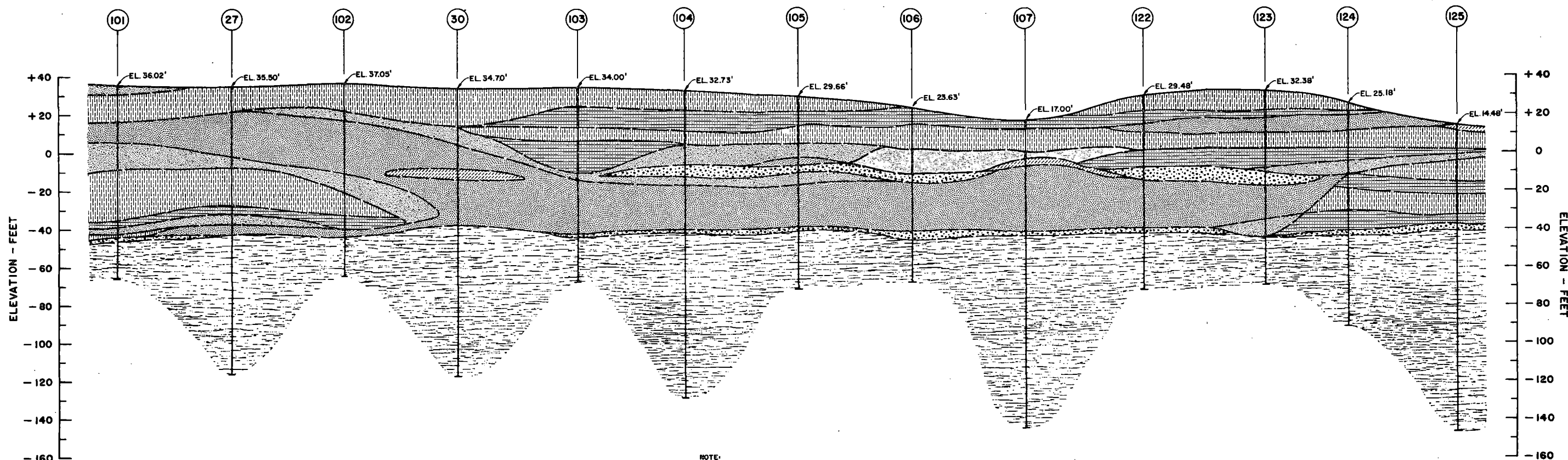


FIGURE 2-4.
SUBSURFACE PROFILES
SURRY POWER STATION-UNITS 1 AND 2



NOTE:
 1. SEE SITE PLOT PLAN (FIGURE 6) FOR PROFILE LOCATION.
 2. ① PROFILE UNIT NUMBERS REFERENCED IN TEXT.

EXPLANATION - REPRESENTATIVE SOIL STRATA
 1. STRATIGRAPHY IS INTERPOLATED FROM BORINGS.
 2. REFER TO BORING LOGS FOR DETAILED SAMPLE DESCRIPTIONS.

- | | |
|---|--|
| <p>① CLAYEY SAND
 GENERALLY, UNIFORM, FINE, 10% TO 30% HIGHLY PLASTIC FINES, MEDIUM DENSE, LIGHT GRAY BROWN. (SC)</p> <p>② CLAY
 GENERALLY, HIGHLY PLASTIC, 5% TO 8% FINE SAND, STIFF, LIGHT GRAY MOTTLED WITH RED BROWN. (CH)</p> <p>③ SILTY SAND
 GENERALLY, UNIFORM, FINE, 10% TO 30% SLIGHTLY TO MODERATELY PLASTIC FINES, MEDIUM DENSE TO DENSE, LIGHT GRAY AND YELLOW BROWN. (SM)</p> <p>④ SANDY GRAVEL OR GRAVELLY SAND
 GENERALLY, WELL GRADED, DENSE TO VERY DENSE, LIGHT GRAY BROWN. (GW OR SW)</p> | <p>⑤ SAND
 GENERALLY, POORLY GRADED, COARSE TO FINE, MOSTLY MEDIUM <10% NON-PLASTIC FINES, MEDIUM DENSE TO DENSE, LIGHT BROWN. (SP, SW OR SP-SM)</p> <p>⑥ CLAYEY SILT
 GENERALLY, MODERATELY PLASTIC, 5% TO 8% FINE SAND, STIFF, MEDIUM GRAY GREEN. (MH)</p> <p>⑦ SILTY CLAY
 GENERALLY, MODERATELY TO HIGHLY PLASTIC, 5% TO 8% FINE SAND, STIFF, MEDIUM GRAY GREEN. (MIOCENE DEPOSITION) (CL OR CH)</p> <p>⑧ INTERBEDDED SAND AND CLAY
 GENERALLY, UNIFORM, FINE, BROWN SAND AND GRAY BROWN CLAY. (SC, CL OR CH)</p> |
|---|--|

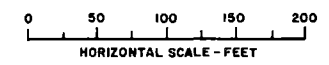
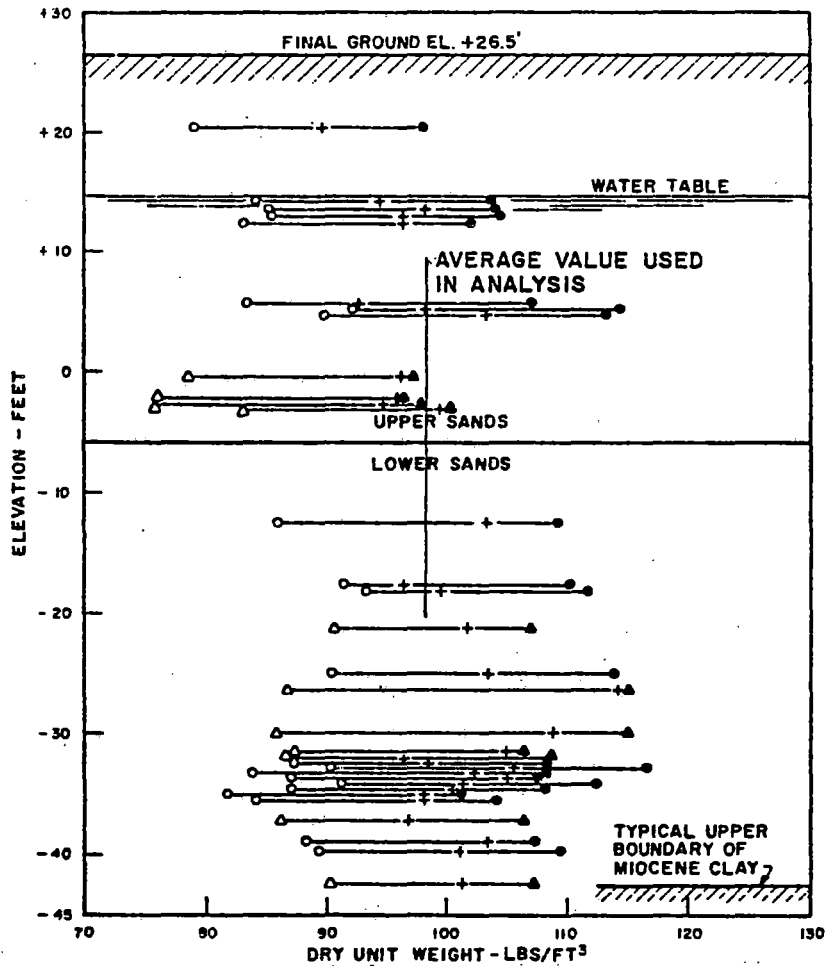


FIGURE 2-5
 SITE SUBSURFACE PROFILE C-C
 SURRY POWER STATION-UNITS 1 AND 2

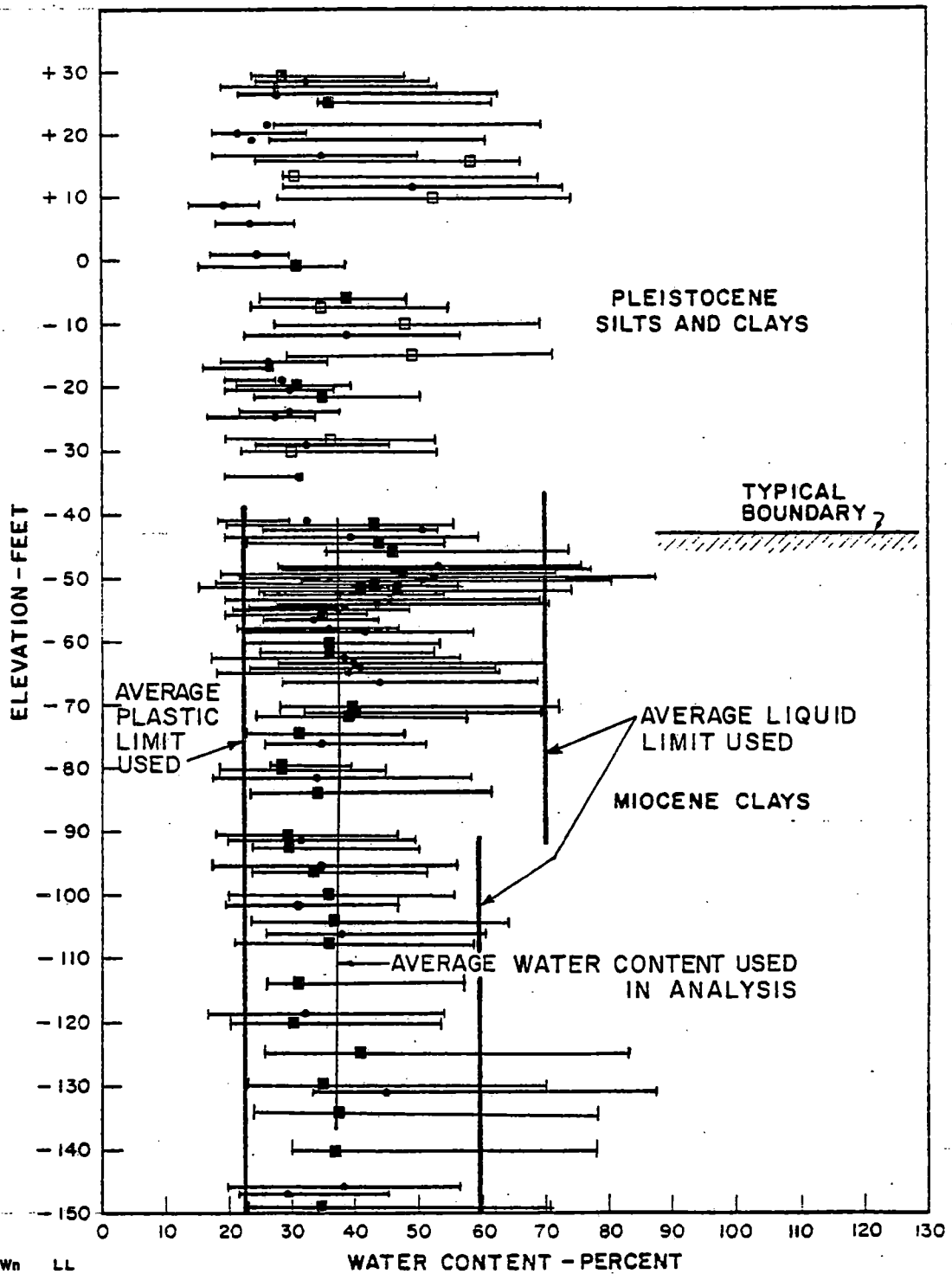
FROM: SURRY 3 AND 4 GEOTECHNICAL REPORT, FIGURE 9



LEGEND

- + IN SITU DRY DENSITY
- MINIMUM DRY DENSITY (STONE & WEBSTER DATA)
- MAXIMUM DRY DENSITY (STONE & WEBSTER DATA)
- △ MINIMUM DRY DENSITY (DAMES & MOORE DATA)
- ▲ MAXIMUM DRY DENSITY (DAMES & MOORE DATA)

FIGURE 2-6
 DENSITY VS ELEVATION FOR
 PLEISTOCENE SANDS
 SURRY POWER STATION - UNITS 1 AND 2



PL Wn LL

DATA FROM UNIT 1&2 ENVIRONMENTAL STUDIES REPORT. B-11, B-13, THRU B-23.

□

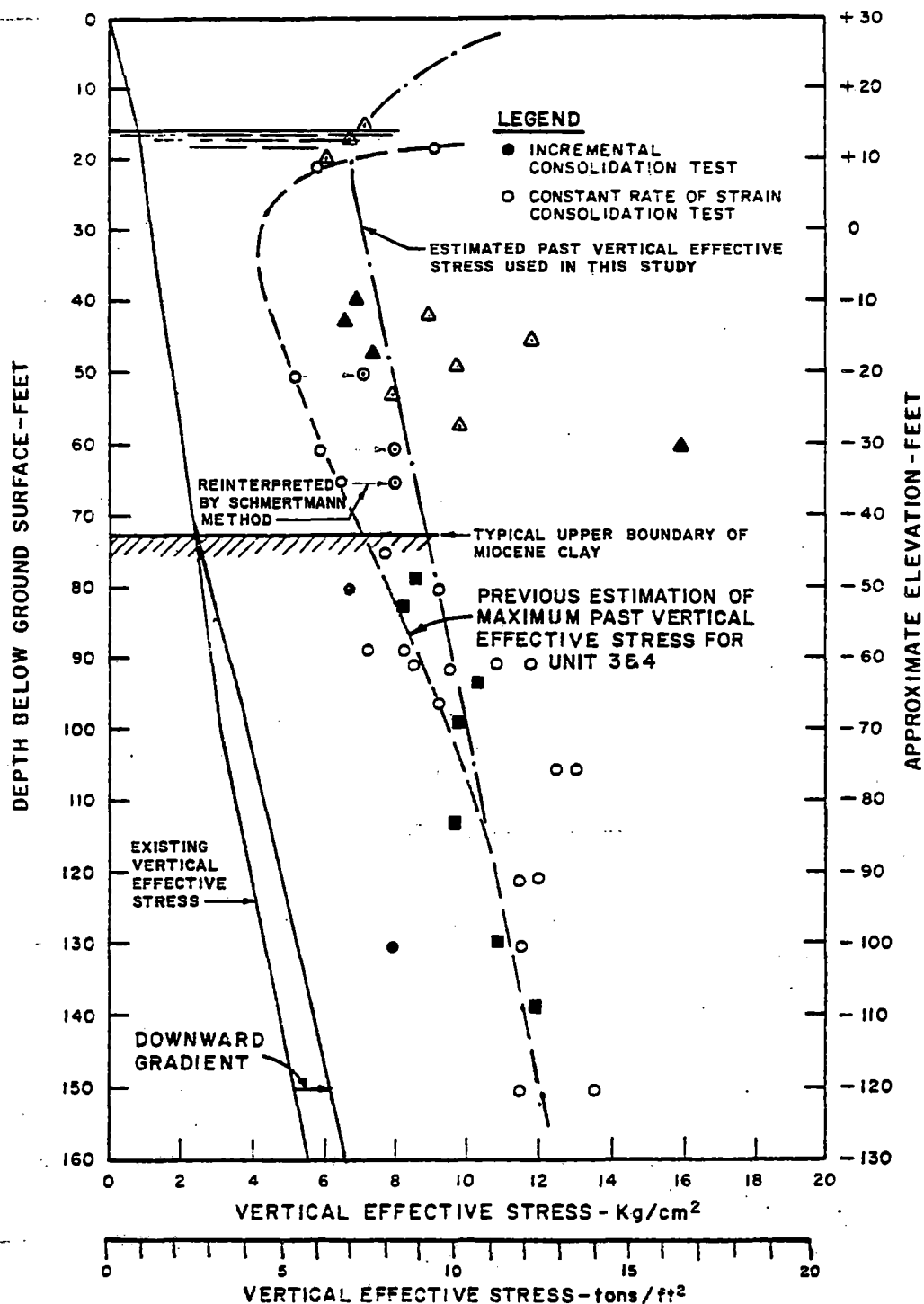
DATA FROM UNIT 1&2 CONDENSATE POLISHER STUDIES

●

DATA FROM SURRY 3 & 4

FIGURE 2-7
WATER CONTENTS AND ATTERBERG-LIMITS vs ELEVATION

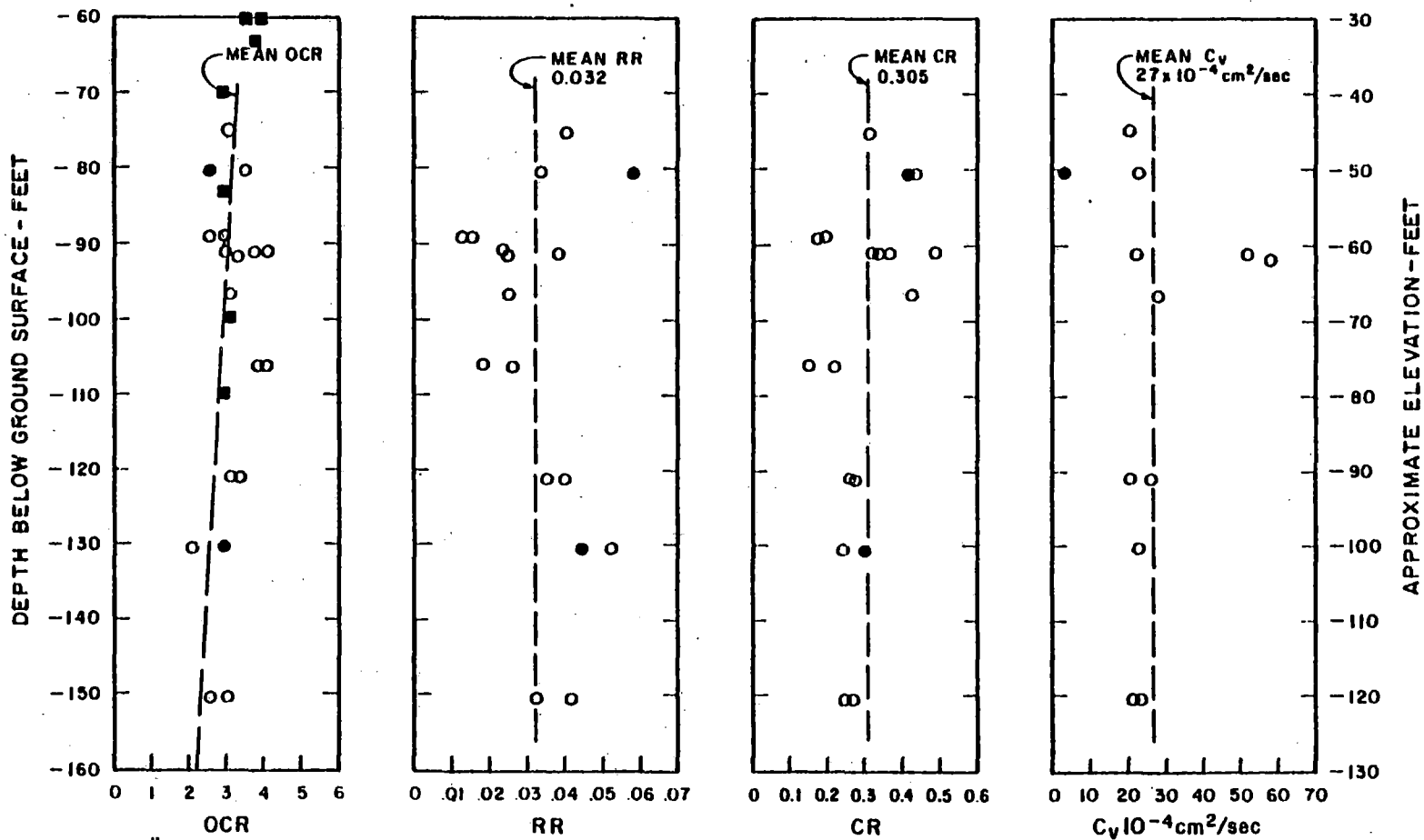
SURRY POWER STATION - UNITS 1 AND 2



- INCREMENTAL CONSOLIDATION TEST FROM UNIT 1&2 ENVIRONMENTAL STUDIES REPORT.
- △ CONSTANT RATE OF STRAIN CONSOLIDATION TEST FROM UNIT 1&2 CONDENSATE POLISHER STUDIES.
- ▲ INCREMENTAL CONSOLIDATION TEST FROM UNIT 1&2 CONDENSATE POLISHER STUDIES.
- DATA FROM SURRY 3&4

FIGURE 2-8
PRECONSOLIDATION STRESSES
IN CLAYS
SURRY POWER STATION-UNITS 1 AND 2

FROM: SURRY 3&4 GEOTECHNICAL REPORT, FIG. 33

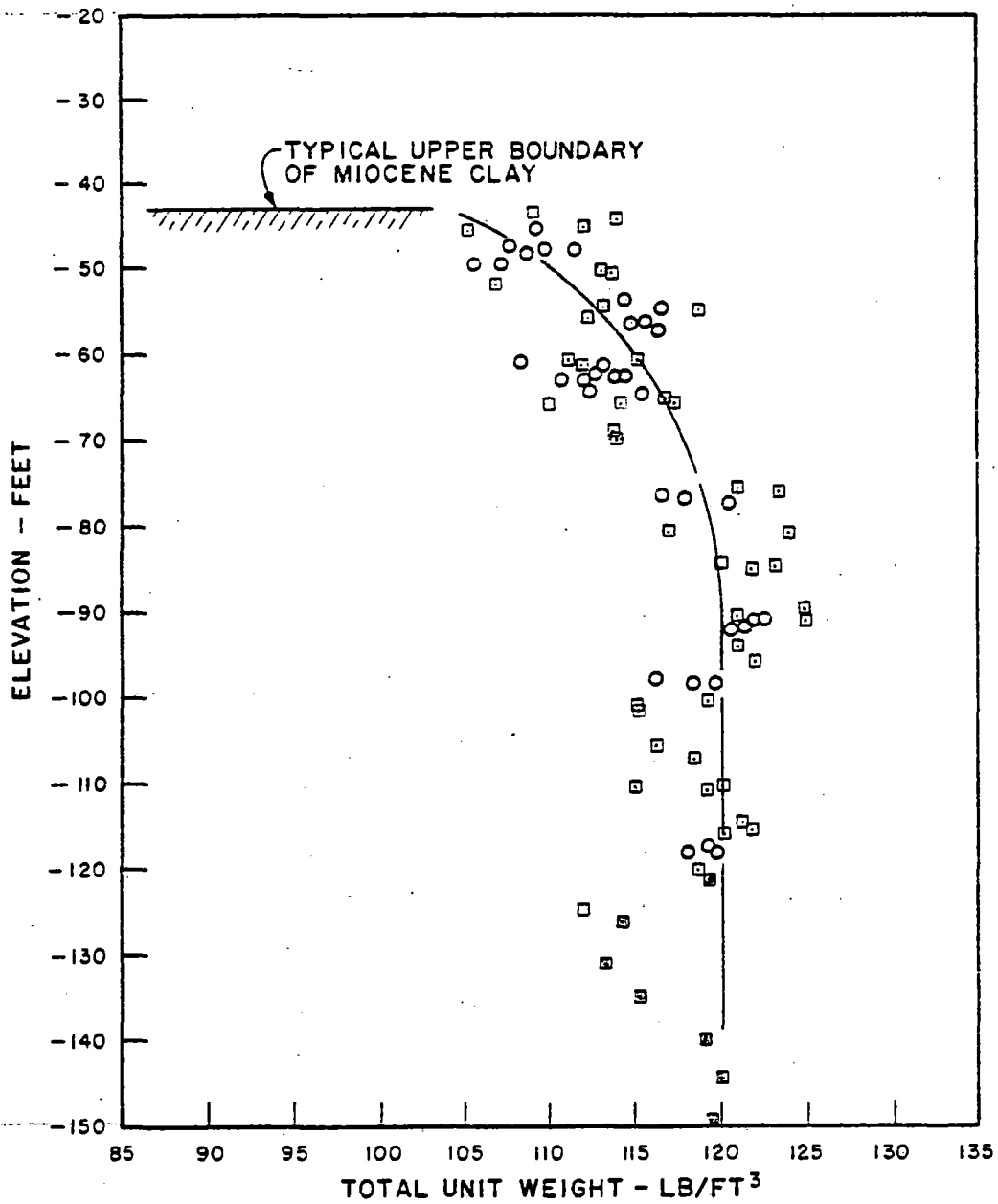


- FROM REPORT: "ENVIROMENTAL STUDIES UNIT 1&2"
 - INCREMENTAL CONSOLIDATION TEST.
 - CONSTANT RATE OF STRAIN CONSOLIDATION TEST.
- OCR OVER CONSOLIDATION RATIO - $\bar{\sigma}_{vm}/\bar{\sigma}_{vo}$
 RR RECOMPRESSION RATIO - $C_R/1+\theta_0$
 CR COMPRESSION RATIO - $C_c/1+\theta_0$
 C_v COEFFICIENT OF CONSOLIDATION.
 $\bar{\sigma}_{vo}$ EXISTING VERTICAL EFFECTIVE STRESS.
 $\bar{\sigma}_{vm}$ MAXIMUM PAST VERTICAL EFFECTIVE STRESS.

NOTE:
 C_v DATA TAKEN AS AVERAGE VALUE ON RECOMPRESSION FROM $\bar{\sigma}_{vo}$ TO $\bar{\sigma}_{vm}$.

FIGURE 2-9
 SUMMARY OF CONSOLIDATION TEST DATA IN MIOCENE CLAYS
 SURRY POWER STATION - UNIT 1 AND 2

FROM: SURRY 3 & 4 GEOTECHNICAL REPORT, FIG. 34

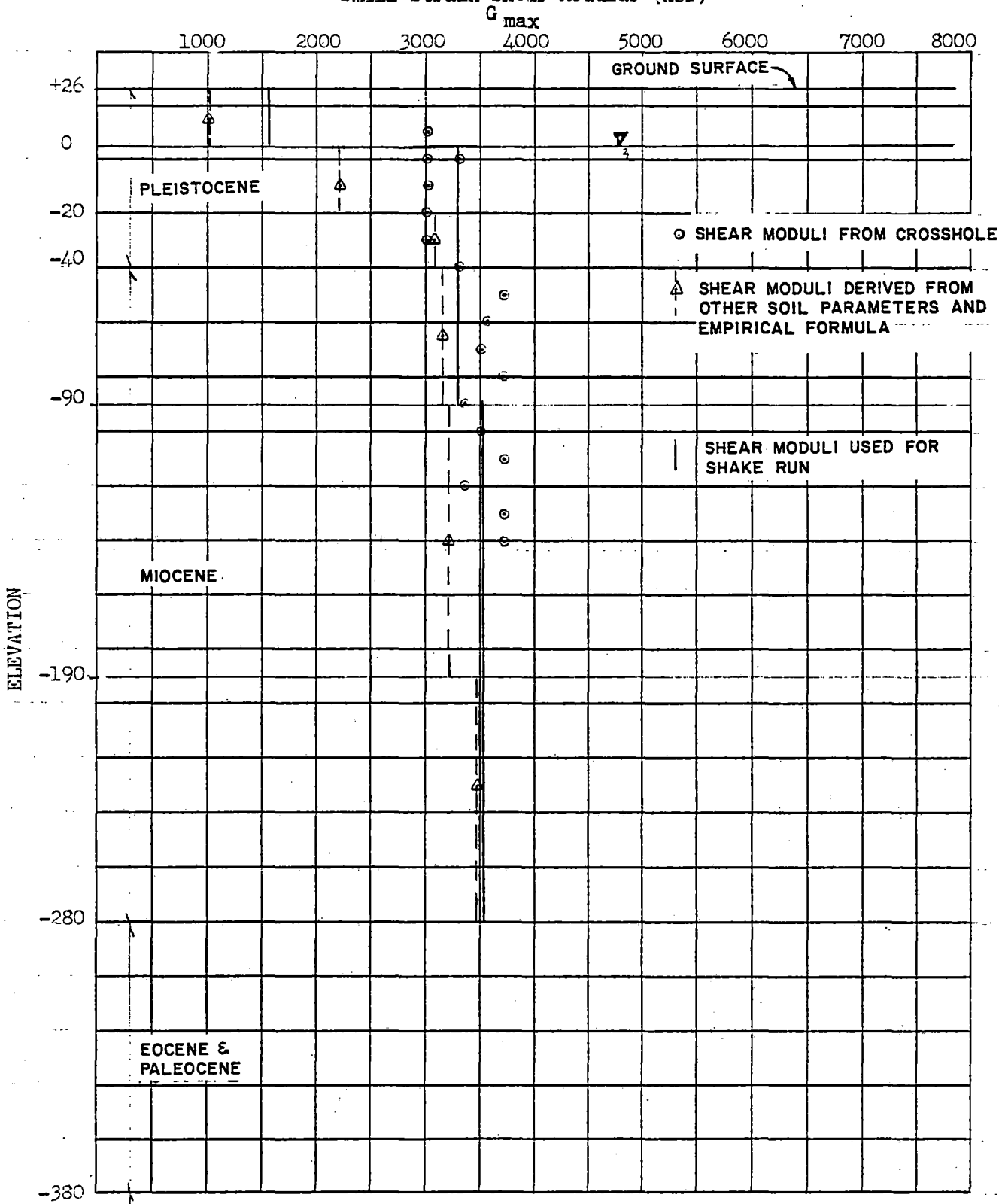


- DATA FROM UNIT 1&2 ENVIRONMENTAL STUDIES REPORT B-11, B-17, B-22.
- DATA FROM UNIT 1&2 ENVIRONMENTAL STUDIES REPORT B-7.
- DATA FROM SURRY 3 & 4 GEOTECHNICAL REPORT

FIGURE 2-10
TOTAL UNIT WEIGHT vs ELEVATION
FOR MIOCENE CLAYS
SURRY POWER STATION - UNIT 1 AND 2

FROM: SURRY 3 & 4 GEOTECHNICAL REPORT, FIG. 29

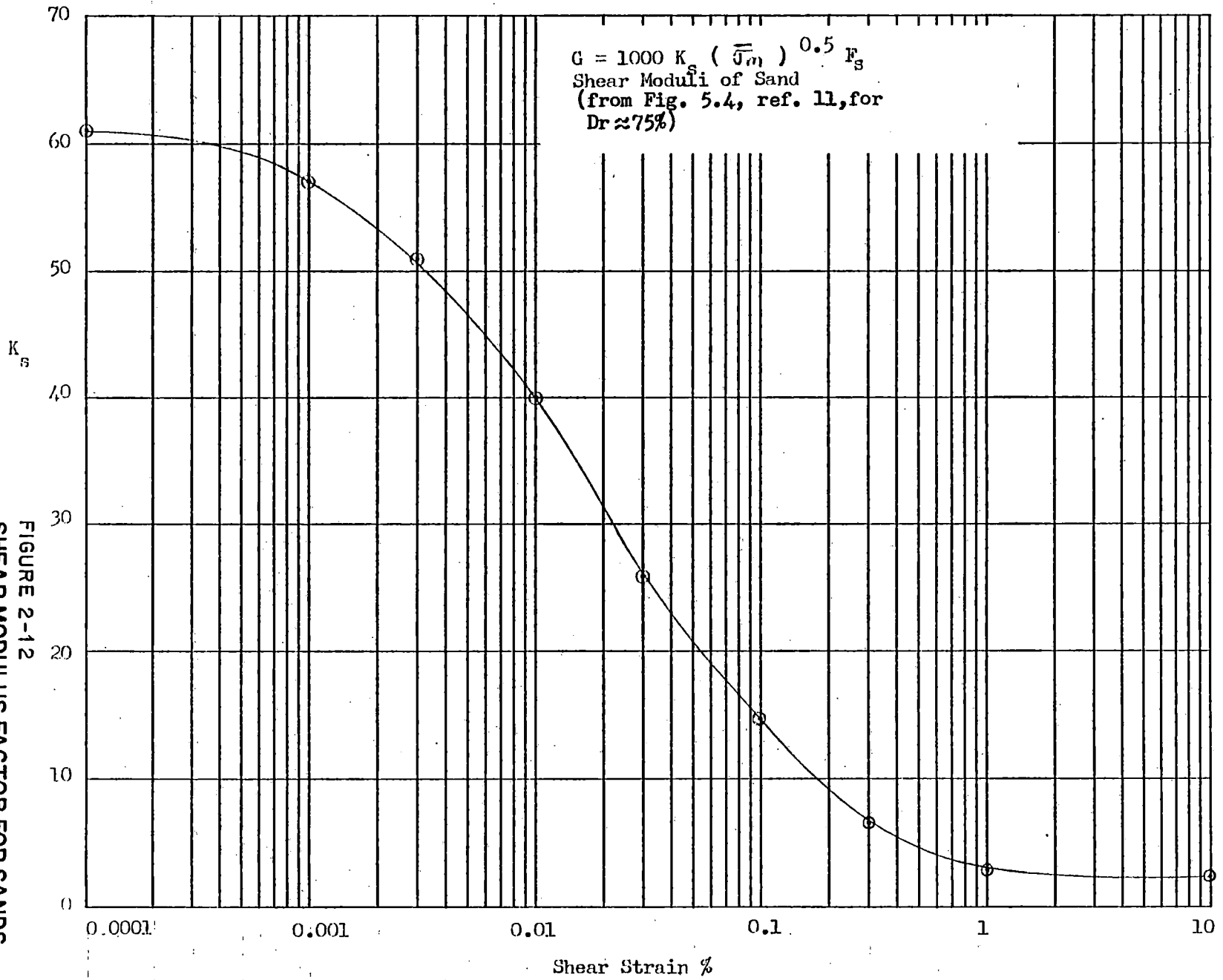
Small Strain Shear Modulus (ksf)



BASE LAYER; $V_s = 2000$ fps
 $G_s = 16770$ ksf

FIGURE 2-11
 SUMMARY OF G_{MAX} VS. ELEVATION
 SURRY POWER STATION-UNITS 1 AND 2

FIGURE 2-12
 SHEAR MODULUS FACTOR FOR SANDS
 SURRY POWER STATION-UNITS 1 AND 2



$G = K_c \cdot F_c$
 Shear Modulus of Clay
 (from Fig. 5.13, ref. 11, for
 $K_{c \text{ max}} = 2300$)

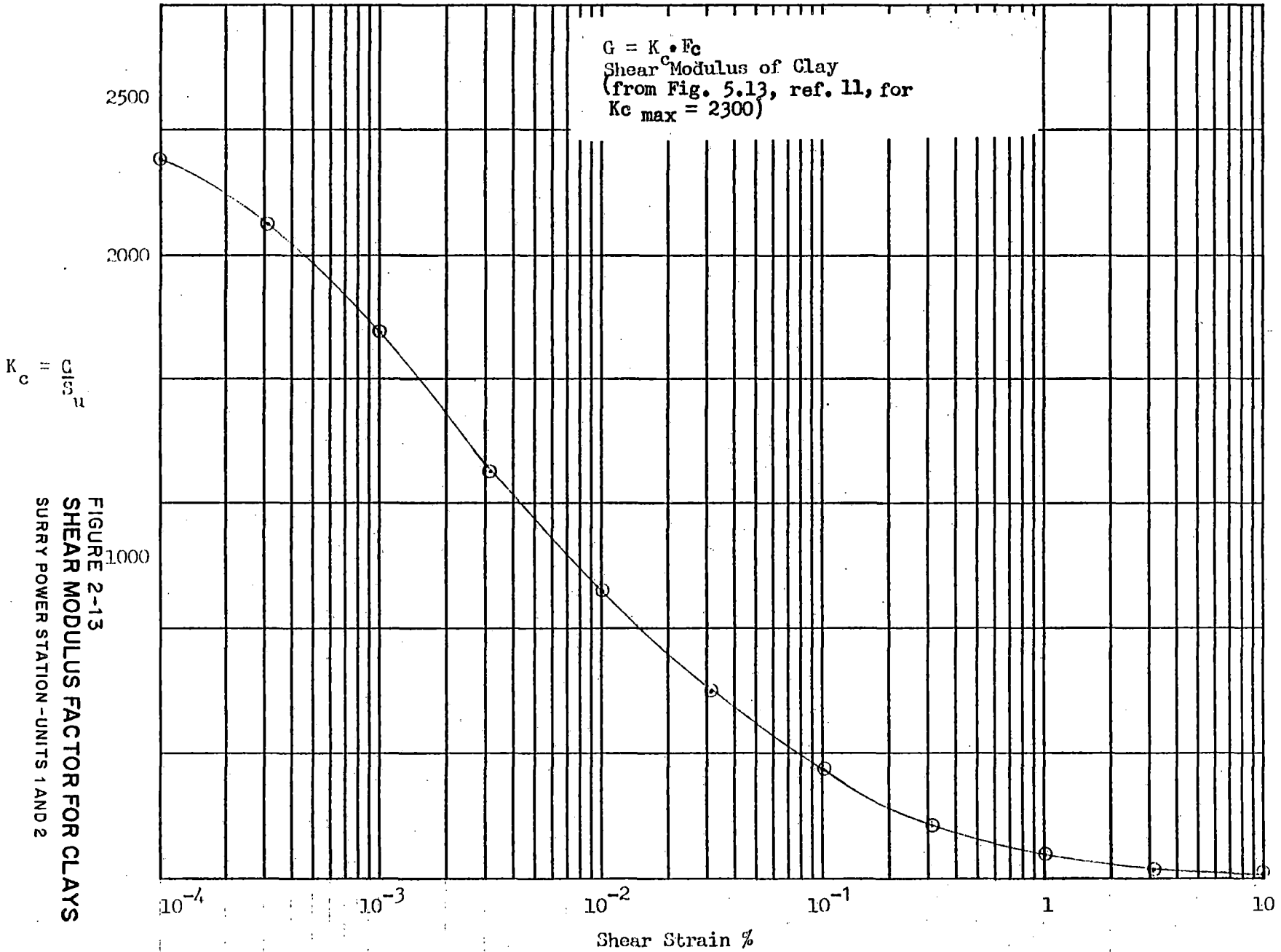


FIGURE 2-13
 SHEAR MODULUS FACTOR FOR CLAYS
 SURRY POWER STATION - UNITS 1 AND 2

Damping Ratio for Sand
(from Fig. 5.9, ref. 11)

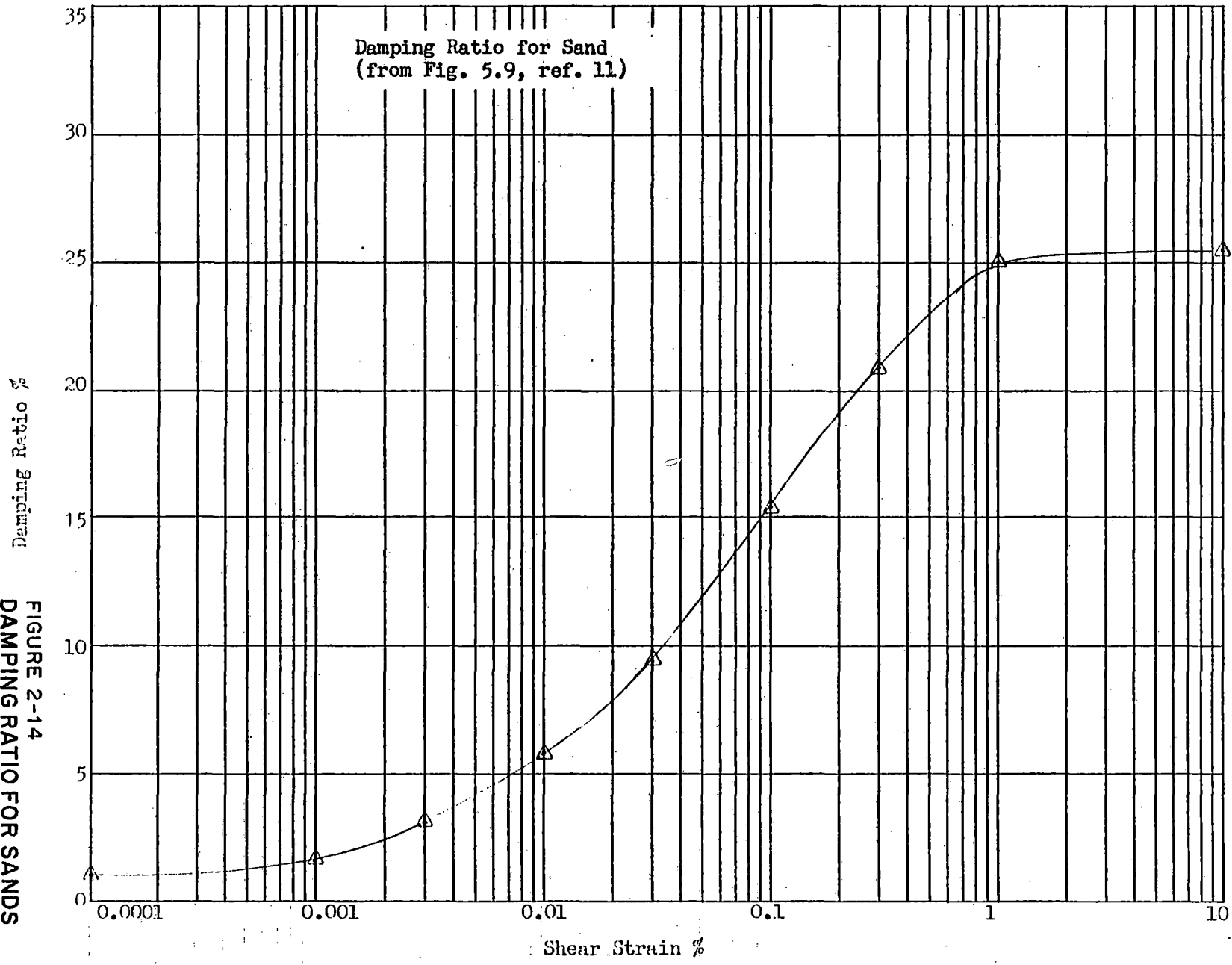
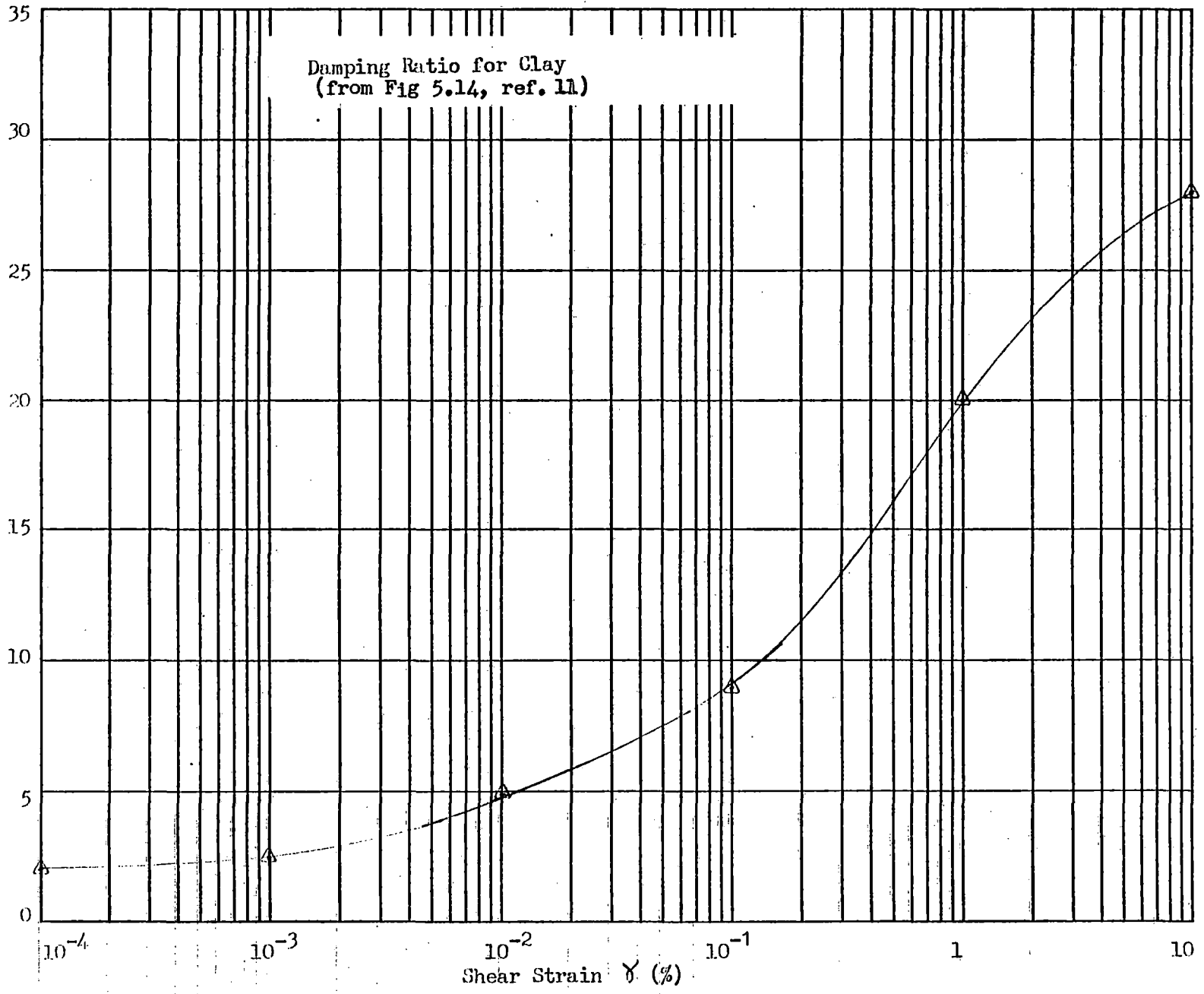
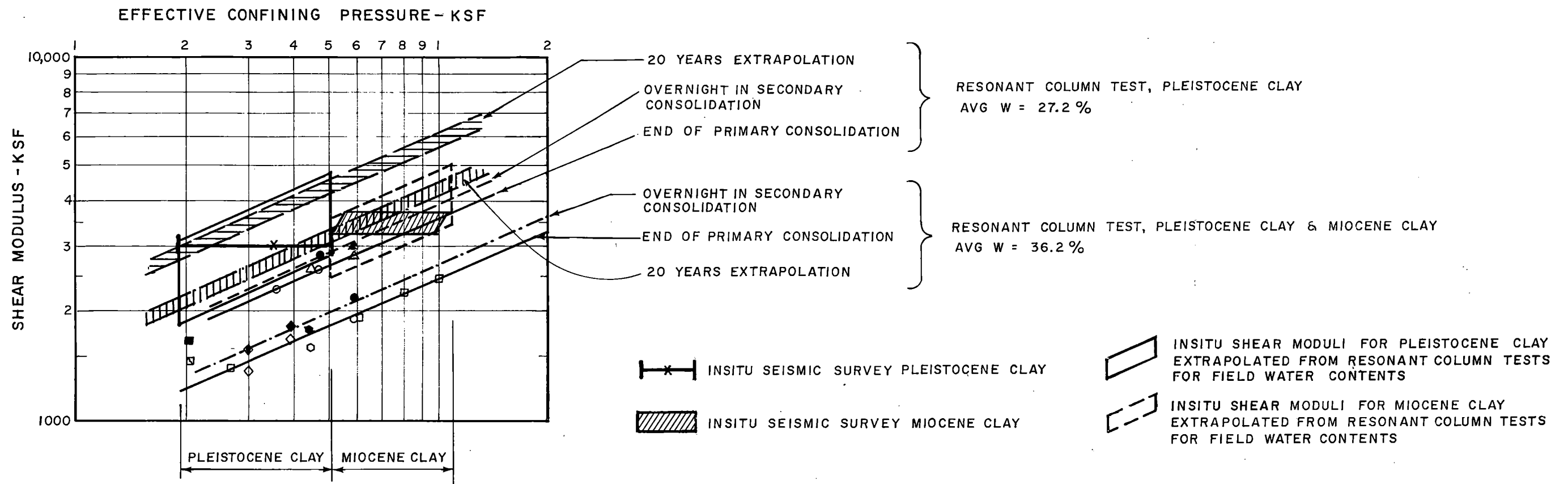


FIGURE 2-14
DAMPING RATIO FOR SANDS
SURRY POWER STATION - UNITS 1 AND 2

FIGURE 2-15
DAMPING RATIO FOR CLAYS
SURREY POWER STATION-UNITS 1 AND 2

Damping Ratio %





LEGEND:

SYMBOL	TEST I.D.	SAMPLE NO.	UNIT	WATER CONTENT (%)	CONSOLIDATION TIME
○	DYNAMIC TEST 1	BLOCK 2	PLEISTOCENE CLAY	29.2	END OF PRIMARY CONSOL. 2-3 HRS
●	"	"	"	29.2	OVERNIGHT IN SECONDARY CONSOL. ≈ 15 HRS
△	DYNAMIC TEST 2	BLOCK 2	PLEISTOCENE CLAY	25.6	END OF PRIMARY CONSOL. 2-3 HRS
▲	"	"	"	25.6	OVERNIGHT IN SECONDARY CONSOL. ≈ 15 HRS
□	DYNAMIC TEST 3	TUBE	MIOCENE CLAY	36.6	END OF PRIMARY CONSOL. 2-3 HRS
▣	"	"	"	"	END OF PRIMARY SWELL 2-3 HRS
■	"	"	"	"	OVERNIGHT IN SECONDARY SWELL ≈ 15 HRS
○	TEST NO. 1	BLOCK 1	PLEISTOCENE CLAY	35.8	END OF PRIMARY CONSOL. 2-3 HRS
●	"	"	"	"	OVERNIGHT IN SECONDARY CONSOL. ≈ 15 HRS
◇	TEST NO. 2	BLOCK 1	PLEISTOCENE CLAY	35.8	END OF PRIMARY CONSOL. 2-3 HRS
◆	"	"	"	"	OVERNIGHT IN SECONDARY CONSOL. ≈ 15 HRS

FIGURE 2-16
COMPARISON OF FIELD AND
LABORATORY MODULUS
DETERMINATIONS
SURRY POWER STATION UNITS 1 AND 2

SOURCE: From Hardin Test Data, Reference 4

SURRY POWER STATION, UNITS 1 AND 2

3.0 GROUND RESPONSE SPECTRA

The selection of seismic design parameters has been discussed in detail in Section 2.5 of the Surry 1 and 2 Final Safety Analysis Report (FSAR). This section of the report describes the smoothed ground response spectra.

3.1 DESIGN BASIS EARTHQUAKE (DBE) AND OPERATIONAL BASIS EARTHQUAKE (OBE)

For a safe and orderly shutdown of the station, a maximum horizontal ground acceleration of 0.15 g is used for the DBE. A horizontal ground acceleration of 0.07 g was established for the OBE. Vertical accelerations are taken as 2/3 the appropriate horizontal accelerations acting simultaneously and in phase to produce maximum loads or stresses.

3.2 GROUND RESPONSE SPECTRA

The ground response spectra used in design are shown in Figures 3-1 and 3-2 for the OBE and DBE, respectively. The spectra were constructed in accordance with the principles of the standard Housner spectra as follows:

For frequencies higher than about 2 cycles per second, the Housner spectra have been followed and normalized to a horizontal ground acceleration of 7 percent of gravity for the OBE and 15 percent of gravity for the DBE.

SURRY POWER STATION, UNITS 1 AND 2

In the frequency range between 0.3 and 2 cycles per second, Housner's average spectra have been normalized to a maximum ground velocity of about 4 inches per second for the OBE and 9 inches per second for the DBE.

For frequencies lower than about 0.3 cycle per second, the spectra were prepared using data suggested by Newmark and Hall in their paper.⁽²⁾

3.3 ARTIFICIAL TIME HISTORY

The artificial time history has a total duration of 15 seconds, with about 3.5 seconds each of rise and fall time, whose ground response spectrum is forced to fit the specified site spectrum. An artificial accelerogram which reproduces the frequency content displayed either in a response spectrum or in a power spectral density function is simulated statistically by using a stochastic model as described in Reference 3. In this model, the earthquake motion is considered to be a wide-band stationary process whose spectral density function, duration, and maximum acceleration are specified. The artificial motion is generated by matching the target or site spectrum for several specified percentages of critical damping at 100 oscillator periods distributed from 0.02 (50 Hz) to 6.666 (0.15 Hz) seconds. For a detailed treatment of the mathematical procedures, see References 4 and 5.

SURRY POWER STATION, UNITS 1 AND 2

The acceleration time history yields ground response spectra at damping values of 0.5, 2, and 5 percent that envelop the smoothed site design ground response spectra for those damping values (see Figure 3-3, for example).

3.4 GROUND RESPONSE SPECTRA AT BASE OF CONTAINMENT

At the request of the NRC, the ground response spectra at the level of the reactor containment mat in the free field were calculated and plotted using SHAKE. The artificial earthquake developed for the Surry site was normalized to the DBE maximum acceleration of .15 g and input at the ground surface of the free-field profile. The earthquake motion was deconvoluted to the base of the profile and the computed motion at El -40 ft, the containment founding grade, was used to calculate the real velocity and acceleration response spectra and the tripartite plot of real displacement, pseudovelocity, and pseudoacceleration vs frequency. These spectra are plotted for damping ratios of .5, 1.0, and 3.0 percent.

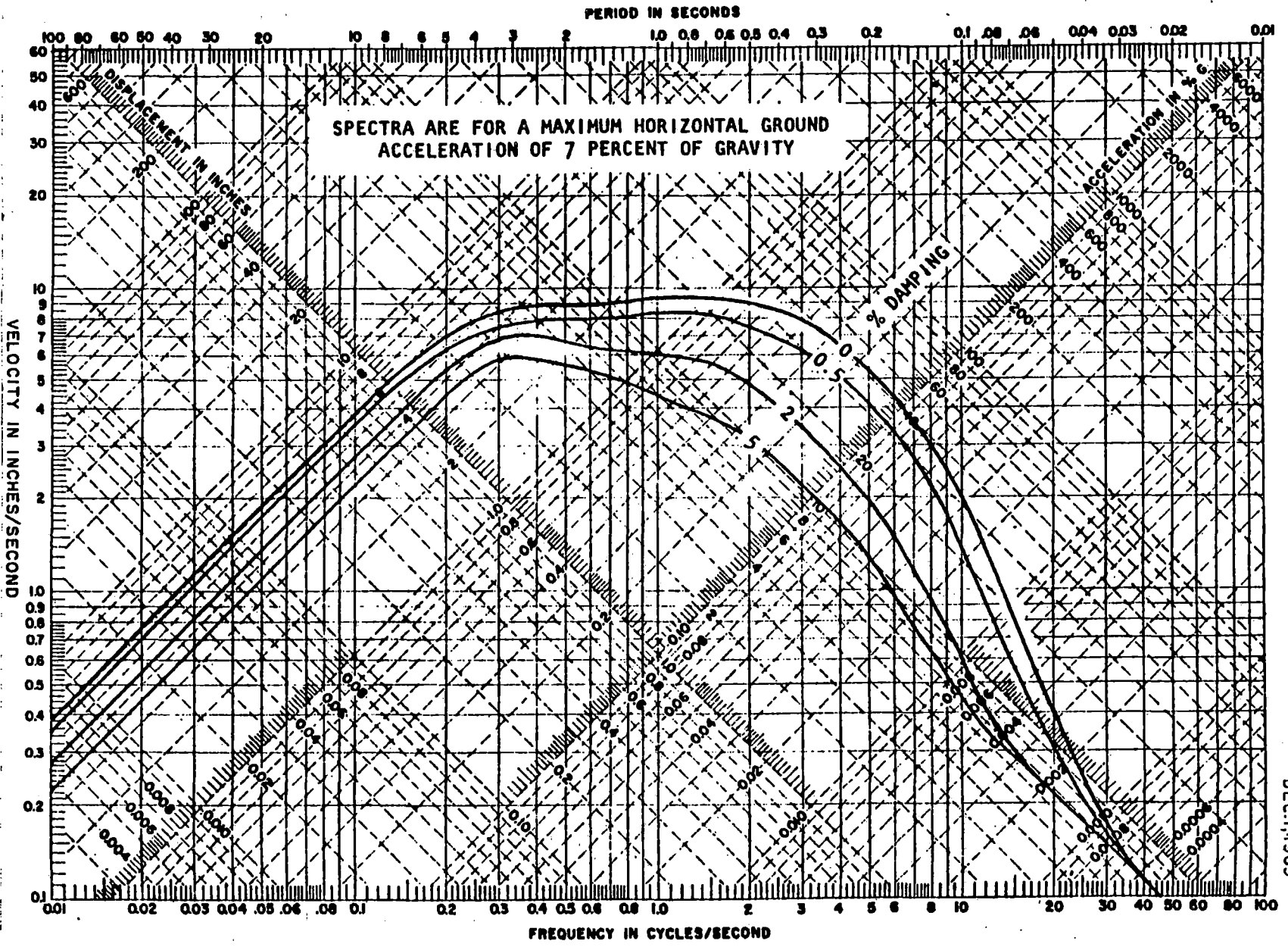
Response spectra were calculated for three soil profiles, represented by the G_{max} calculated from seismic cross-hole surveys and discussed in Section 2.4.1, G_{max} plus 50 percent, and G_{max} minus 50 percent. The spectra for each soil profile are plotted in Figures 3-4, 3-5, and 3-6, respectively. Also plotted in these figures is the envelope for .5 percent damping, as

SURRY POWER STATION, UNITS 1 AND 2

presented in Figure 2.5-5 of the Surry 1 and 2 FSAR, (1) and Figure 3-2 of this report.

3.5 REFERENCES

1. Virginia Electric & Power Company, Final Safety Analysis Report. Surry Power Station, Units 1 and 2, Part B, Volume 1, December 1969.
2. Newmark, N.O., and Hall, W.J., Seismic Design Criteria for Nuclear Reactor Facilities. May 25, 1967.
3. Hou, S.N., Earthquake Simulation Models and their Applications. Research Report R68-17, Department of Civil Engineering, MIT, 1968.
4. Rascon, O.A. and Cornell, C.A., Strong Motion Earthquake Simulation. Research Report R68-15, Department of Civil Engineering, MIT, 1968.
5. Tsai, N.C., Spectrum Compatible Motions for Design Purposes. Journal of Engineering Mechanics Division, ASCE, Vol 98, No. EM2, Rev. 4, Paper 8807, April 1972, p 345-356.



FROM: SURRY 1 AND 2 FSAR, FIGURE 2.5-4

FIGURE 3-1
 RESPONSE SPECTRA
 OPERATIONAL BASIS EARTHQUAKE
 SURRY POWER STATION-UNITS 1 AND 2

DEC 11, 1969

2.5-1

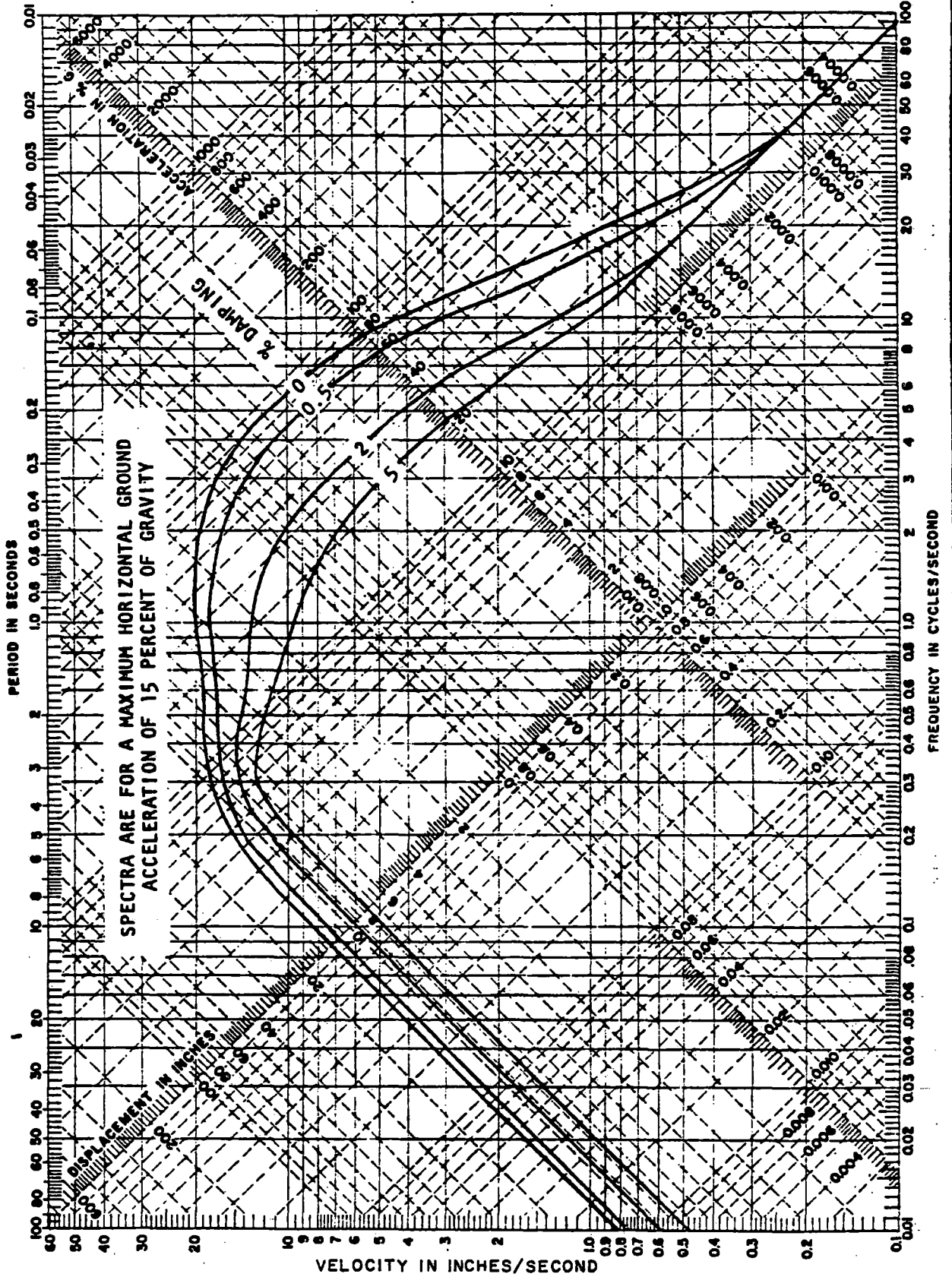
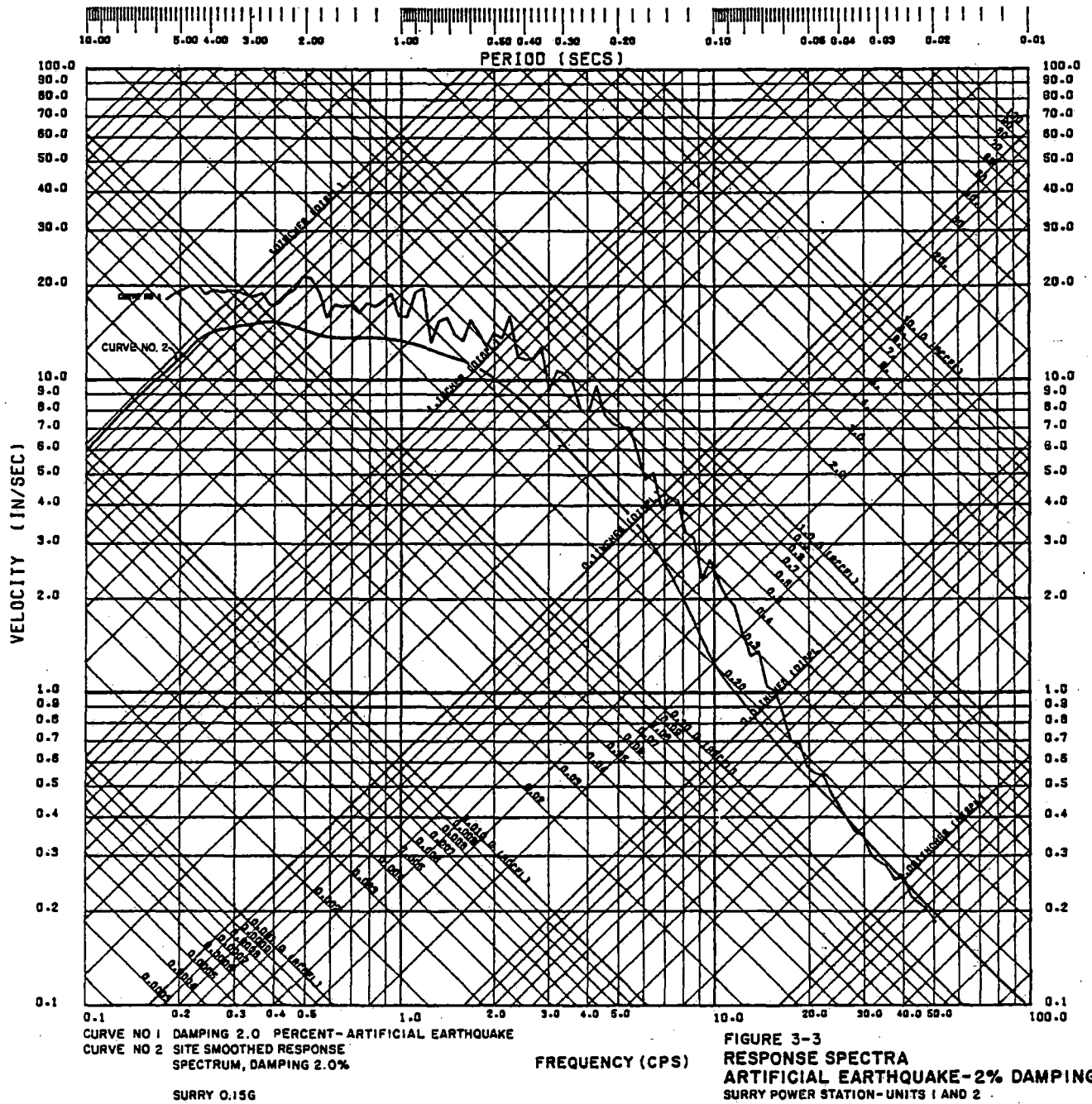
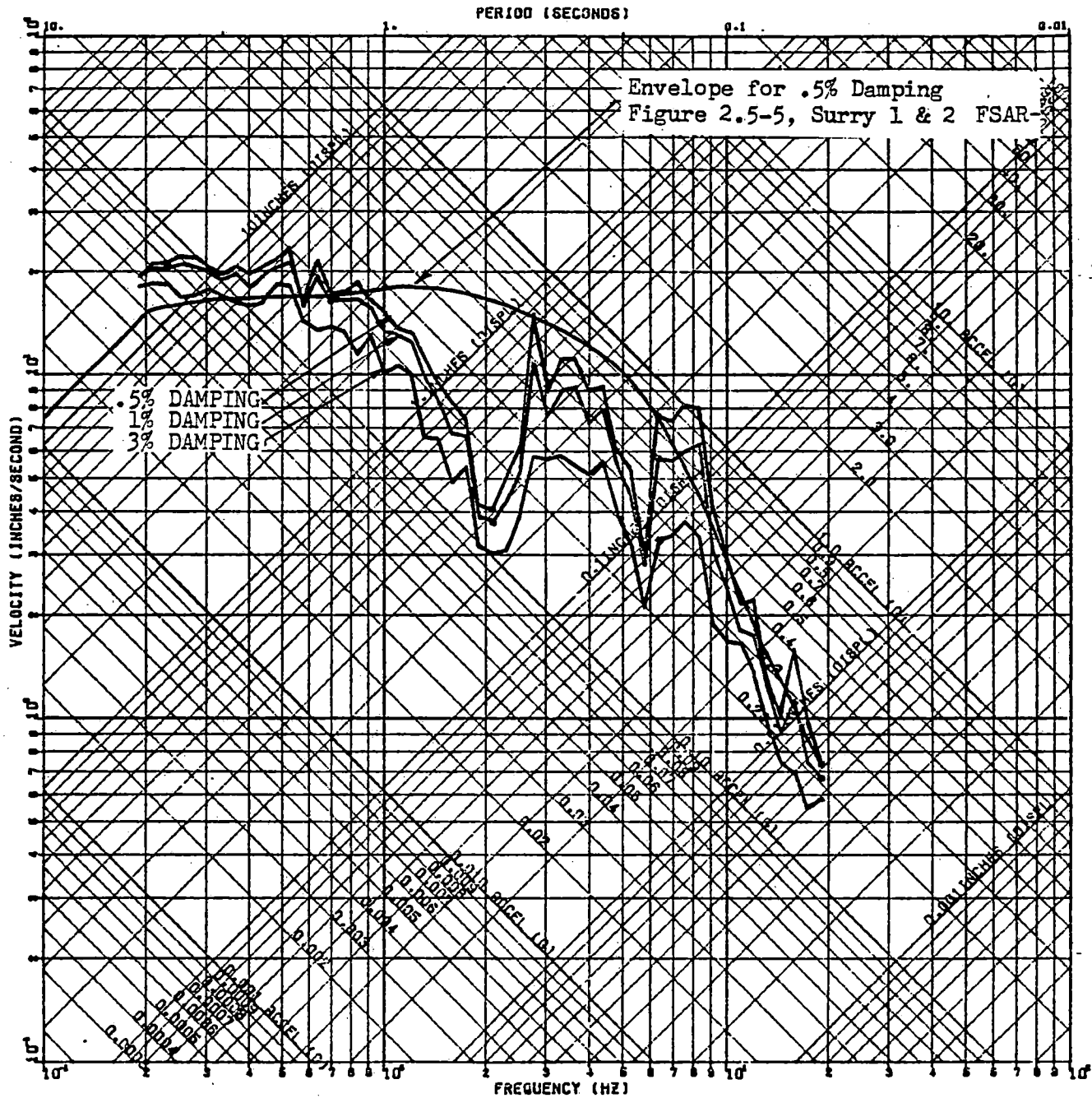


FIGURE 3-2
RESPONSE SPECTRA
DESIGN BASIS EARTHQUAKE
SURREY POWER STATION-UNITS 1 AND 2

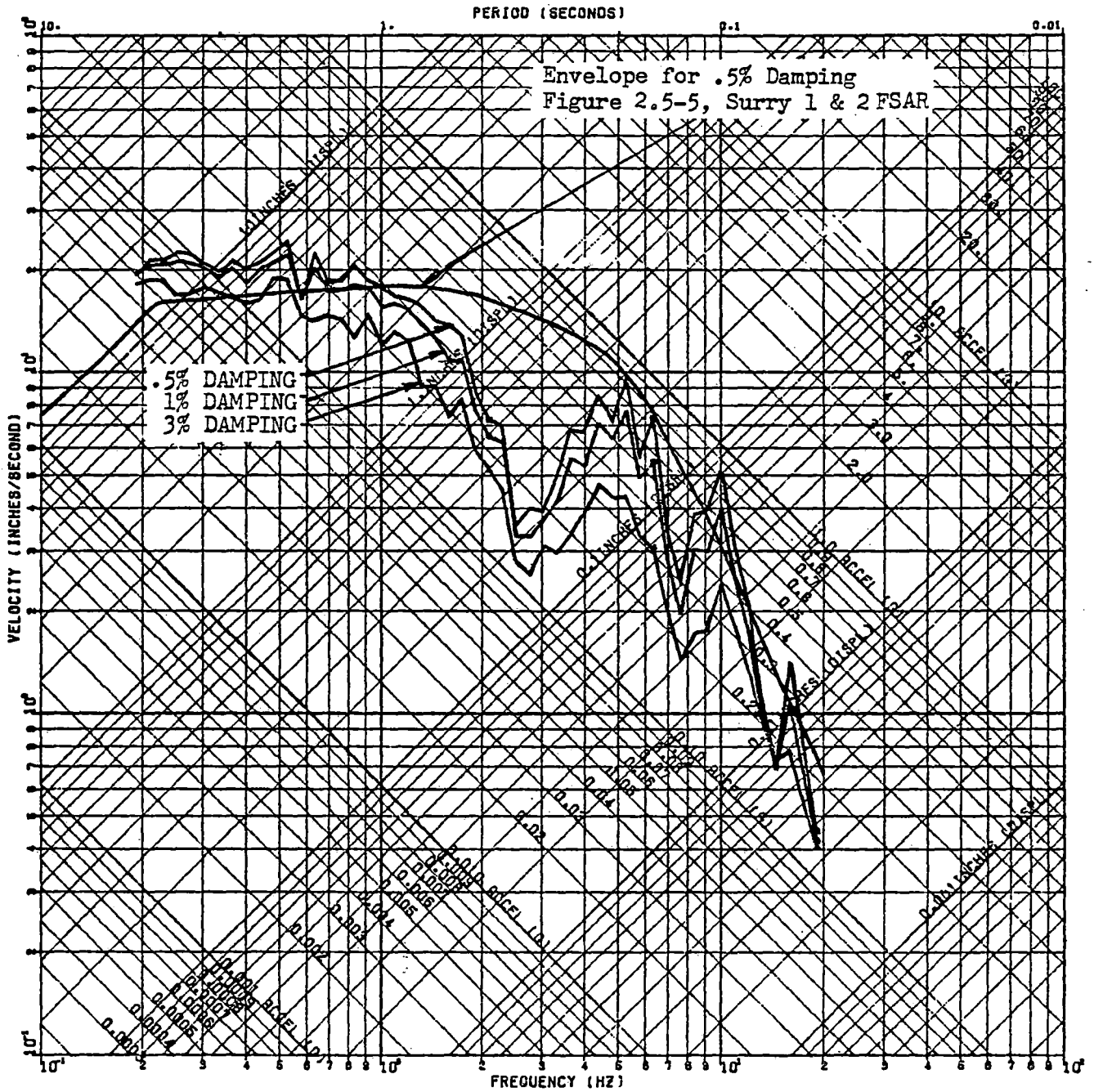
FROM: SURREY 1 AND 2 FSAR, FIGURE 2.5-5





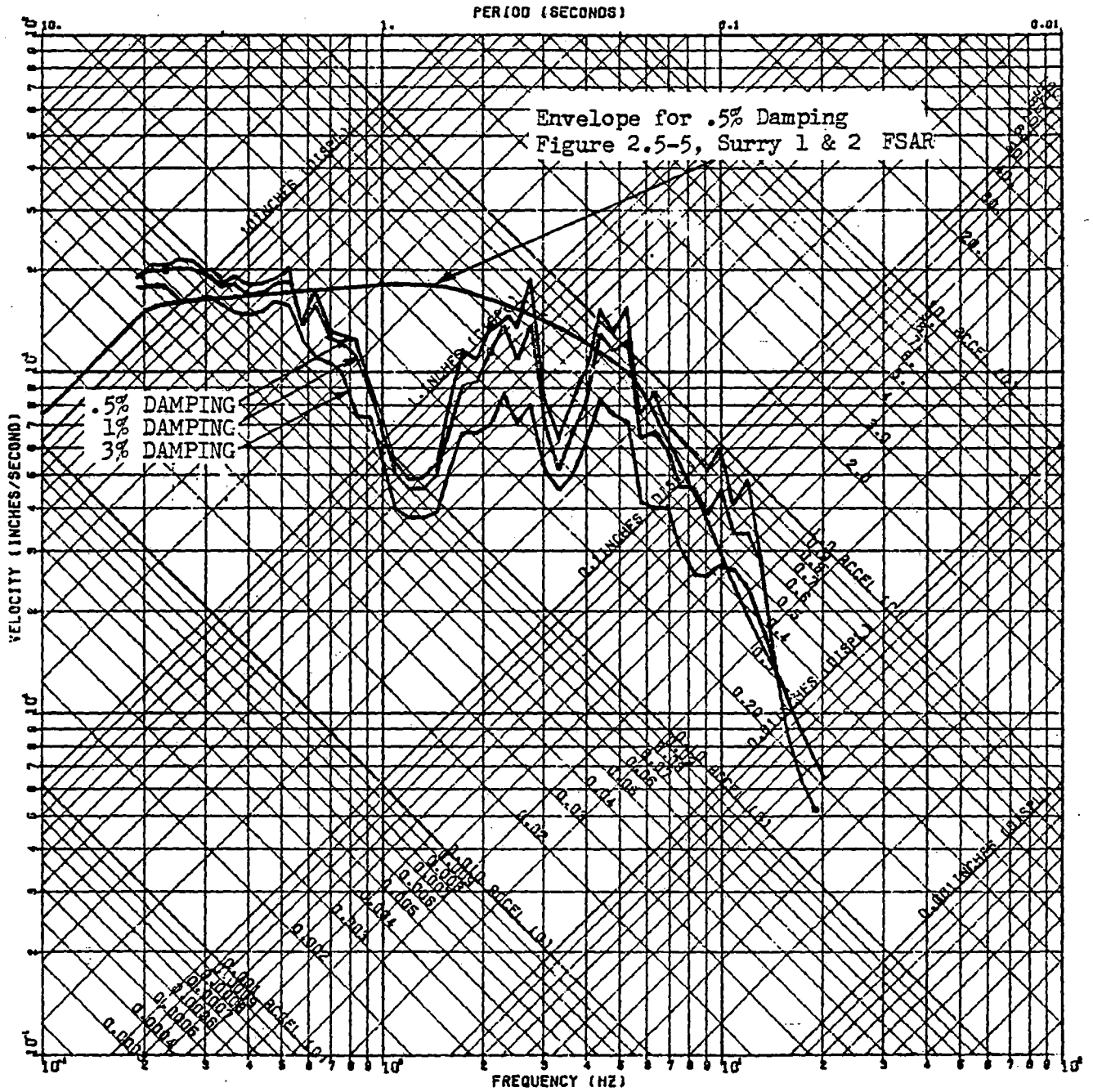
ART EQ(OBE)-FREE FIELD FREE FIELD DECONVOLUTE(MAX)
SPECTRA FOR TOP OF LAYER 4
DAMPING VALUES
 □ 0.005
 ○ 0.010
 ▲ 0.030

FIGURE 3-4
GROUND RESPONSE SPECTRA
G max
SURRY POWER STATION - UNITS 1 AND 2



ARTIFICIAL EG FREE FIELD FREE FIELD DECONVOLUTE(+50ZOMAX)
 SPECTRA FOR TOP OF LAYER 4
 DAMPING VALUES
 □ 0.005
 ○ 0.010
 ▲ 0.030

FIGURE 3-5
 GROUND RESPONSE SPECTRA
 Gmax +50%
 SURRY POWER STATION - UNITS 1 AND 2



ARTIFICIAL EQ. (DBE)-FREE FIELD

FREE FIELD DECONVOLUTE(-50%GMAX)
SPECTRA FOR TOP OF LAYER 4

DAMPING VALUES

□ 0.005

○ 0.010

▲ 0.030

FIGURE 3-6

GROUND RESPONSE SPECTRA

Gmax-50%

SURRY POWER STATION - UNITS 1 AND 2

4.0 AMPLIFIED RESPONSE ANALYSIS

Soil-structure interaction analysis can be performed using a direct finite element solution in which the dynamic model is composed of detailed representations of both the structure and the supporting medium. In a direct interaction analysis, the effects of embedment upon stiffness and control motion are automatically included. Although such a procedure may appear to be efficient, analyses become more difficult to manage when large, complex structures are founded upon greatly stratified media. Also, this procedure does not produce any intermediate results, which are often useful in making engineering assessments.

Many different procedures may be used to reduce such an analysis to more manageable steps. For example, a detailed finite element soil model can be used to compute frequency-dependent stiffnesses that are then used in a second step for seismic analysis of a detailed structural model. For embedded structures, however, some method that redefines the control motion must be included. An earthquake with a specified amplitude and frequency content at the site surface is not necessarily a reasonable input to the detailed model in the second step.

A multiple-step analysis need not rely upon finite element representations of soil. The three-step solution described below is based upon the theory of

elasticity, and includes a solution for the problem of definition of the control motion in the case of embedded structures.

4.1 DESCRIPTION OF THE THREE-STEP ANALYSIS

The solution of soil-structure interaction problems can be reduced to the following three steps:

1. calculations of frequency-dependent soil stiffnesses
2. modification of the specified surface motion to account for structure embedment
3. interaction analysis

These steps are illustrated in Figure 4-1 (see Reference 2).

4.1.1 Frequency-Dependent Soil Stiffness

The frequency-dependent stiffnesses of a rectangular footing founded at the surface of a layered medium are computed with the program REFUND, discussed in Section 9.3. The program solves the problem of forced vibration of a rigid plate on a viscoelastic, layered stratum using numerical solutions to the

generalized problems of Cerrutti and Boussinesq (see Figure 4-2). The effects of unit horizontal and vertical point loads are combined by superposition to produce the behavior of a rectangular plate.

Solutions to the problem of a point load on the surface of continuum require an assumption about the behavior of the medium directly under the load; for example, see Timoshenko and Goodier.⁽¹⁾ In REFUND, a solution directly under the load is achieved by employing a column of elements for which a linear displacement function is assumed. Away from this central column, in the "far-field," the solution for a viscoelastic layered medium is obtained (see Figure 4-3).

If the central column under the point load is removed and replaced by equivalent distributed forces corresponding to the internal stresses, the dynamic equilibrium of the far field is preserved. Since no other prescribed forces act on the far field, the displacements at the boundary (and any other point in the far field) are uniquely defined in terms of these boundary forces. The problem is thus to find the relations between these boundary forces and the corresponding boundary displacements.

It is always possible to express the displacements in the far field in terms of eigenfunctions corresponding to the natural modes of wave propagation in the stratum, each having a characteristic wave number k . In an unbounded

SURRY POWER STATION, UNITS 1 AND 2

medium, any value of the wave number k , and hence any wavelength, is admissible; for a layered stratum, however, only a numerable set of values of k (each one with a corresponding propagation mode) satisfies the boundary conditions. There are thus, at a given frequency, an infinite but numerable set of propagation modes and wave numbers k that can be found by solving a transcendental eigenvalue problem. For each eigenfunction the distribution of stresses can be determined up to a multiplicative constant, the participation factor of the mode. By combining these modal stresses to match any given distribution of stresses at the boundary, the participation factors and the corresponding dynamic stiffness function relating boundary stresses to boundary displacements can be determined. . .

In REFUND's cylindrical coordinates, loads and displacements are expanded in Fourier series around the axis:

$$\begin{aligned} u_r &= \sum_0^{\infty} u_r^n \cos n\theta & p_r &= \sum_0^{\infty} p_r^n \cos n\theta \\ u_y &= \sum_0^{\infty} u_y^n \cos n\theta & p_y &= \sum_0^{\infty} p_y^n \cos n\theta \\ u_\theta &= \sum_0^{\infty} -u_\theta^n \sin n\theta & p_\theta &= \sum_0^{\infty} -p_\theta^n \sin n\theta \end{aligned}$$

For the problem at hand, only the first two components of the series are needed. The (unit) vertical force case corresponds to the Fourier component of order zero ($n=0$), and the horizontal unit force case corresponds to the

SURRY POWER STATION, UNITS 1 AND 2

Fourier component of order one ($n=1$). The cartesian displacement (flexibility) matrix at a point then follows from the cylindrical displacement components:

$$\left\{ \begin{array}{c|c|c} \frac{1}{2}(u_r^1 + u_\theta^1) + \frac{1}{2}(u_r^1 - u_\theta^1) \cos 2\theta & u_r^0 \cos \theta & \frac{1}{2}(u_r^1 - u_\theta^1) \sin 2\theta \\ \hline u_y^1 \cos \theta & u_y^0 & u_y^1 \sin \theta \\ \hline \frac{1}{2}(u_r^1 - u_\theta^1) \sin 2\theta & u_r^0 \sin \theta & \frac{1}{2}(u_r^1 + u_\theta^1) - \frac{1}{2}(u_r^1 - u_\theta^1) \cos 2\theta \end{array} \right\}$$

and the displacement vector for arbitrary loading is

$$U = FP$$

where

$$U = \begin{Bmatrix} u_x \\ u_y \\ u_z \end{Bmatrix} \quad P = \begin{Bmatrix} p_x \\ p_y \\ p_z \end{Bmatrix}$$

U is the displacement vector at a point $(x,0,z)$ while P is the load vector at $(0,0,0)$. The coordinate system is illustrated in Figure 4-4.

For points along the free surface, the reciprocity theorem requires that $U_r^0 = U_y^1$. Hence, F is chessboard symmetric/antisymmetric. REFUND then

SURRY POWER STATION, UNITS 1 AND 2

computes the cylindrical displacement components for the two loading cases, and determines the cartesian flexibility matrix F under the load (axis), at the boundary, and at selected points beyond the boundary.

To compute the subgrade stiffness functions for a rigid, rectangular plate, the program discretizes the foundation into a number of points and computes the global flexibility matrix F from the nodal submatrices F using the technique just described. Imposing then the conditions of unit rigid body displacements and rotations, it is possible to solve for the global load vector from the equation

$$FP = U$$

where U is the global displacement vector satisfying the rigid body condition.

It follows that U is of the form

$$U = TV$$

where V is a (6x1) vector containing the rigid body translations or rotations of the plate and T is linear transformation matrix assembled with the

coordinates of the nodal points. The stiffness functions are then obtained from

$$Z = T^T P$$

which corresponds formally to

$$Z = T^T F^{-1} T V$$

A comparison of REFUND results with another method is shown in Section 9.3.

4.1.2 Embedment Correction

The effects of foundation embedment on the impedances are included by employing correction factors described by Kausel et al.⁽²⁾ These correction factors are determined from parametric studies of embedded foundations and are of the form

$$C_R = (1 + C_1 \frac{R}{H})(1 + C_2 \frac{E}{R})(1 + C_3 \frac{E}{H})$$

in which

SURRY POWER STATION, UNITS 1 AND 2

C_R = correction factor

R = foundation radius

E = embedment depth

H = depth to bedrock

C_i = constants, different values for each degree of freedom.

The frequency dependent stiffnesses, K , determined by REFUND are modified to become

$$K^1 = K \times C_R$$

4.1.3 Kinematic Interaction

In the second step of the analysis shown in Figure 4-1, "kinematic interaction" modifies the purely translational input specified at the surface of the stratum to both a translational and rotational motion at the base of the rigid, massless foundation. The existence of the additional input can be inferred from Figure 4-5. In a stratum undergoing translational motion only,

SURRY POWER STATION, UNITS 1 AND 2

the boundary conditions at the "excavation" require the foundation to rotate. Ignoring the rotational component would result in an unconservative solution.

Note that the modified motion at the base of the foundation is not equivalent to a deconvolution. The specified surface motion is modified so that

$$\ddot{y}_1(t) = \text{IFT} \begin{cases} F(\Omega) \left[\cos\left(\frac{\pi f}{2f_n}\right) \right], f \leq 0.7f_n \\ F(\Omega) [0.453], f > 0.7f_n \end{cases}$$

and

$$\ddot{\phi}_1(t) = \text{IFT} \begin{cases} F(\Omega) \left[0.257 \left(1 - \cos \frac{\pi f}{2f_n}\right) / R \right], f \leq f_n \\ F(\Omega) [0.257/R], f > f_n \end{cases}$$

$F(\Omega)$ = Fourier Transform of surface motion

IFT = inverse transform

R = foundation radius

f_n = fundamental shear beam frequency of the column of soil between the embedment level and the free surface

These relationships are taken from Kausel et al. (2)

A finite element analysis of a rigid, massless, embedded foundation provides a demonstration that the relations above are reasonable and conservative. Such a comparison is shown in Section 9.4.

4.1.4 Interaction Analysis

The third step of the procedure illustrated schematically in Figure 4-1 is the analysis of the structural model supported on the frequency-dependent springs from Step 1 for the modified seismic input from Step 2. The solution is achieved using the program FRIDAY.

FRIDAY evaluates the dynamic response of an assembly of cantilever structures supported by a common mat and subjected to a seismic excitation. The support of the mat can be rigid, or it can consist of frequency-dependent/independent springs and dashpots (subgrade stiffnesses). The equations of motion are solved in the frequency domain, determining response time histories by convolution of the transfer functions and the Fourier transform of the input excitation. The dynamic equilibrium equations can be written in matrix notation as:

$$M\ddot{U} + C\dot{Y} + KY = 0 \quad (1)$$

SURRY POWER STATION, UNITS 1 AND 2

where M , C , K are the mass, damping and stiffness matrices, respectively, and U , Y are the absolute and relative (to the moving support) displacement vectors.

These two vectors are related by:

$$U = Y + EU_g$$

(2)

where U_g is the base excitation vector (3 translations and 3 rotations), and E is the matrix:

$$E = \left\{ \begin{array}{cc} I & T_1 \\ O & I \\ I & T_2 \\ O & I \\ & \vdots \\ I & T_n \\ O & I \end{array} \right\}$$

(3)

SURRY POWER STATION, UNITS 1 AND 2

where I is the (3x3) identity matrix, O is the null matrix, and

$$T_i = \left\{ \begin{array}{c|c|c} O & Z_i - Z_0 & -(Y_i - Y_0) \\ \hline -(Z_i - Z_0) & O & X_i - X_0 \\ \hline Y_i - Y_0 & -(X_i - X_0) & O \end{array} \right\}$$

with x_i, y_i, z_i being the coordinates of the corresponding mass point; x_0, y_0, z_0 are the coordinates of the common support.

In the frequency response method, the transfer functions are determined by setting, one at a time, the ground motion components equal to a unit harmonic of the form $u_i = e^{i\omega t}$. It follows then that U, Y are also harmonic:

$$\begin{aligned} \ddot{U} &= H_j e^{i\omega t} & \ddot{Y} &= (H_j - E_j) e^{i\omega t} \\ \dot{U} &= \frac{1}{i\omega} H_j e^{i\omega t} & \dot{Y} &= \frac{1}{i\omega} (H_j - E_j) e^{i\omega t} \\ U &= -\frac{1}{\omega^2} H_j e^{i\omega t} & Y &= -\frac{1}{\omega^2} (H_j - E_j) e^{i\omega t} \end{aligned} \tag{4}$$

where $H_j = H_j(\omega)$ is the vector containing the transfer functions for the j^{th} input ground motion, and E_j is the j^{th} column of E in Eq. 3. Substitution of Eq 4 into Eq 1 yields

$$(-\omega^2 M + i\omega C + K)H_j = (i\omega C + K)E_j \quad (5)$$

If the damping matrix is of the form $C = \frac{1}{\omega} D$, which corresponds to a linear hysteretic damping situation, the equation reduces to

$$(-\omega^2 M + K + iD)H_j = (K + iD)E_j \quad (6)$$

In view of the correspondence principle, it is possible to generalize the equation of motion allowing at this stage elements in the stiffness matrix K with an arbitrary variation with frequency. This enables the use of frequency-dependent stiffness functions or impedance (inverse of flexibility functions or compliances).

Defining the dynamic stiffness matrix:

$$K_d = K + iD - \omega^2 M \quad (7)$$

The solution for the transfer functions follows formally from:

$$\begin{aligned}
 H_j &= -K_d^{-1} (K + iD) E_j \\
 &= -(I + \omega^2 K_d^{-1} M) E_j
 \end{aligned}
 \tag{8}$$

Note that the dynamic stiffness matrix K_d does not depend on the loading condition E_i . Also, for $\omega = 0$, $H_i(0) = E_i$.

Having found the transfer functions, the acceleration time-histories follow then from the inverse Fourier transformation:

$$\ddot{U} = \frac{1}{2\pi} \int_{-\infty}^{\infty} \left\{ \sum_{j=1}^{j=6} H_j f_j \right\} e^{i\omega t} d\omega
 \tag{9}$$

where, $f_j = f_j(\omega)$ is the Fourier transform of the j^{th} input acceleration component:

$$f_j = \int_0^T \ddot{u}_j e^{-i\omega t} dt
 \tag{10}$$

SURRY POWER STATION, UNITS 1 AND 2

The procedure consists then of determining the dynamic stiffness matrix K_d , solving Eq 6 for the six loading conditions $H = \{H_i\}$, determining the six Fourier transforms of the input components $F = \{f_i\}$, and performing the inverse transformation (Eq 9), which corresponds formally to:

$$\ddot{U} = \frac{1}{2\pi} \int_{-\infty}^{\infty} HF e^{i\omega t} d\omega$$

The dynamic equations are solved in FRIDAY by Gaussian elimination, and the Fourier transforms are computed by subroutines using the Cooley-Tuckey FFT (fast Fourier transform) algorithm. A comparison of the results of FRIDAY with another solution is shown in Section 9.5.

4.2 STRUCTURAL MODELING

The level of detail in mathematical models of structures is determined by consideration of the following:

1. distribution of mass in the building
2. symmetry/asymmetry of building arrangement
3. locations at which output is required
4. approximate frequency content of input

SURRY POWER STATION, UNITS 1 AND 2

The models used in the analysis, typically, are generalized, three-dimensional, multi-mass representations. The total number of degrees of freedom included is more than sufficient to encompass all significant frequencies; the number of masses being governed, as a practical matter, by the locations at which amplified response spectra (ARS) are required.

Eccentricity between the center of mass and center of stiffness at every level is included, except where insignificant. As a result, the effects of torsion upon the modes and frequencies is automatically determined. A typical model is shown in Figure 4-6. The generalized dynamic members connecting the centers of mass have stiffness matrices determined by tensor transformation from the matrices of the structural elements connecting the centers of stiffness.

To demonstrate the effects of torsion on the results, a comparison was made between the results of analyses using a generalized three-dimensional model and a planar model of the containment. As expected, the amplified response spectra are not sensitive to the details of structural modeling for this site. The results for the generalized three-dimensional model are virtually identical to those obtained for the planar model.

SURRY POWER STATION, UNITS 1 AND 2

4.4 RESULTS

Output from the third step FRIDAY includes structural response as well as ARS for all coordinates in each structure analyzed. In general, a structural coordinate coincides with a building floor level. Typical structural displacement and acceleration profiles are shown in Figures 4-6 and 4-7. ARS are generated for two orthogonal horizontal and the vertical directions at each structural coordinate for both OBE and DBE earthquakes. Typical ARS are shown in Section 5. For use in pipe stress problems, ARS peaks are automatically broadened ± 15 percent to account for variations in soil and structural material properties.

Comparisons of ARS generated by the three-step REFUND/FRIDAY method and the finite element PLAXLY method as well as those based on the FSAR earthquake and the Regulatory Guide 1.60 earthquakes were made at the request of the NRC. The ARS generated for these comparisons used strain compatible soil parameters from the last iteration of the SHAKE program.

Comparisons were also made of ARS generated from the REFUND/FRIDAY programs for a variety of soil parameters as requested by the NRC.

All ARS comparisons are described in Section 5.

SURRY POWER STATION, UNITS 1 AND 2

4.4 REFERENCES

1. Timoshenko & Goodier, Theory of Elasticity, 3rd Edition. McGraw-Hill Book Co., p 97-109.
2. Kausel, Whitman, Morray, & Elsabee, The Spring Method for Embedded Foundations. Nuclear Engineering and Design 48(1978): 377-392.

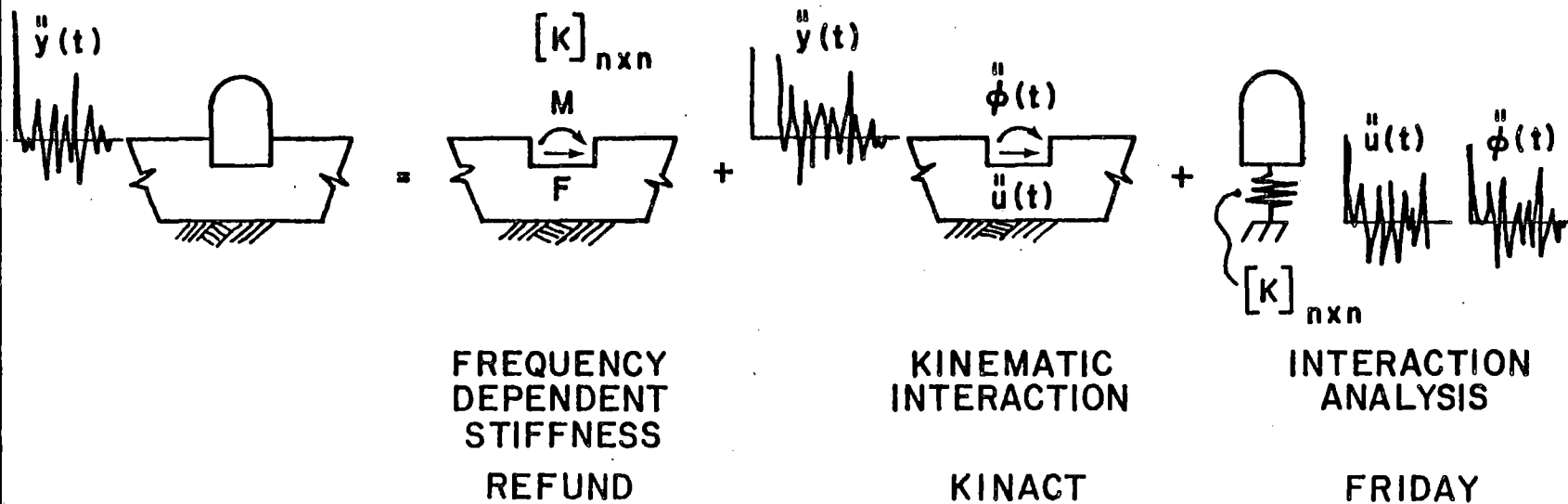
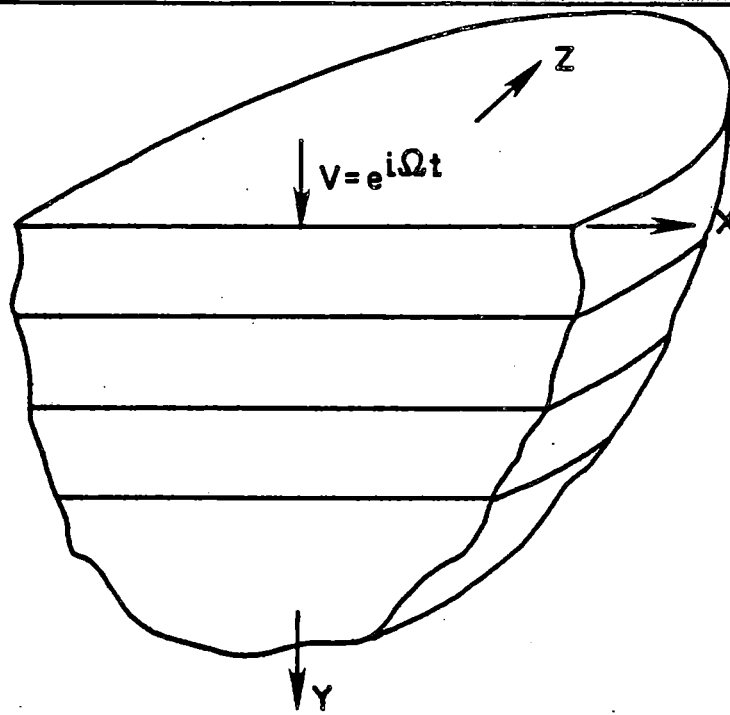
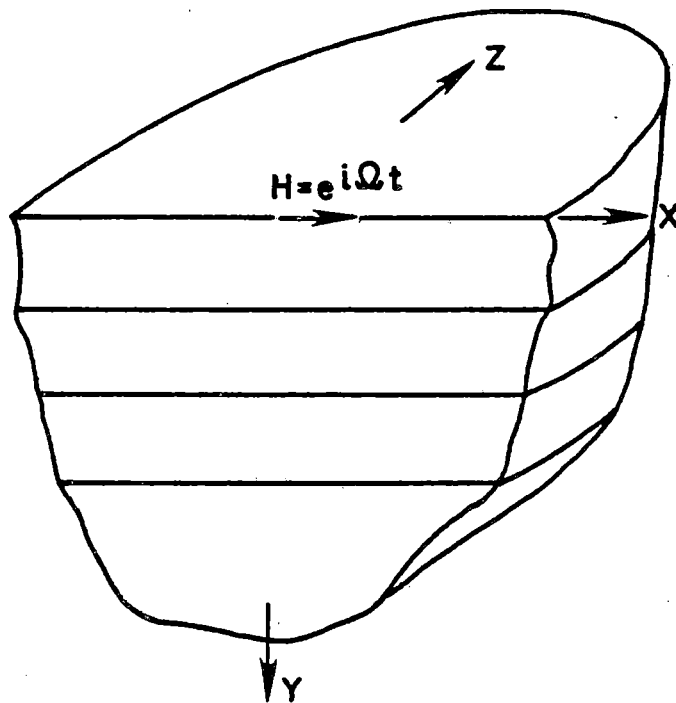


FIGURE 4-1

THE THREE STEP SOLUTION
 SURRY POWER STATION - UNITS 1 AND 2



BOUSSINESQ



CERRUTI

FIGURE 4-2
THE BOUSSINESQ AND CERRUTI PROBLEMS
SURRY POWER STATION - UNITS 1 AND 2

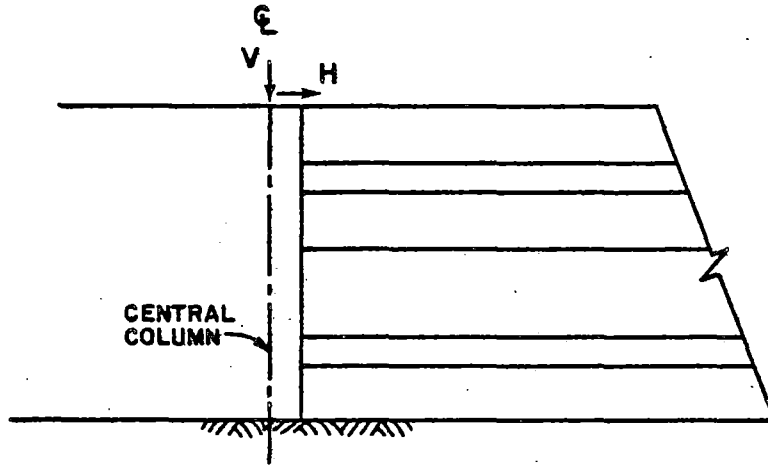


FIGURE 4-3
 IDEALIZATION OF THE BASIC 'REFUND'
 SOLUTION FOR CONCENTRATED LOADS
 SURRY POWER STATION-UNITS 1 AND 2

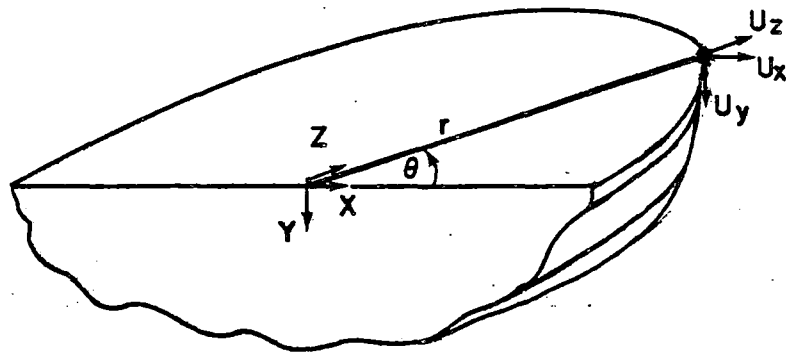
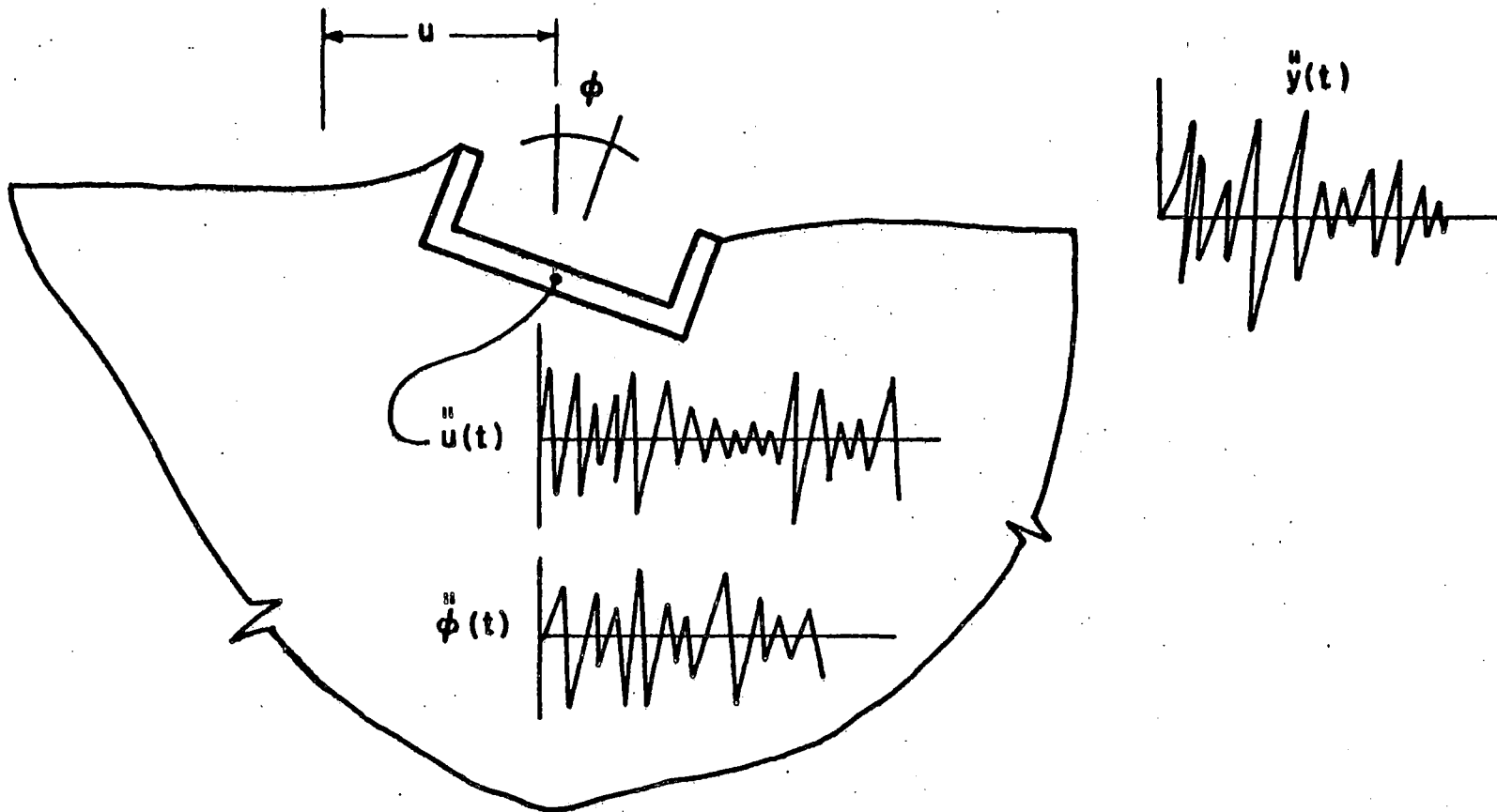


FIGURE 4-4
 'REFUND' COORDINATE SYSTEM
 SURRY POWER STATION-UNITS 1 AND 2



$\ddot{u}(t)$ = TRANSLATIONAL ACCELERATION AT
BASE OF RIGID, MASSLESS FOUNDATION

$\ddot{\phi}(t)$ = ROTATIONAL ACCELERATION

FIGURE 4-5
KINEMATIC INTERACTION
SURREY POWER STATION - UNITS 1 AND 2

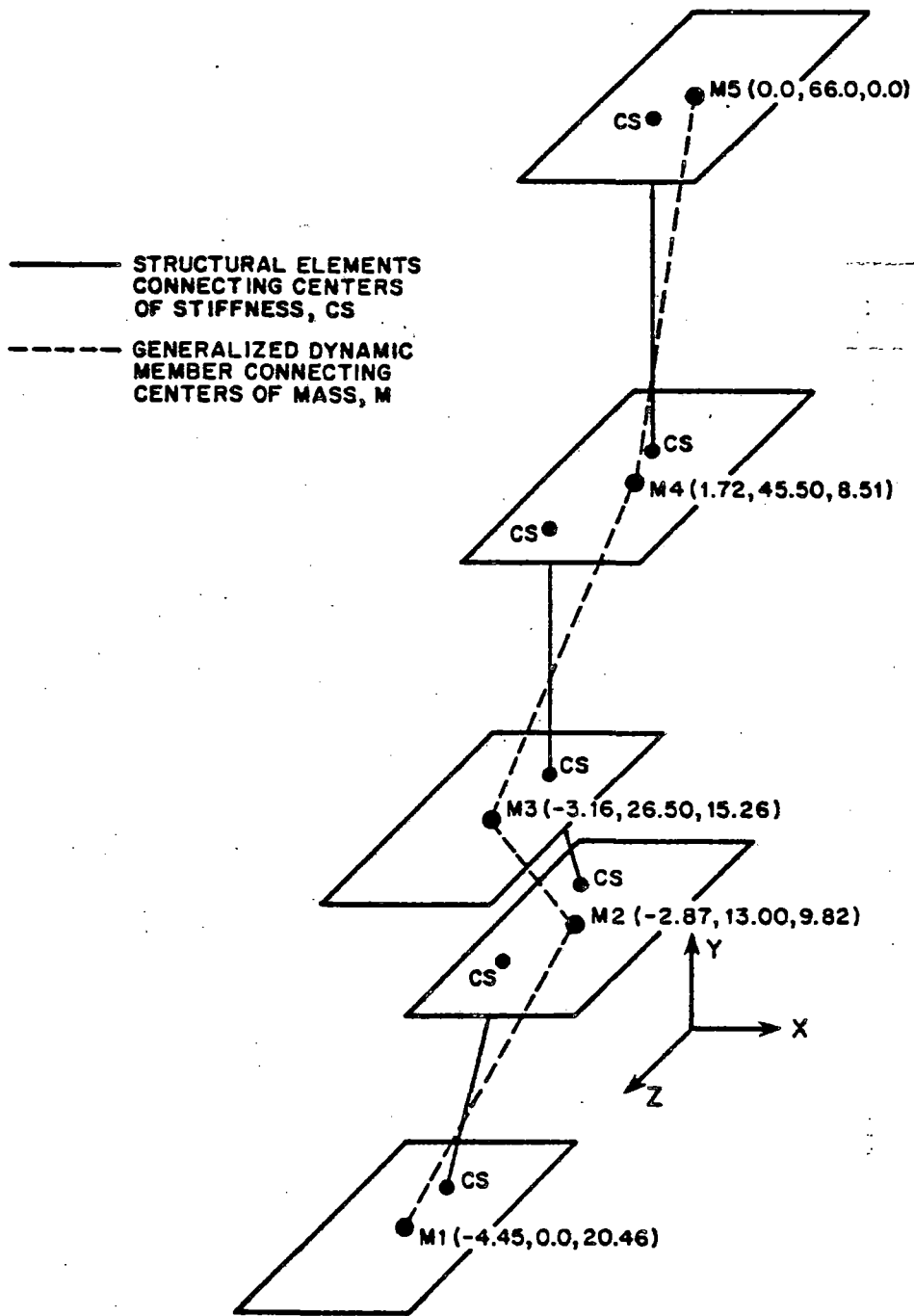
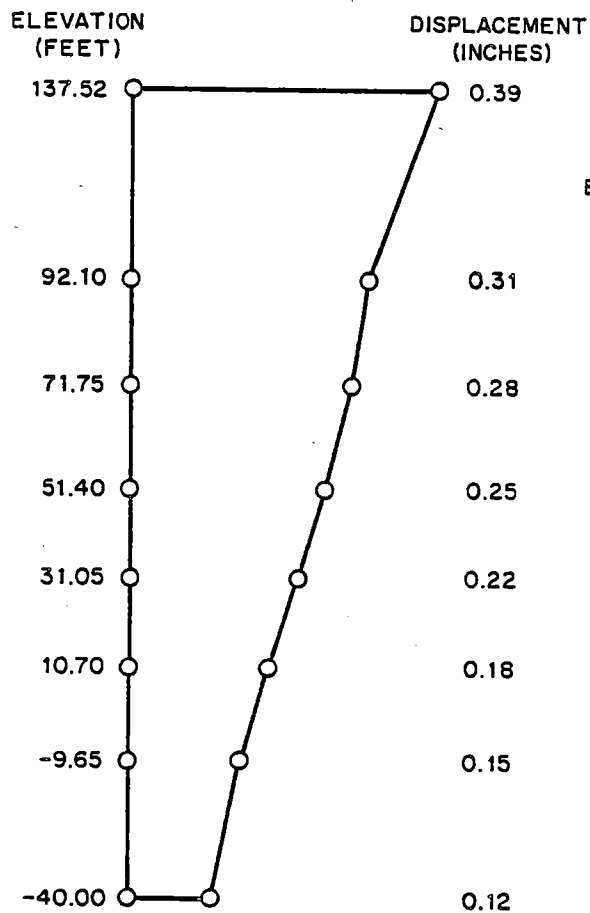
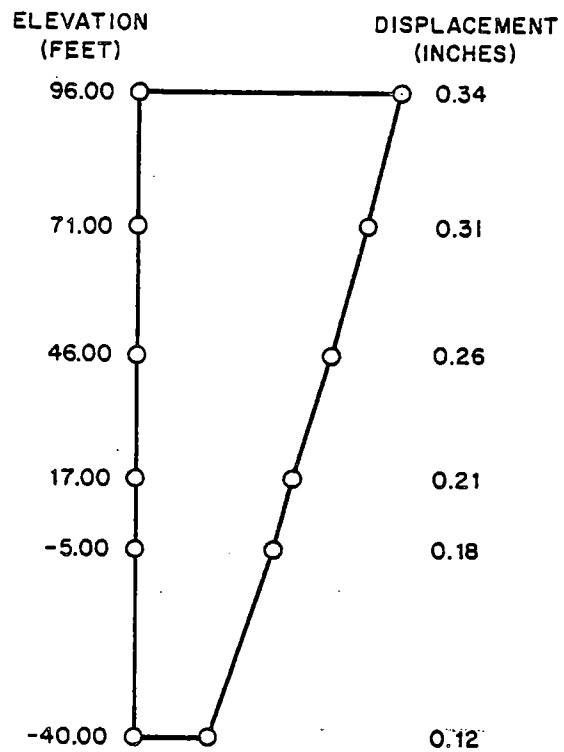


FIGURE 4-6
 GENERALIZED DYNAMIC MODEL
 OF A CATEGORY I STRUCTURE
 SURRY POWER STATION-UNITS 1 AND 2

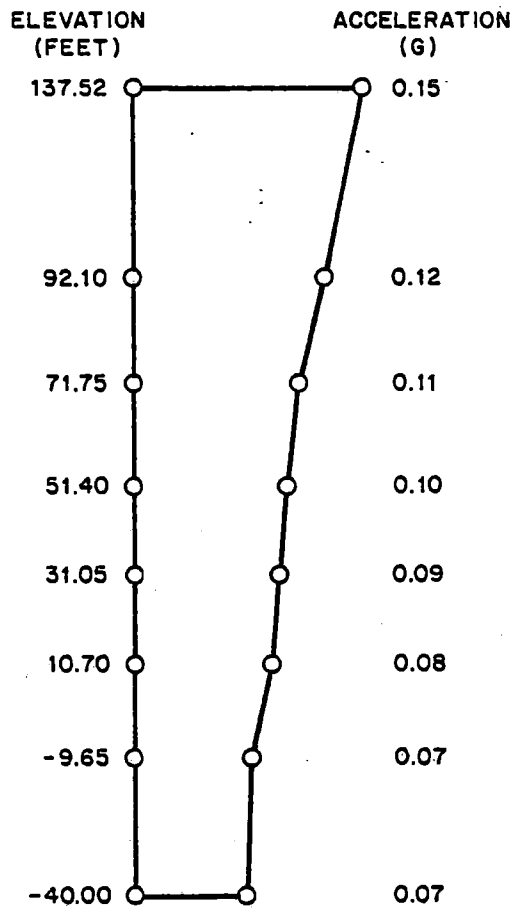


SHELL

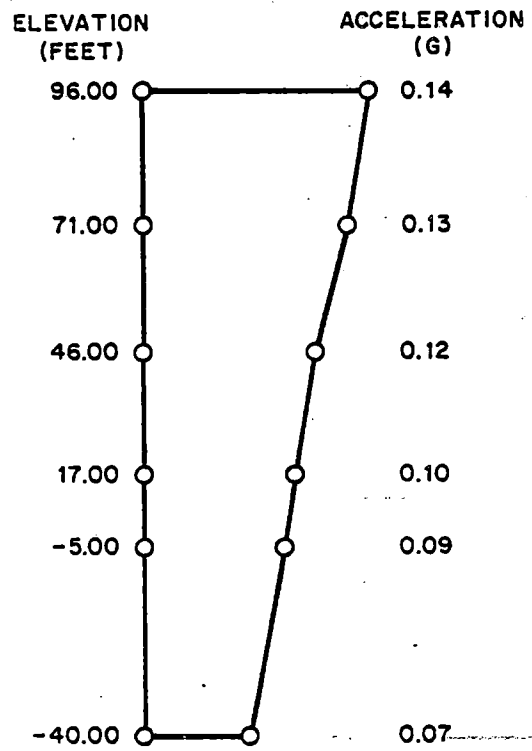


INTERNALS

FIGURE 4-7
 TYPICAL DISPLACEMENT PROFILES
 SURRY POWER STATION-UNITS 1 AND 2



SHELL



INTERNALS

FIGURE 4-8
TYPICAL ACCELERATION PROFILES
SURRY POWER STATION-UNITS 1 AND 2

SURRY POWER STATION, UNITS 1 AND 2

5.0 COMPARISONS OF RESULTS

Comparisons of amplified response spectra (ARS) were prepared for the following cases:

1. Methodology - REFUND/FRIDAY vs PLAXLY
2. Earthquake - FSAR vs Regulatory Guide 1.60
3. Soil Parameter Variation - low strain, first and last iterations from SHAKE; ± 50 percent variation of low strain input to SHAKE.

5.1 REFUND/FRIDAY VS PLAXLY

The containment structure was analyzed two ways for purposes of comparison using strain compatible soil parameters from the SHAKE program.

1. A one-step analysis using the finite element program PLAXLY
2. A three-step analysis using the methodology described in Section 4.1

The following observations can be made about the ARS shown in Figures 5-1 through 5-3.:

SURRY POWER STATION, UNITS 1 AND 2

1. At the mat level, the results of the two methods are very close.
2. With increasing elevation, the REFUND/FRIDAY results become more conservative with respect to the PLAXLY results. This is a consequence of the conservative assumption made about the rotational part of the input in the kinematic interaction step (see, for example, Figure 9.4-2).

5.2 FSAR EARTHQUAKE VS REGULATORY GUIDE 1.60 EARTHQUAKE

Additional analyses were performed at the request of the NRC using the three-step method (REFUND/FRIDAY) to compare the design earthquake in the FSAR to that specified by Regulatory Guide 1.60. The ARS shown in Figures 5-4 through 5-6 are comparisons of consistent piping analysis bases; that is, the spectra for equipment dampings associated with the Regulatory Guide 1.60 earthquake (2 and 3 percent) are displayed with the 1 percent spectra for the FSAR earthquake. The soil shear moduli and damping used for these analyses are from the last iteration of the SHAKE program.

Even though the Regulatory Guide 1.60 earthquake is significantly more energetic than the FSAR earthquake, the results are very close.

SURRY POWER STATION, UNITS 1 AND 2

5.3 VARIATION OF SOIL PROPERTIES

At the request of the NRC, ARS were generated for a range of soil shear modulus and damping ratio:

1. The low-strain soil shear modulus (Gmax) with soil damping ratio equal to 0.05.
2. Shear modulus and damping after one iteration in SHAKE, starting from the low-strain modulus (Gmax).
3. Shear modulus and damping consistent with earthquake amplitude, but calculated by the program SHAKE starting from 1 1/2 times the low-strain modulus (Gmax plus 50 percent).
4. Shear modulus and damping consistent with earthquake amplitude, but calculated by SHAKE starting from 1/2 of the low-strain modulus (Gmax minus 50 percent).
5. Shear modulus and damping from the last iteration of SHAKE, starting with the low strain modulus (Gmax).

SURRY POWER STATION, UNITS 1 AND 2

The ARS for Cases 1, 2, and 5 are compared in Figures 5-7 through 5-16 for piping damping ratios of .005, .010, and .030. They indicate that the analysis is sensitive to extreme variations in parameters but that, within the limits of the iterations of SHAKE, both the amplitudes and frequency content are well-behaved.

The ARS for Cases 3, 4 and 5 are shown in Figures 5-17 through 5-24 for piping damping ratios of .005, .010, and .030. Beginning the SHAKE analysis with 1/2 the low-strain modulus (Gmax minus 50 percent) results in extremely low moduli for the final iteration. Again, while apparently sensitive to extreme variations of input parameters, the amplified response analysis is relatively insensitive to variations of modulus and damping in the reasonable middle range of values.

5.4 SAMPLE PIPE STRESS PROBLEMS

On the basis of discussions with the NRC Staff on 20 April 1979, pipe stress analyses were done for three systems in the containment building. These are analyses for the DBE condition in accordance with the code equation:

$$S_p + S_{DL} + S_{DBE} = 1.8 S_h$$

where S_p = Pressure stress

SURRY POWER STATION, UNITS 1 AND 2

S_{DL} = Dead weight stress

S_{DBE} = DBE earthquake stress due to restraint displacement and inertia effects

S_h = Allowable stress at operating temperature

These analyses were done using NUPIPE for (a) the original ARS; and ARS using soil structure interaction by REFUND/FRIDAY, (b) Regulatory Guide 1.60 spectra and 1.61 damping values, and (c) FSAR ground response spectra for piping damping values equal to 0.5 to 1 percent.

Note that, for the purposes of these stress analysis comparisons, the ARS for conditions (b) and (c) outlined above were not peak broadened.

Tables 5-1 through 5-3 show pipe stress summaries for three samples.

SURRY POWER STATION, UNITS 1 AND 2

TABLE 5-1

SAMPLE PROBLEM 706

PIPE STRESS SUMMARY, PSI

Location Point	Stress* Per Original ARS		Stress* Per SSI Reg. Guides 1.60 & 1.61 ARS		Stress* Per SSI FSAR ARS			
	1/2% Damping		2% Damping		1/2% Damping		1% Damping	
	Inertia	Total	Inertia	Total	Inertia	Total	Inertia	Total
10**	4,631	11,174	3,480	9,933	2,508	8,535	2,300	8,350
10	3,869	9,944	2,913	8,951	2,103	7,854	1,965	7,706
32	2,223	8,047	1,646	7,549	948	6,867	873	6,822
40**	3,223	10,140	2,390	9,161	1,394	7,723	1,282	7,613
40	2,425	8,974	1,799	8,241	1,060	7,167	975	7,084
15**	5,665	12,693	4,259	11,152	3,083	9,479	2,828	9,226
15	3,269	9,687	2,460	8,789	1,800	7,811	1,651	7,665
75	2,122	9,364	1,617	8,828	1,378	8,298	1,261	8,199
100	690	8,995	528	8,642	398	7,764	364	7,741
115	980	7,851	874	7,697	627	7,223	569	7,169
130**	1,189	10,376	919	9,807	685	8,632	628	8,577
130	891	9,327	691	8,901	513	8,021	470	7,979
155**	486	7,605	473	7,493	272	7,055	243	7,034
155	363	7,253	354	7,169	204	6,843	182	6,827

NOTES:

* Computed using NUPIPE computer program for DBE
 ** Elbow

Allowable Stress = $1.8S_h = 30,769$ psi
 Fundamental Frequency = 4.864 CPS

SURRY POWER STATION, UNITS 1 AND 2

TABLE 5-2

SAMPLE PROBLEM 1020

PIPE STRESS SUMMARY, PSI

Location Point	Stress* Per Original ARS		Stress* Per SSI Reg. Guides 1.60 & 1.61 ARS		Stress* Per SSI FSAR ARS			
	1/2% Damping		2% Damping		1/2% Damping		1% Damping	
	Inertia	Total	Inertia	Total	Inertia	Total	Inertia	Total
2	2,058	8,812	2,378	8,622	1,558	6,582	1,352	6,379
12**	703	7,645	752	7,237	539	5,673	471	5,607
12	542	6,612	580	6,285	415	5,050	363	4,999
24	1,032	5,624	1,040	5,480	812	4,862	707	4,759
34	2,215	16,311	2,286	14,937	2,014	10,783	1,727	10,545
34**	2,868	20,206	2,959	18,437	2,608	13,091	2,236	12,783
38	4,780	21,991	5,024	20,407	3,778	14,322	3,275	13,824
38**	6,165	27,211	6,483	25,225	4,870	17,500	4,220	16,857
50	1,343	10,072	1,488	9,823	1,077	8,695	917	8,560
55	869	8,706	911	8,482	623	7,645	543	7,578
62	386	9,696	459	9,397	498	8,477	406	8,396
80**	404	10,629	416	10,209	441	8,974	364	8,897
80	308	9,530	317	9,212	332	8,280	274	8,223
86	1,170	13,110	1,282	12,418	926	10,189	791	10,058

NOTES:

- * Computed using NUPIPE computer program for DBE
- ** Elbow

Allowable Stress = $1.8S_h = 33,750$ psi
 Fundamental Frequency = 5.231 CPS

SURRY POWER STATION, UNITS 1 AND 2

TABLE 5-3

SAMPLE PROBLEM 1555

PIPE STRESS SUMMARY, PSI

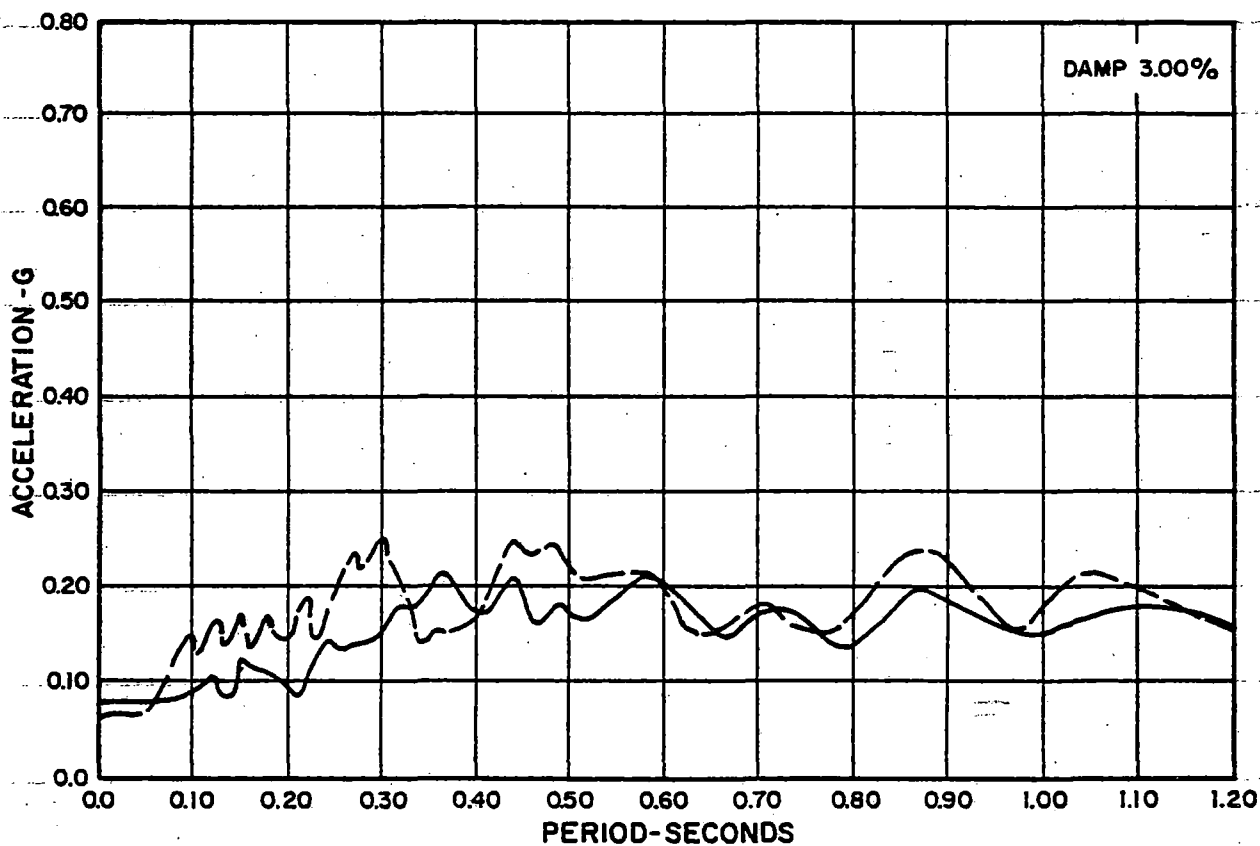
Location Point	Stress* Per Original ARS		Stress* Per SSI Reg. Guides 1.60 & 1.61 ARS		Stress* Per SSI FSAR ARS			
	1/2% Damping		2% Damping		1/2% Damping		1% Damping	
	Inertia	Total	Inertia	Total	Inertia	Total	Inertia	Total
1	2,863	5,309	844	3,108	1,063	3,080	860	2,880
5	2,441	4,744	756	2,894	938	2,845	759	2,668
5**	3,055	5,604	941	3,280	1,172	3,219	947	2,997
15	1,198	3,310	526	2,540	599	2,425	484	2,316
37	6,174	7,974	1,538	3,273	2,071	3,695	1,673	3,304
45**	9,691	11,926	2,379	4,441	3,225	5,069	2,605	4,450
45	7,724	9,781	1,900	3,819	2,573	4,317	2,079	3,823
57	3,246	4,976	878	2,635	1,123	2,794	913	2,596
57**	3,895	5,765	1,053	2,933	1,344	3,130	1,093	2,888
65	3,080	4,687	912	2,548	1,114	2,616	908	2,424
105	5,181	7,328	1,317	3,397	1,735	3,532	1,408	3,209
105**	6,402	8,756	1,623	3,887	2,144	4,059	1,739	3,657

NOTES:

* Computed using NUPIPE computer program for DBE

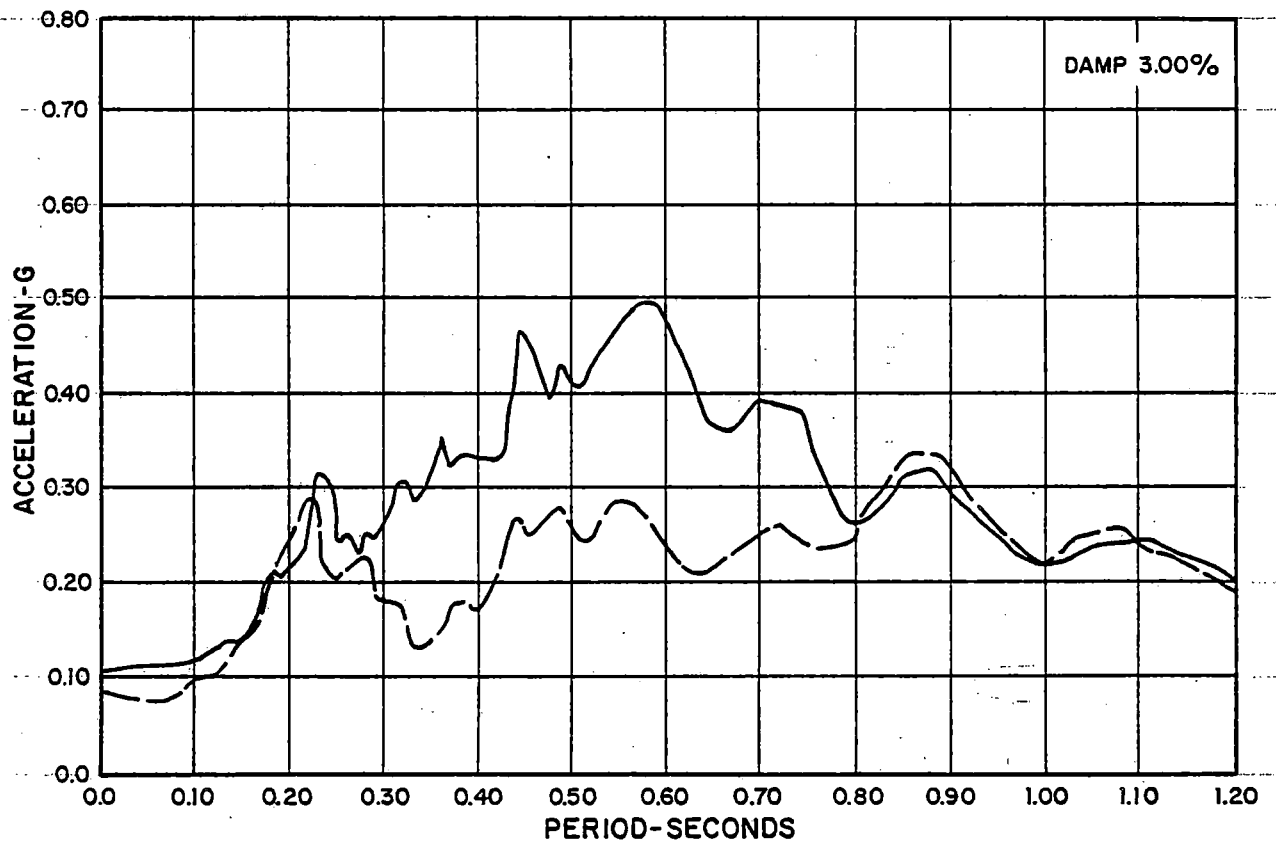
** Elbow

Allowable Stress - $1.8S_h = 30,882$ psi
 Fundamental Frequency = 4.070 CPS



LEGEND
 — REFUND/FRIDAY
 - - - PLAXLY

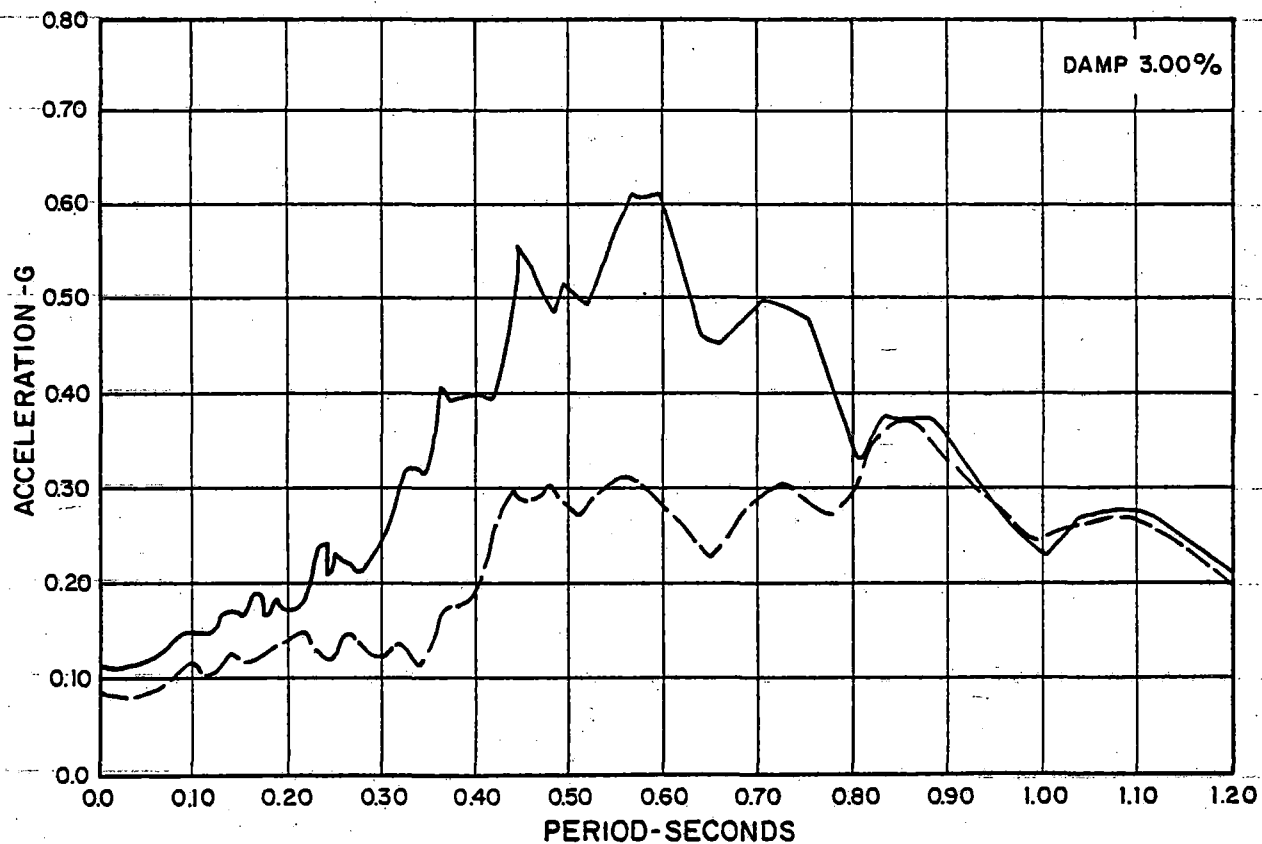
FIGURE 5-1
COMPARISON OF REFUND/FRIDAY AND
PLAXLY RESULTS -ARS AT MAT
 SURRY POWER STATION - UNITS 1 AND 2



LEGEND

———— REFUND/FRIDAY
 - - - - - PLAXLY

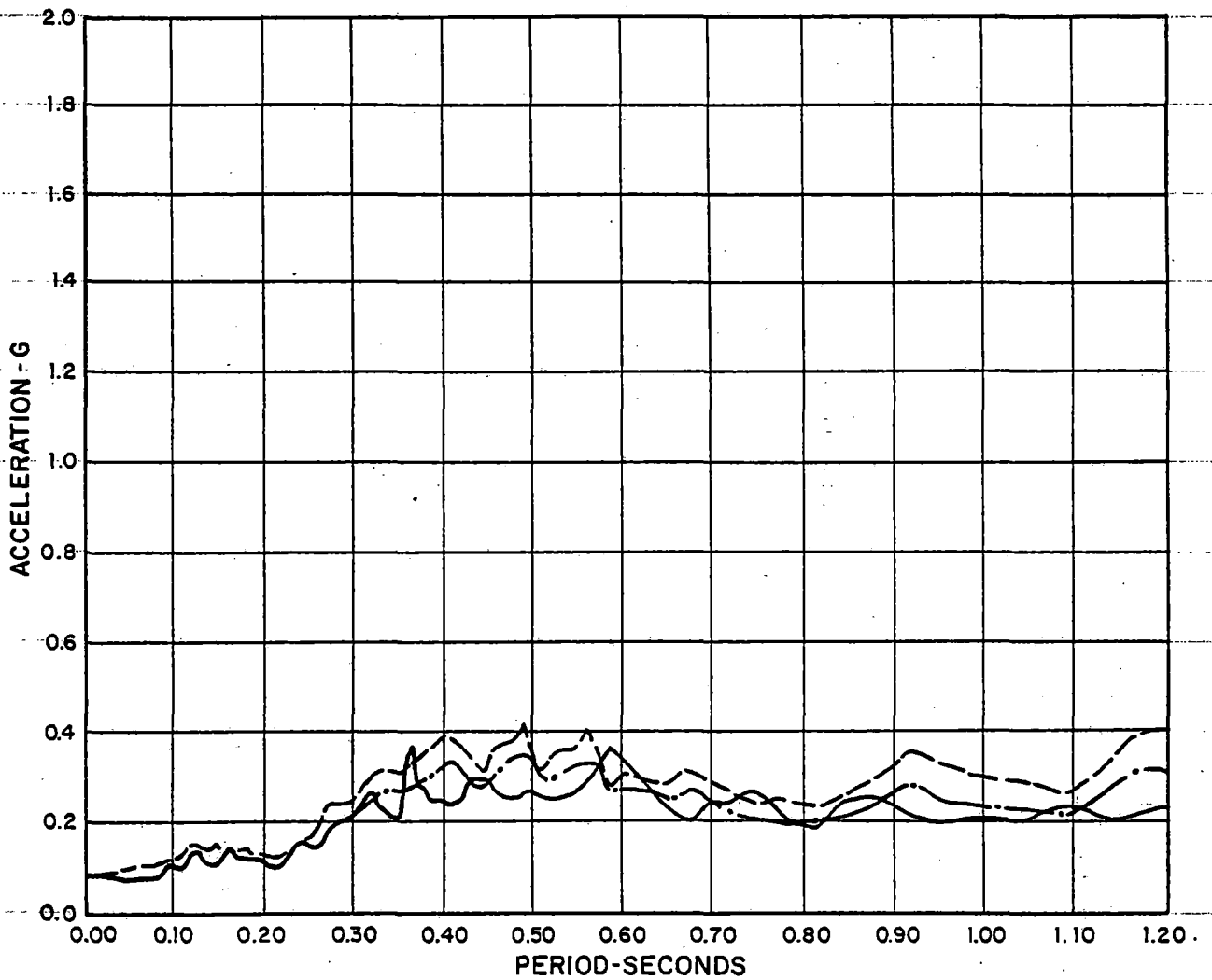
FIGURE 5-2
 COMPARISON OF REFUND/FRIDAY AND
 PLAXLY - ARS AT OPERATING FLOOR
 SURRY POWER STATION-UNITS 1 AND 2



LEGEND

- REFUND/FRIDAY
- - - PLAXLY

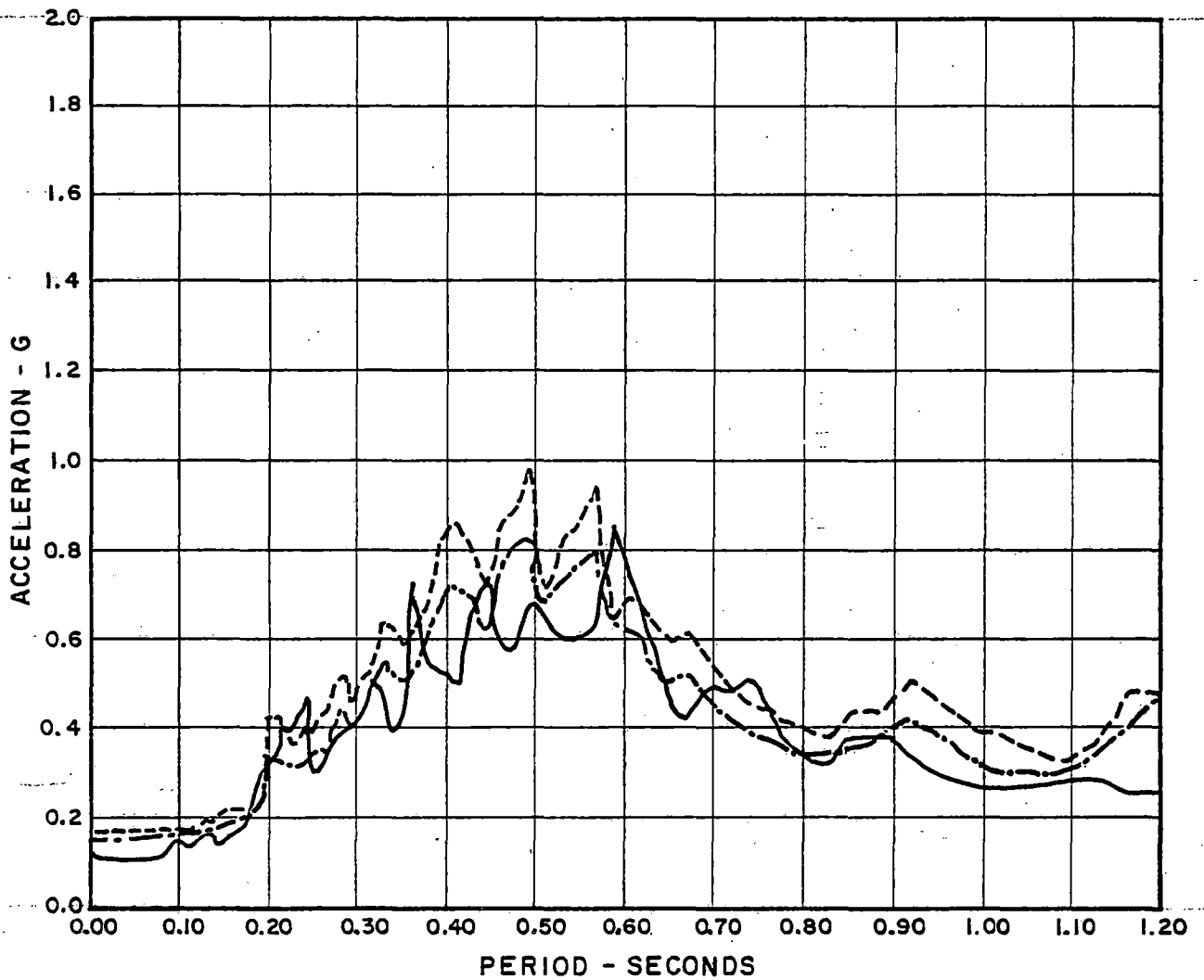
FIGURE 5-3
 COMPARISON OF REFUND/FRIDAY AND
 PLAXLY - ARS AT SPRINGLINE
 SURRY POWER STATION-UNITS 1 AND 2



LEGEND

- FSAR EARTHQUAKE 1% DAMPING
- REGULATORY GUIDE 1.60 EARTHQUAKE 2% DAMPING
- . - . REGULATORY GUIDE 1.60 EARTHQUAKE 3% DAMPING

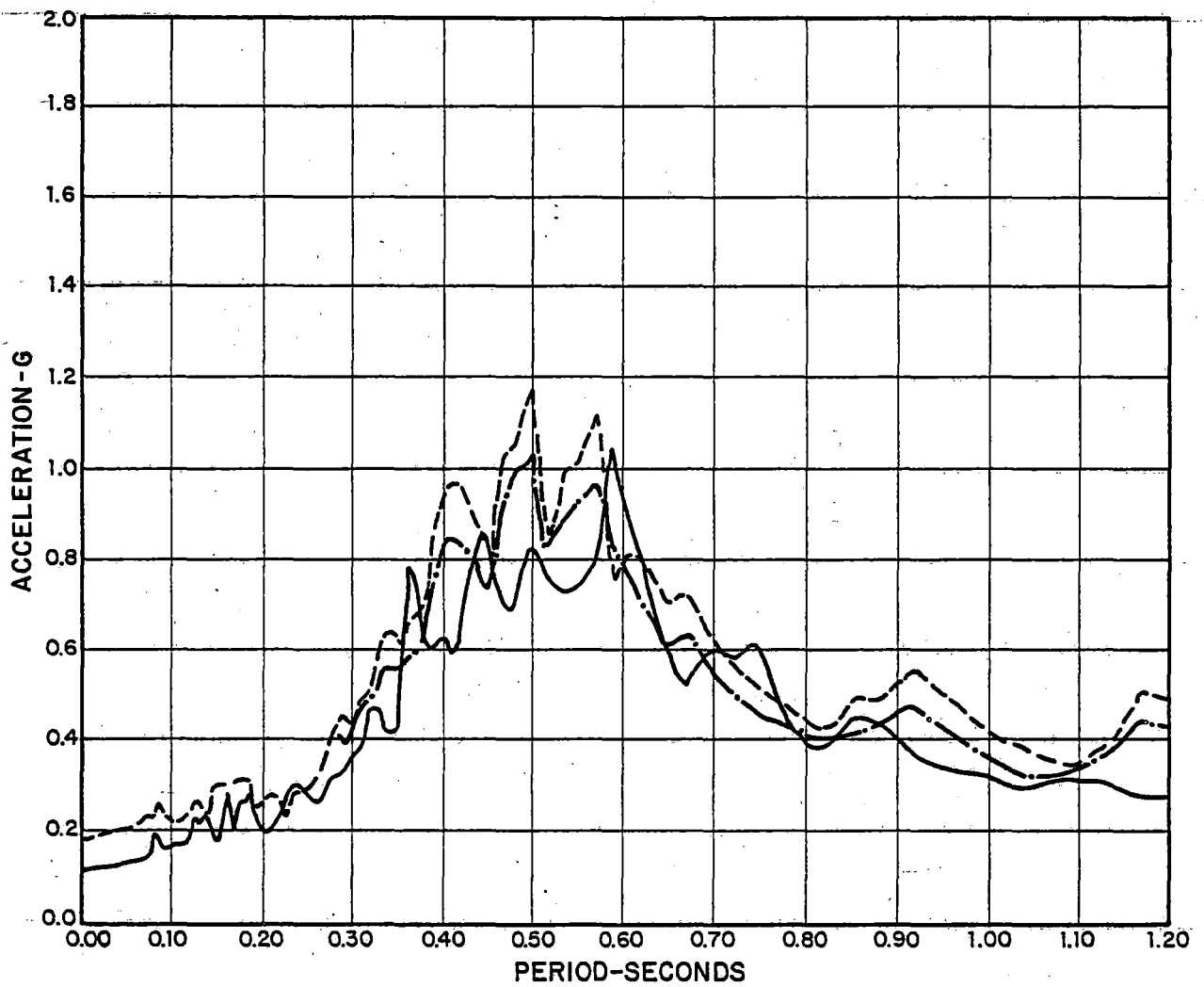
**FIGURE 5-4
 COMPARISON OF
 THE FSAR AND REGULATORY GUIDE
 1.60 EARTHQUAKES-ARS AT MAT
 SURRY POWER STATION - UNITS 1 AND 2**



LEGEND:

- FSAR EARTHQUAKE 1% DAMPING
- REGULATORY GUIDE 1.60 EARTHQUAKE 2% DAMPING
- · - · - REGULATORY GUIDE 1.60 EARTHQUAKE 3% DAMPING

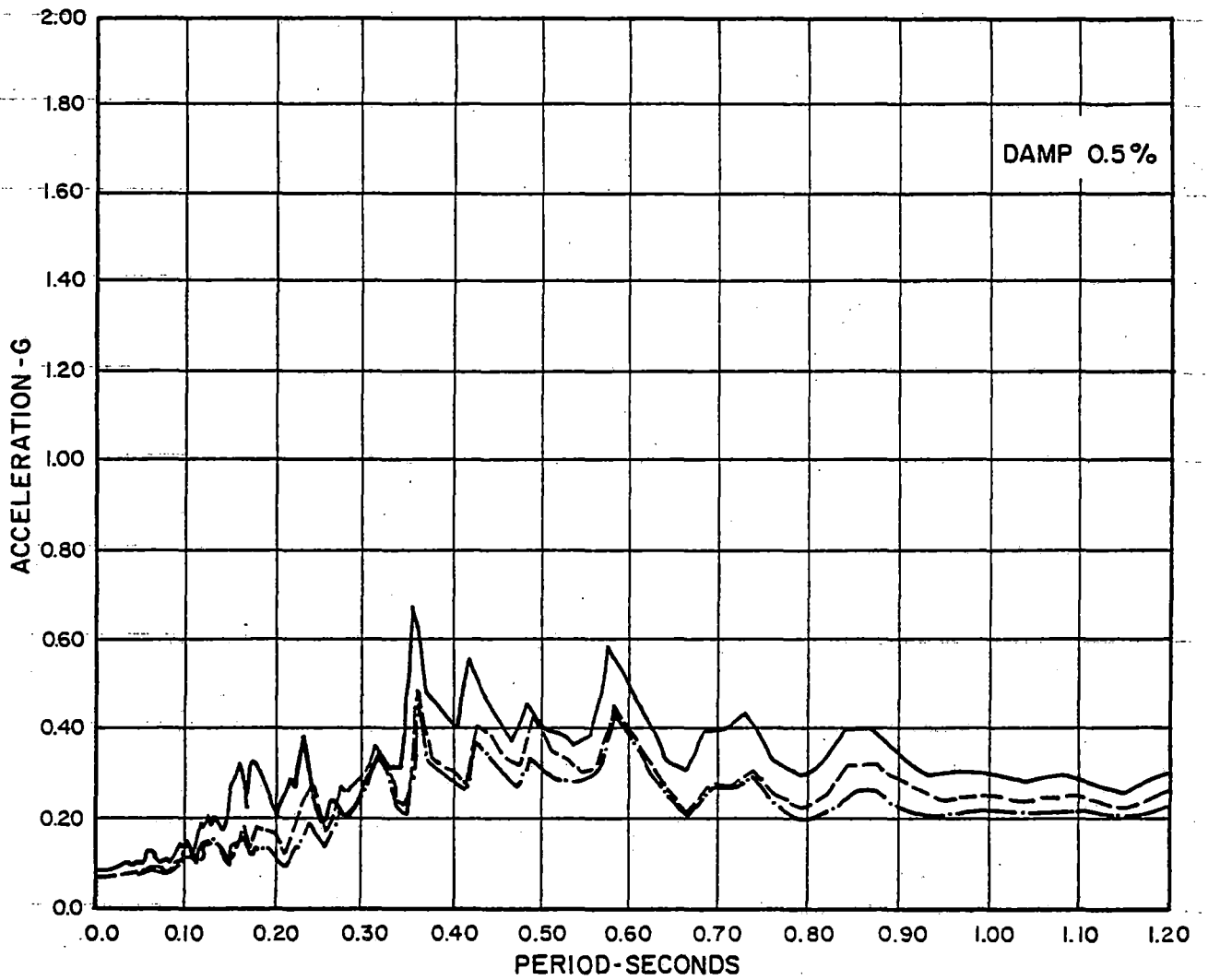
FIGURE 5-5
 COMPARISON OF FSAR AND REGULATORY GUIDE
 1.60 EARTHQUAKES-ARS AT OPERATING FLOOR
 SURRY POWER STATION-UNITS 1 AND 2



LEGEND

- FSAR EARTHQUAKE 1% DAMPING
- - - - - REGULATORY GUIDE 1.60 EARTHQUAKE 2% DAMPING
- · - · - REGULATORY GUIDE 1.60 EARTHQUAKE 3% DAMPING

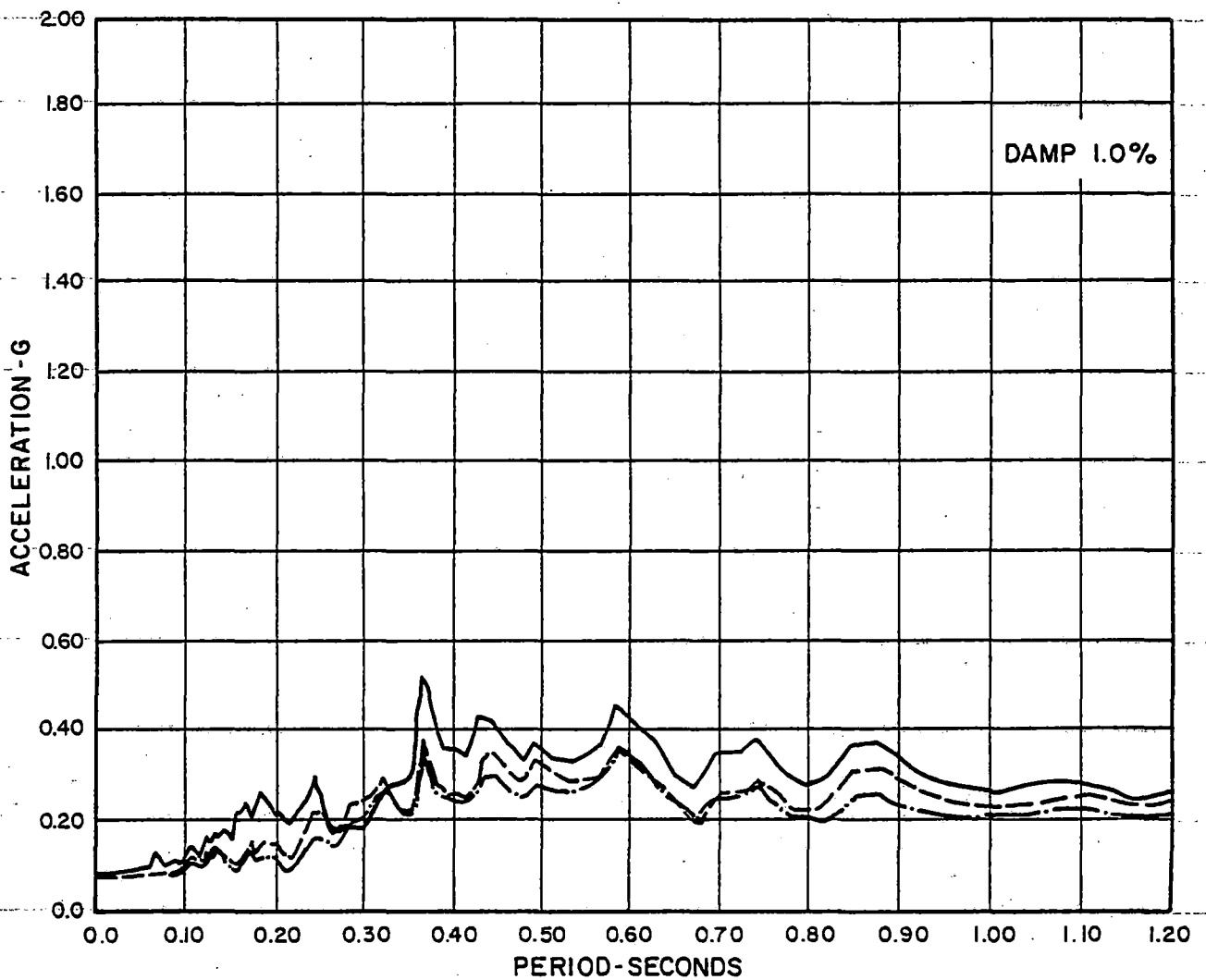
**FIGURE 5-6
COMPARISON OF
THE FSAR AND REGULATORY GUIDE
1.60 EARTHQUAKES-ARS AT SPRINGLINE
SURRY POWER STATION-UNITS 1 AND 2**



LEGEND

- LOW STRAIN G_{max}
- - - - - FIRST ITERATION FROM SHAKE
- · - · - LAST ITERATION FROM SHAKE

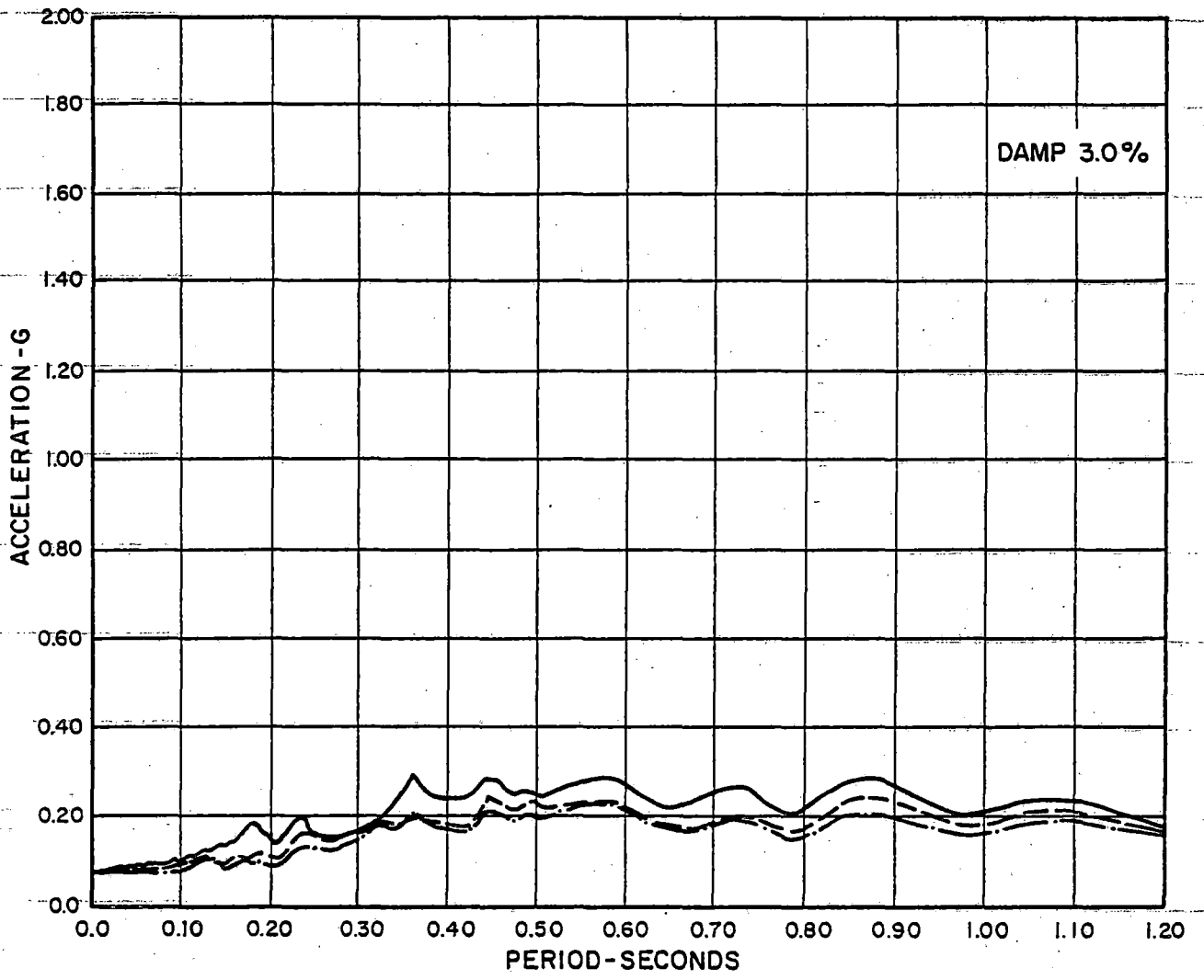
FIGURE 5-7
COMPARISON OF ARS FOR
SOIL PARAMETER VARIATIONS
HORIZONTAL RESPONSE SPECTRUM AT MAT
SURRY POWER STATION-UNITS 1 AND 2



LEGEND

- LOW STRAIN G_{max}
- - - - - FIRST ITERATION FROM SHAKE
- · - · - LAST ITERATION FROM SHAKE

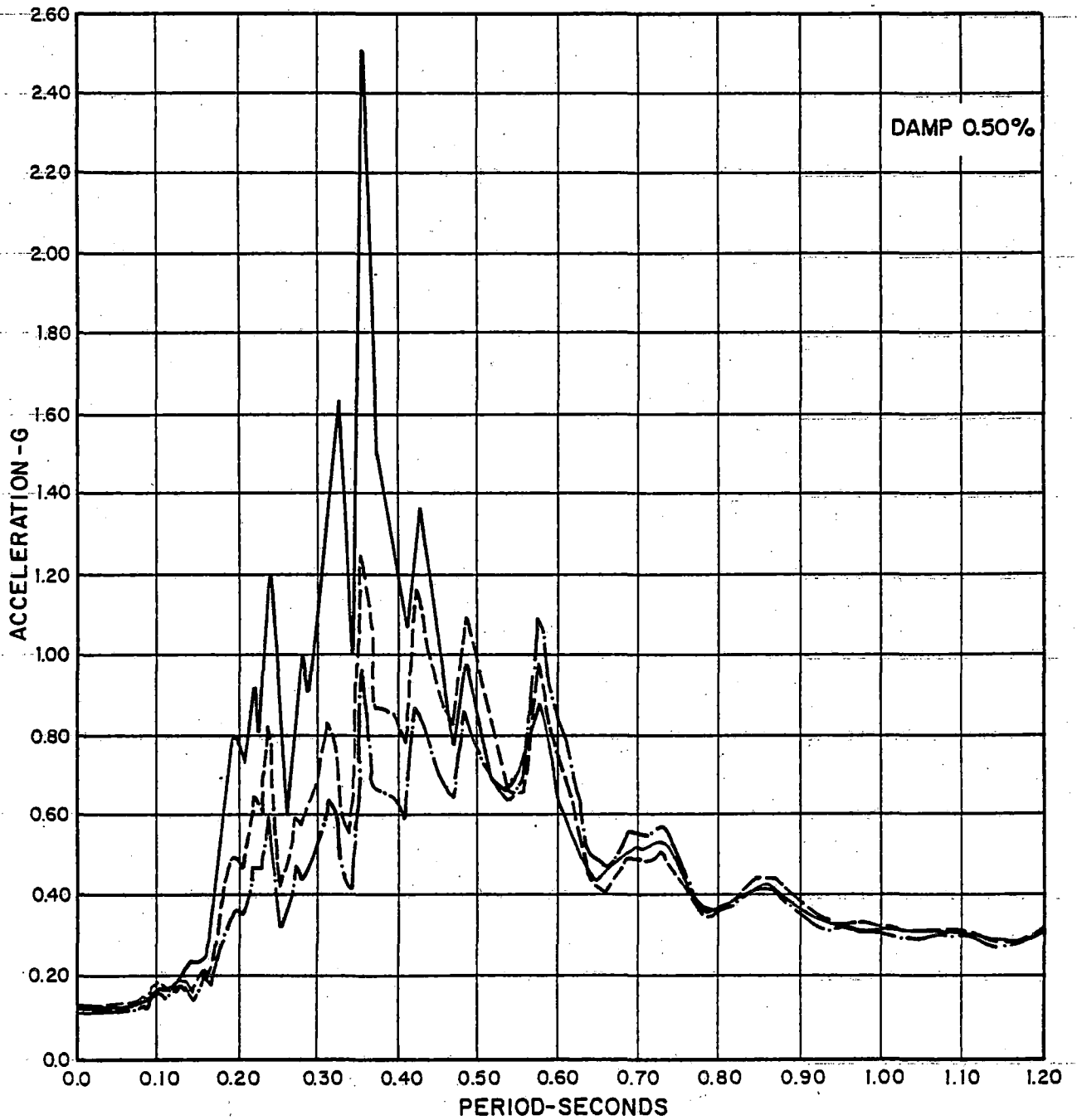
FIGURE 5-8
COMPARISON OF ARS FOR
SOIL PARAMETER VARIATIONS
 HORIZONTAL RESPONSE SPECTRUM AT MAT
 SURRY POWER STATION-UNITS 1 AND 2



LEGEND

- LOW STRAIN G_{max}
- - - - - FIRST ITERATION FROM SHAKE
- · - · - LAST ITERATION FROM SHAKE

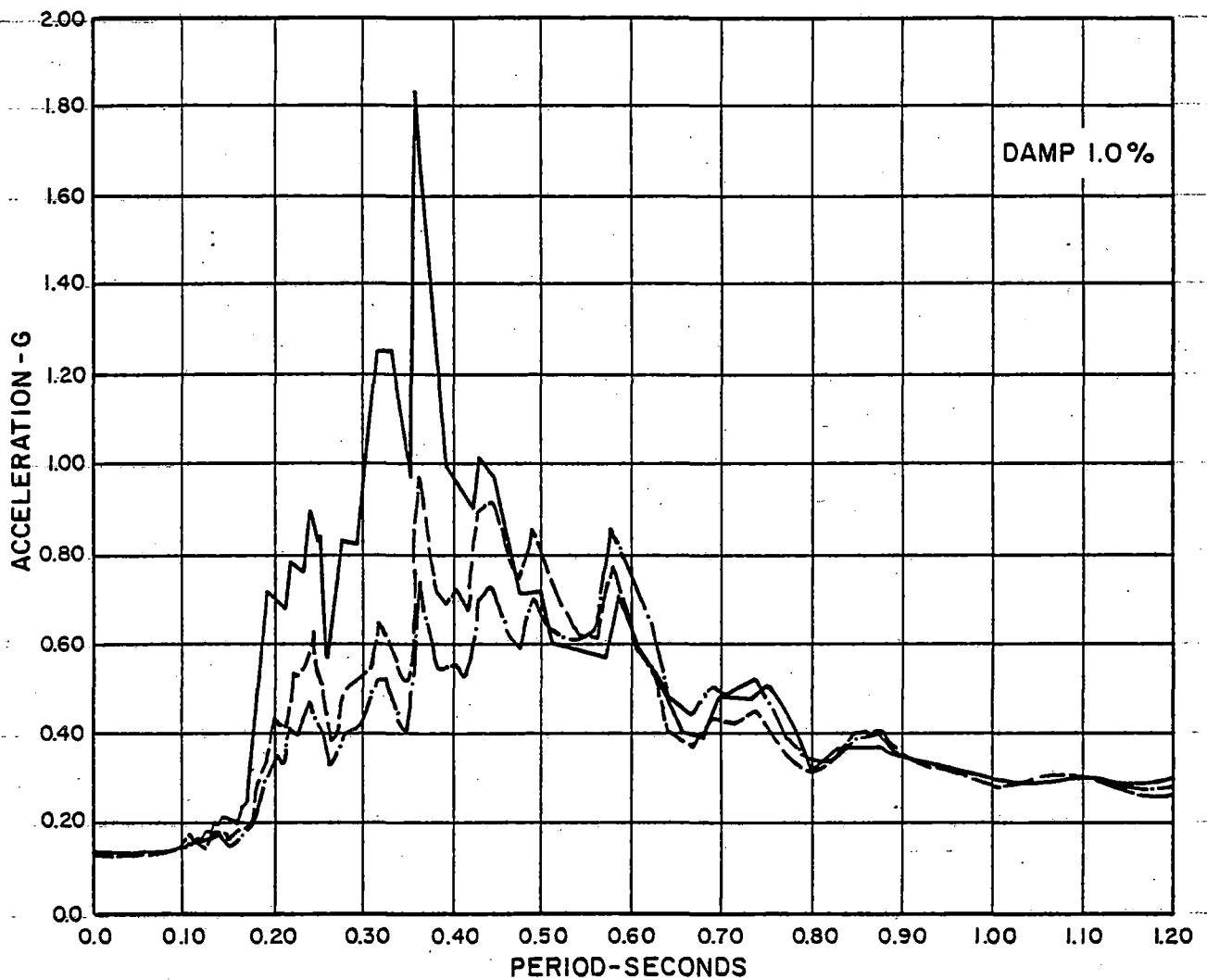
FIGURE 5-9
COMPARISON OF ARS FOR
SOIL PARAMETER VARIATIONS
HORIZONTAL RESPONSE SPECTRUM AT MAT
SURRY POWER STATION-UNITS 1 AND 2



LEGEND

- LOW STRAIN G_{max}
- - - - - FIRST ITERATION FROM SHAKE
- · - · - LAST ITERATION FROM SHAKE

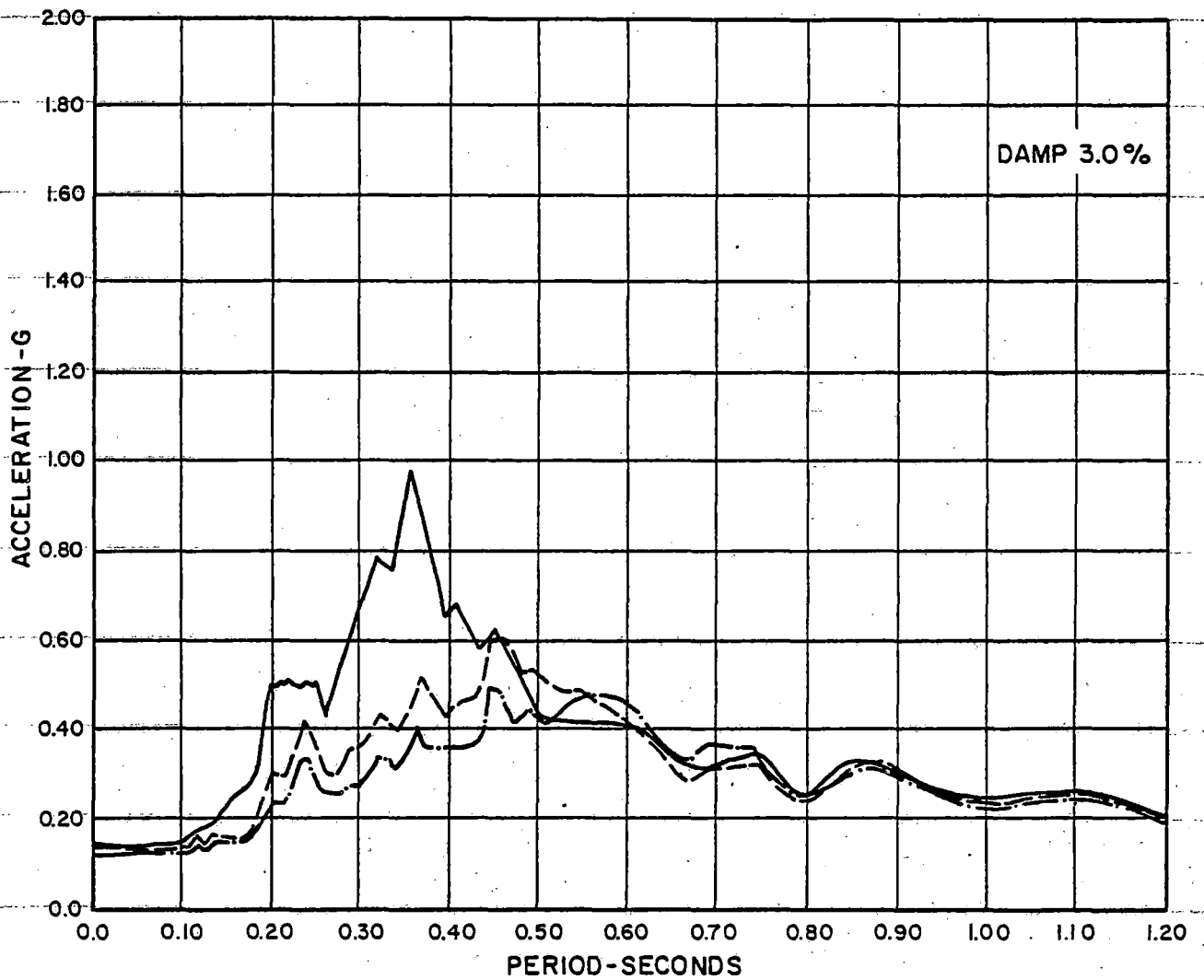
FIGURE 5-10
COMPARISON OF ARS FOR
SOIL PARAMETER VARIATIONS
HORIZONTAL RESPONSE SPECTRUM
AT OPERATING FLOOR
SURRY POWER STATION-UNITS 1 AND 2



LEGEND

- LOW STRAIN G_{max}
- FIRST ITERATION FROM SHAKE
- · - · - LAST ITERATION FROM SHAKE

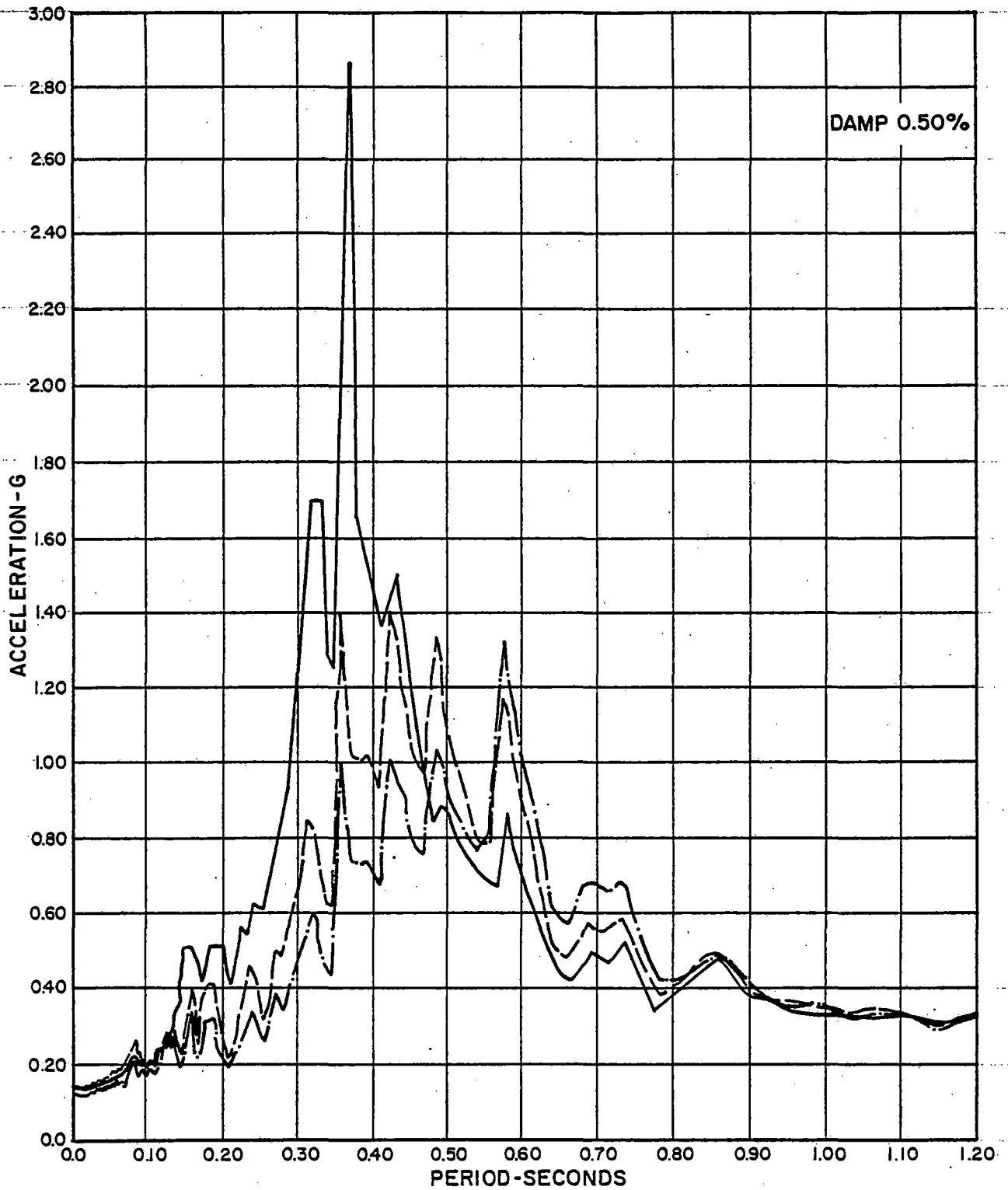
FIGURE 5-11
COMPARISON OF ARS FOR
SOIL PARAMETER VARIATIONS
HORIZONTAL RESPONSE SPECTRUM
AT OPERATING FLOOR
SURRY POWER STATION-UNITS 1 AND 2



LEGEND

- LOW STRAIN G_{max}
- - - - - FIRST ITERATION FROM SHAKE
- · - · - LAST ITERATION FROM SHAKE

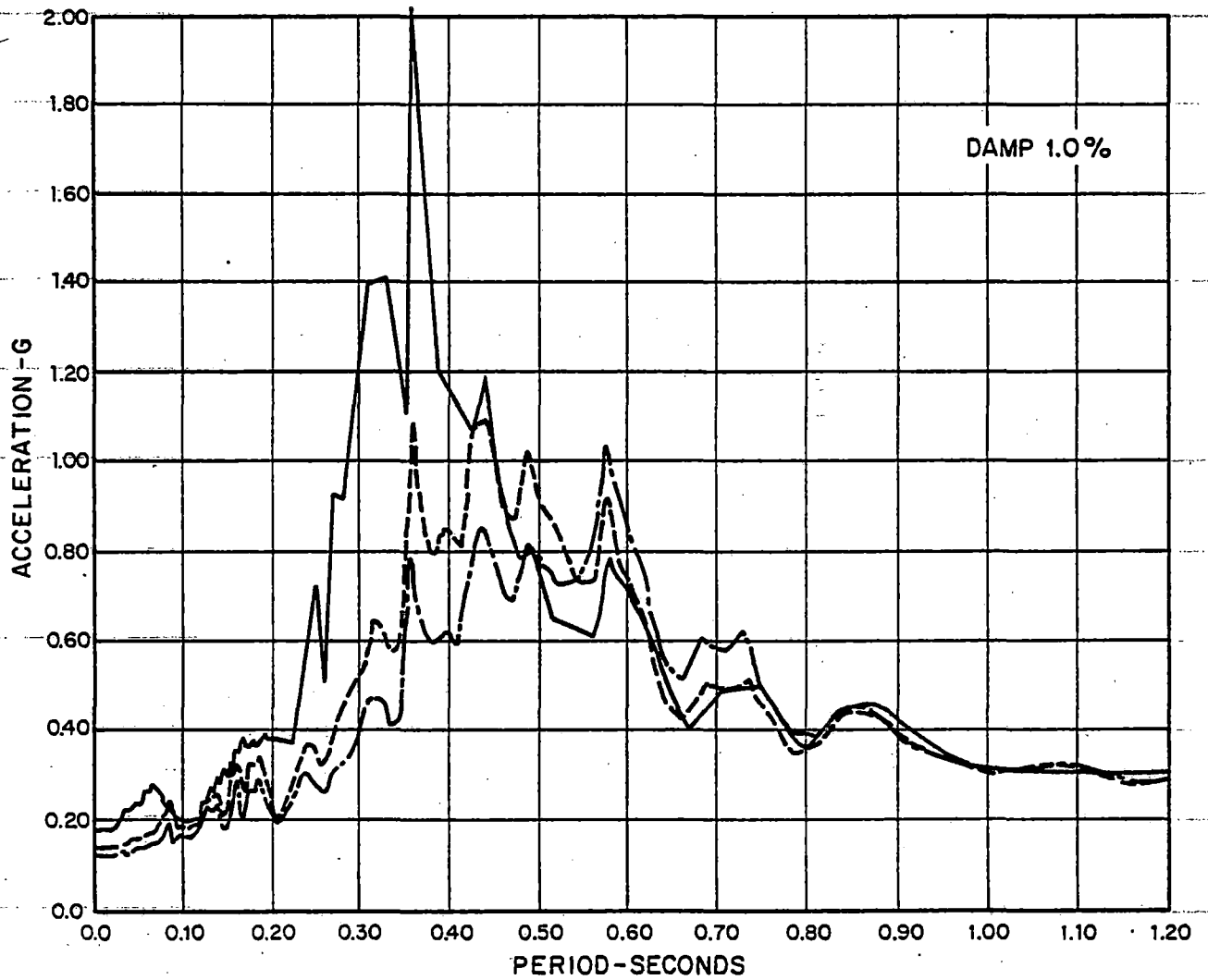
FIGURE 5-12
COMPARISON OF ARS FOR
SOIL PARAMETER VARIATIONS
HORIZONTAL RESPONSE SPECTRUM
AT OPERATING FLOOR
SURRY POWER STATION - UNITS 1 AND 2



LEGEND

- LOW STRAIN G_{max}
- - - FIRST ITERATION FROM SHAKE
- · - LAST ITERATION FROM SHAKE

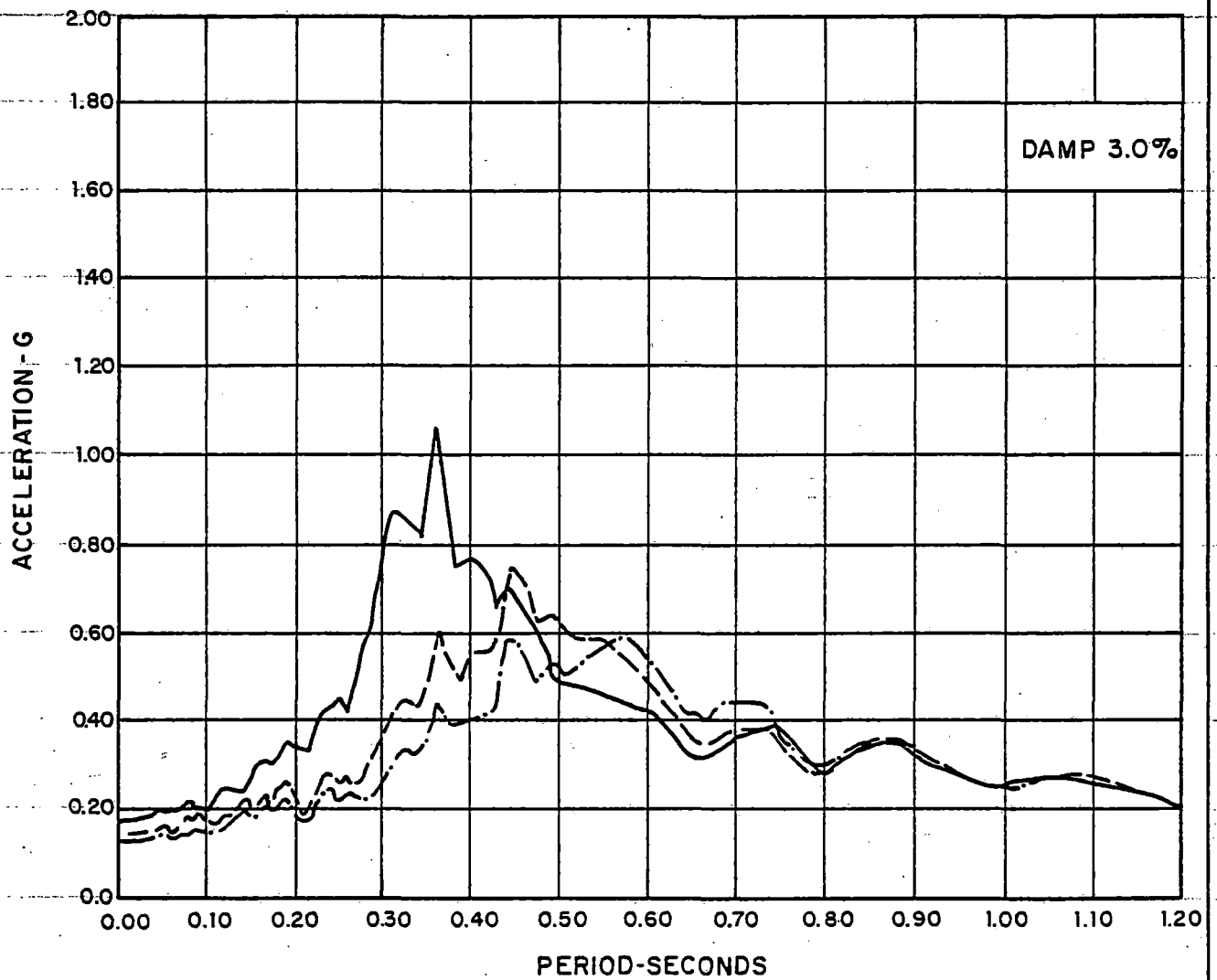
FIGURE 5-13
COMPARISON OF ARS FOR
SOIL PARAMETER VARIATIONS
 HORIZONTAL RESPONSE SPECTRUM
 AT SPRINGLINE
 SURRY POWER STATION-UNITS 1 AND 2



LEGEND

- LOW STRAIN G_{max}
- - - - - FIRST ITERATION FROM SHAKE
- · - · - LAST ITERATION FROM SHAKE

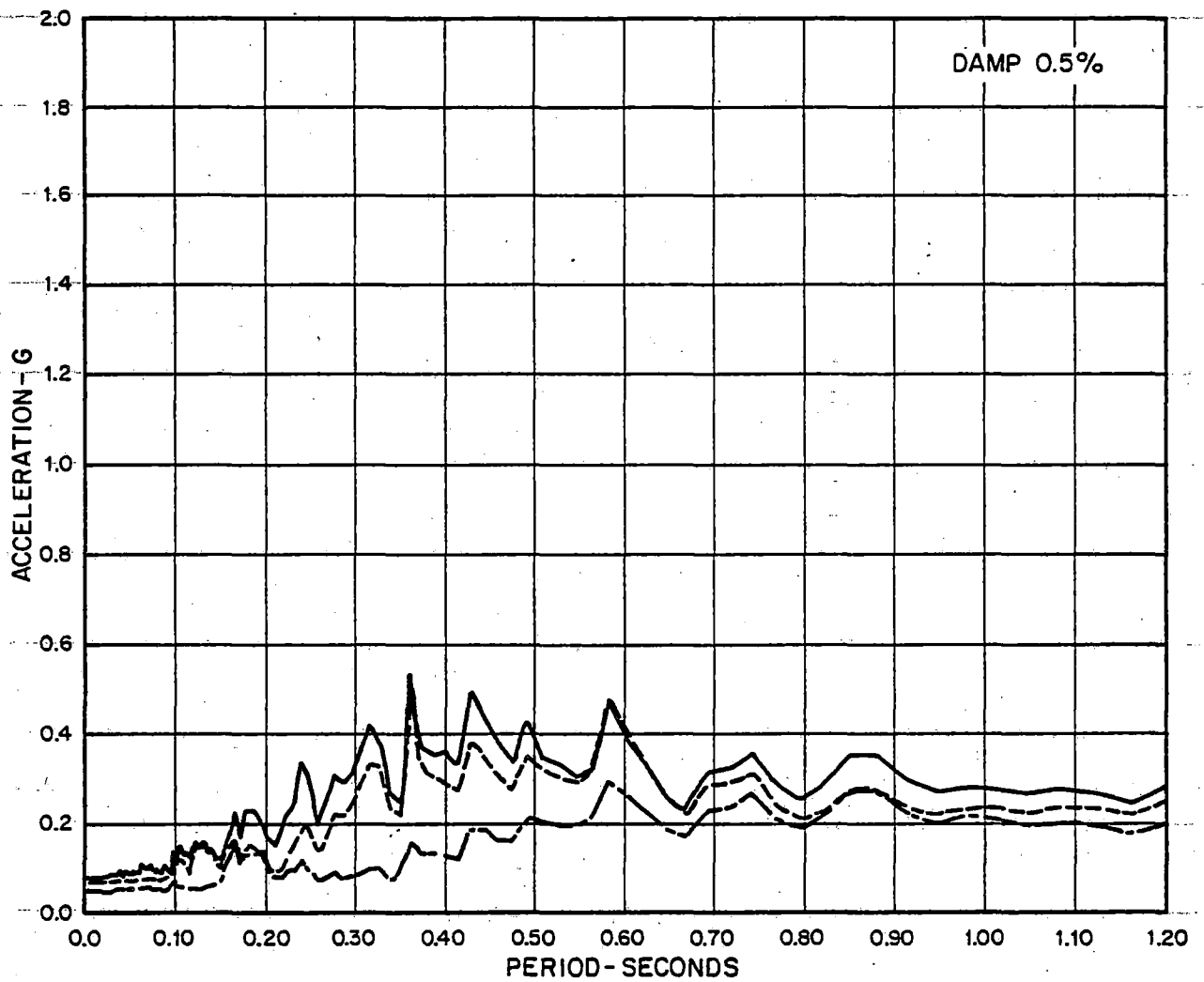
FIGURE 5-14
 COMPARISON OF ARS FOR
 SOIL PARAMETER VARIATIONS
 HORIZONTAL RESPONSE SPECTRUM
 AT SPRINGLINE
 SURRY POWER STATION - UNITS 1 AND 2



LEGEND

- LOW STRAIN G_{max}
- - - - - FIRST ITERATION FROM SHAKE
- . - . - LAST ITERATION FROM SHAKE

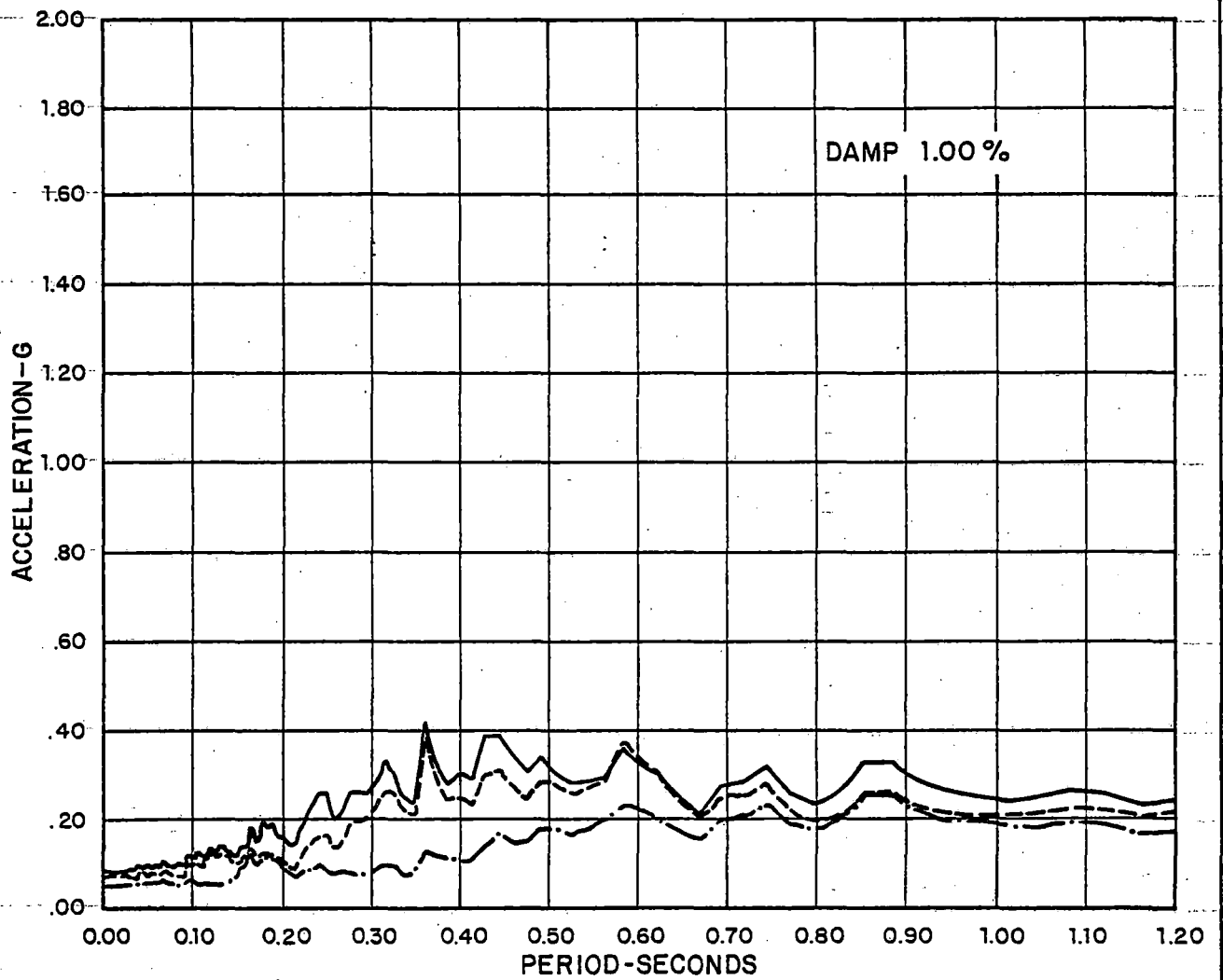
FIGURE 5-15
 COMPARISON OF ARS FOR
 SOIL PARAMETER VARIATIONS
 HORIZONTAL RESPONSE SPECTRUM
 AT SPRINGLINE
 SURRY POWER STATION-UNIT 1 AND 2



LEGEND

- LAST ITERATION FROM SHAKE USING $G_{max} + 50\%$
- - - - LAST ITERATION FROM SHAKE USING G_{max}
- · - · LAST ITERATION FROM SHAKE USING $G_{max} - 50\%$

FIGURE 5-16
COMPARISON OF ARS FOR
SOIL PARAMETER VARIATIONS
 HORIZONTAL RESPONSE SPECTRUM AT MAT
 SURRY POWER STATION - UNITS 1 AND 2



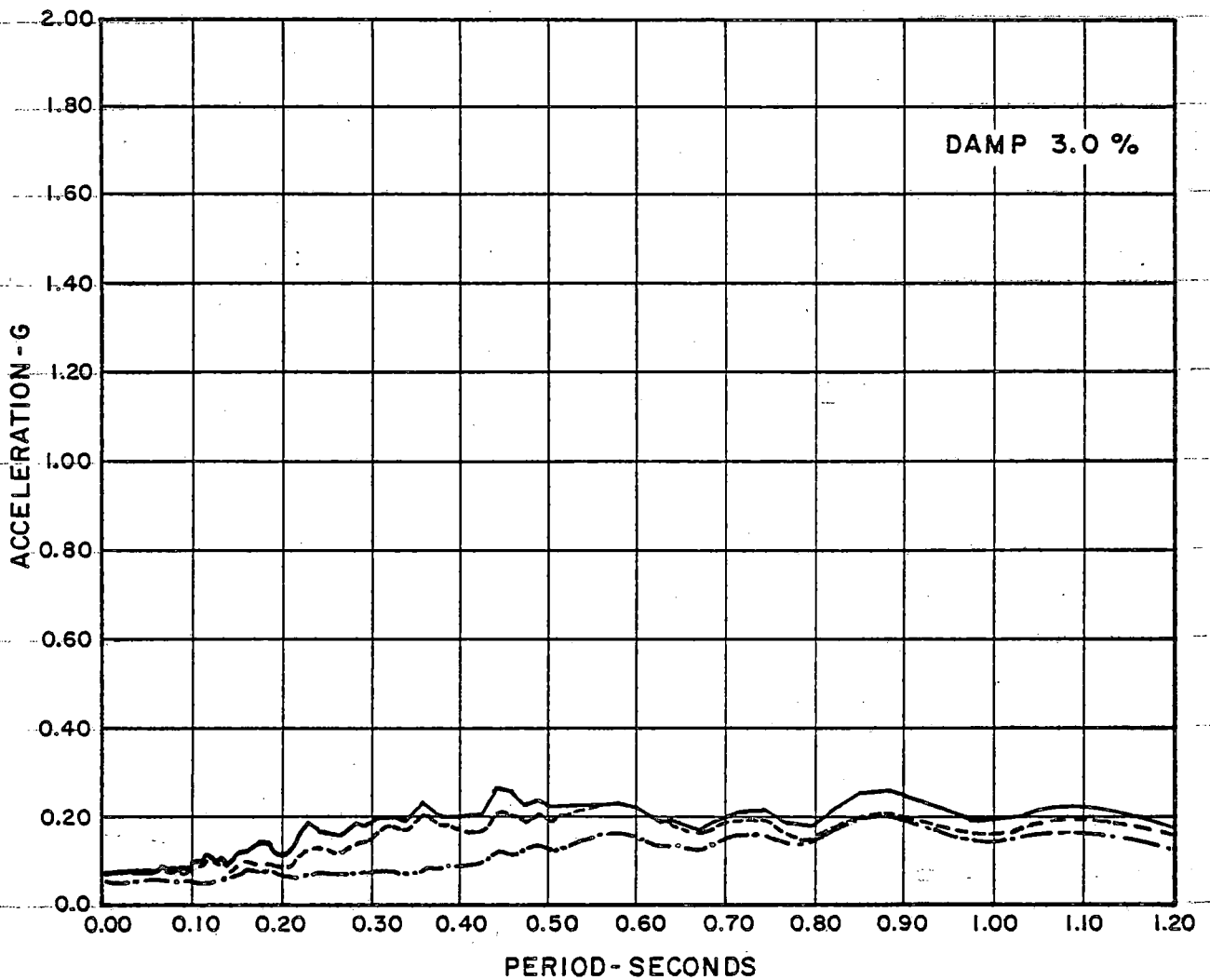
LEGEND

- LAST ITERATION FROM SHAKE USING $G_{max} + 50\%$
- LAST ITERATION FROM SHAKE USING G_{max}
- · - · - LAST ITERATION FROM SHAKE USING $G_{max} - 50\%$

FIGURE 5-17

**COMPARISON OF ARS FOR
SOIL PARAMETER VARIATIONS**

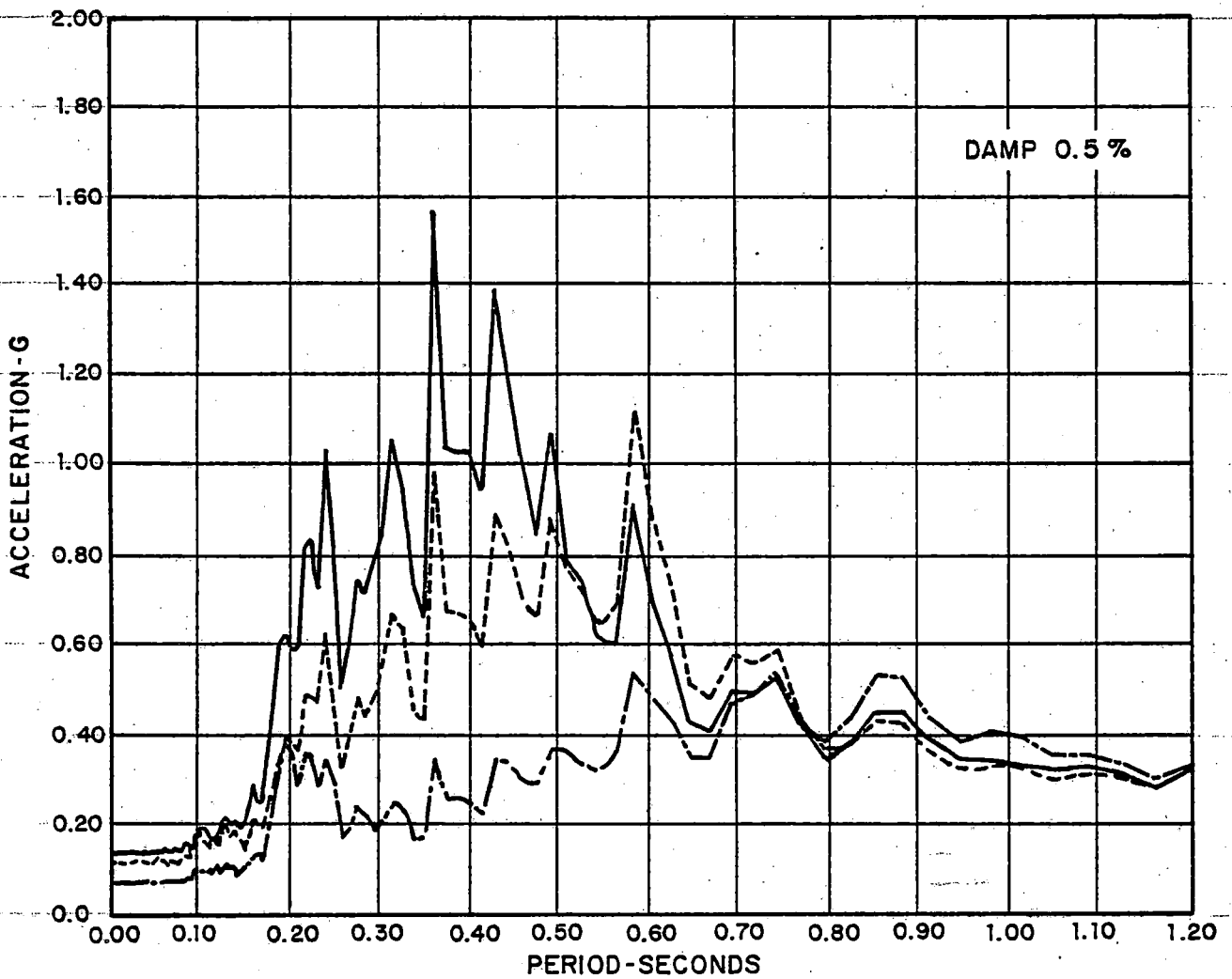
**HORIZONTAL RESPONSE SPECTRUM AT MAT
SURRY POWER STATION - UNITS 1 AND 2**



LEGEND:

- LAST ITERATION FROM SHAKE USING $G_{max} + 50\%$
- - - LAST ITERATION FROM SHAKE USING G_{max}
- · - · LAST ITERATION FROM SHAKE USING $G_{max} - 50\%$

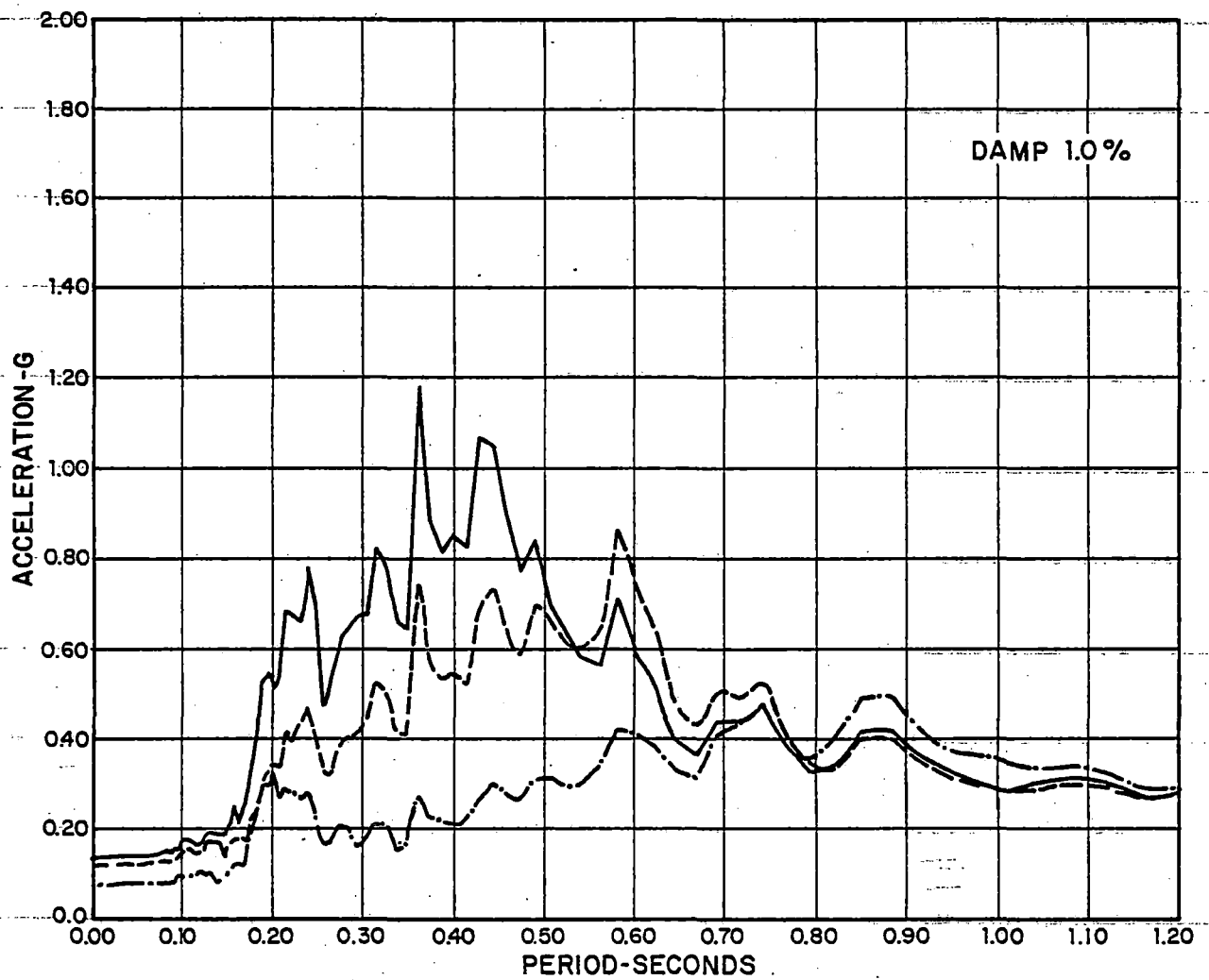
FIGURE 5-18
COMPARISON OF ARS FOR
SOIL PARAMETER VARIATIONS
 HORIZONTAL RESPONSE SPECTRUM AT MAT
 SURRY POWER STATION-UNITS 1 AND 2



LEGEND

- LAST ITERATION FROM SHAKE USING $G_{max} + 50\%$
- LAST ITERATION FROM SHAKE USING G_{max}
- · - · - LAST ITERATION FROM SHAKE USING $G_{max} - 50\%$

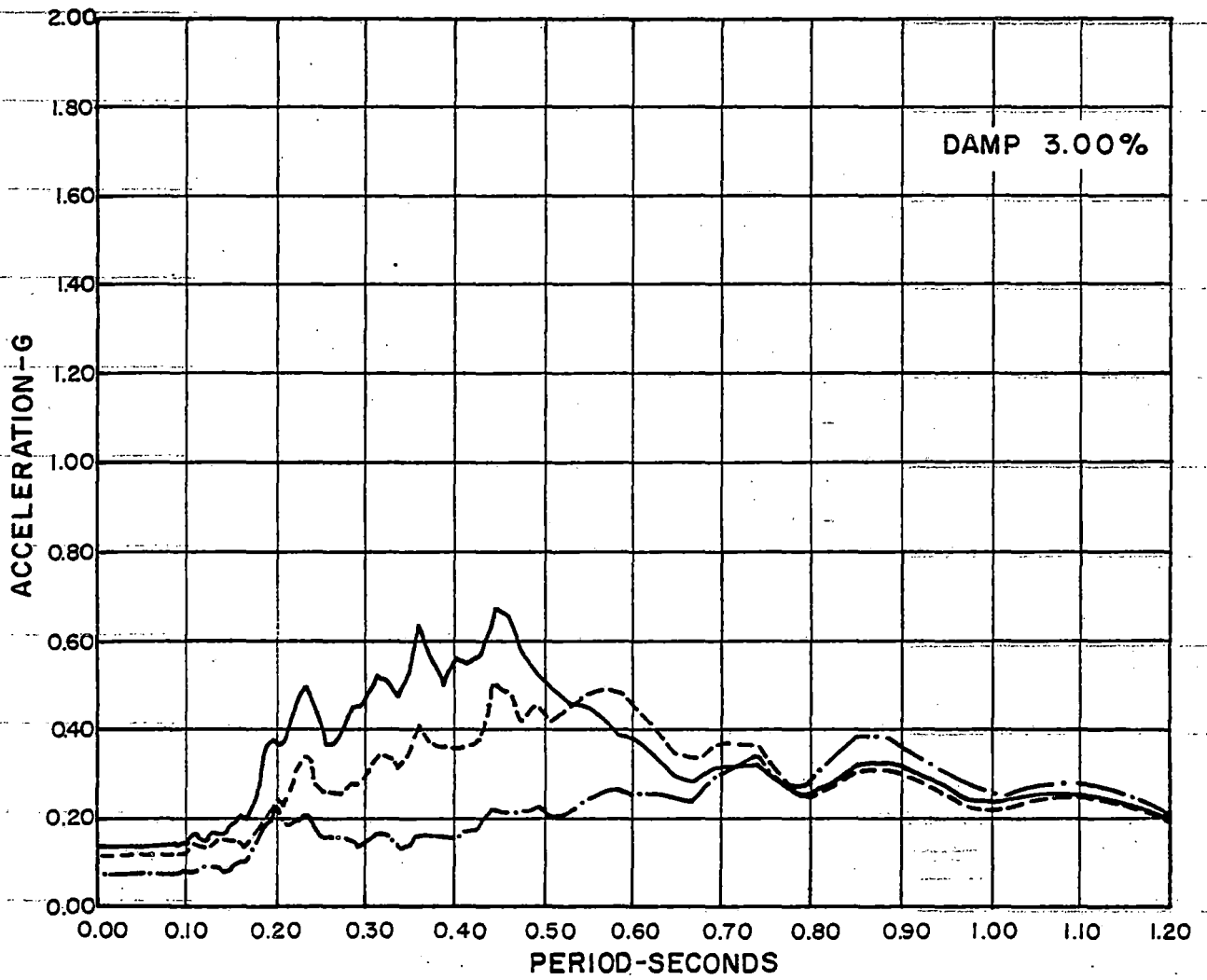
FIGURE 5-19
COMPARISON OF ARS FOR
SOIL PARAMETER VARIATIONS
 HORIZONTAL RESPONSE SPECTRUM
 AT OPERATING FLOOR
 SURRY POWER STATION - UNITS 1 AND 2



LEGEND

- LAST ITERATION FROM SHAKE USING $G_{max} + 50\%$
- LAST ITERATION FROM SHAKE USING G_{max}
- · - · - LAST ITERATION FROM SHAKE USING $G_{max} - 50\%$

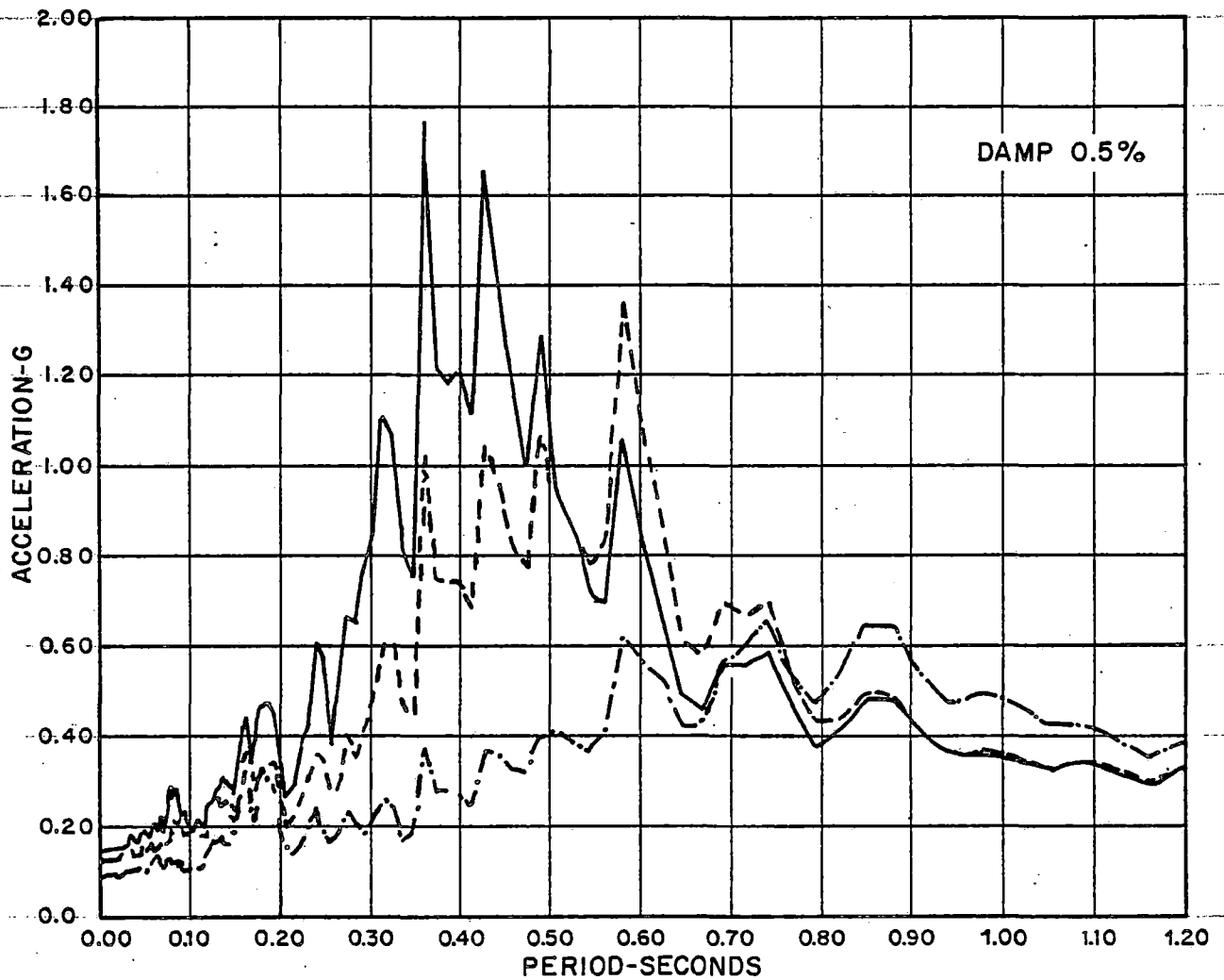
FIGURE 5-20
COMPARISON OF ARS FOR
SOIL PARAMETER VARIATIONS
 HORIZONTAL RESPONSE SPECTRUM
 AT OPERATING FLOOR
 SURRY POWER STATION - UNITS 1 AND 2



LEGEND

- LAST ITERATION FROM SHAKE USING $G_{max} + 50\%$
- - - - - LAST ITERATION FROM SHAKE USING G_{max}
- · - · - LAST ITERATION FROM SHAKE USING $G_{max} - 50\%$

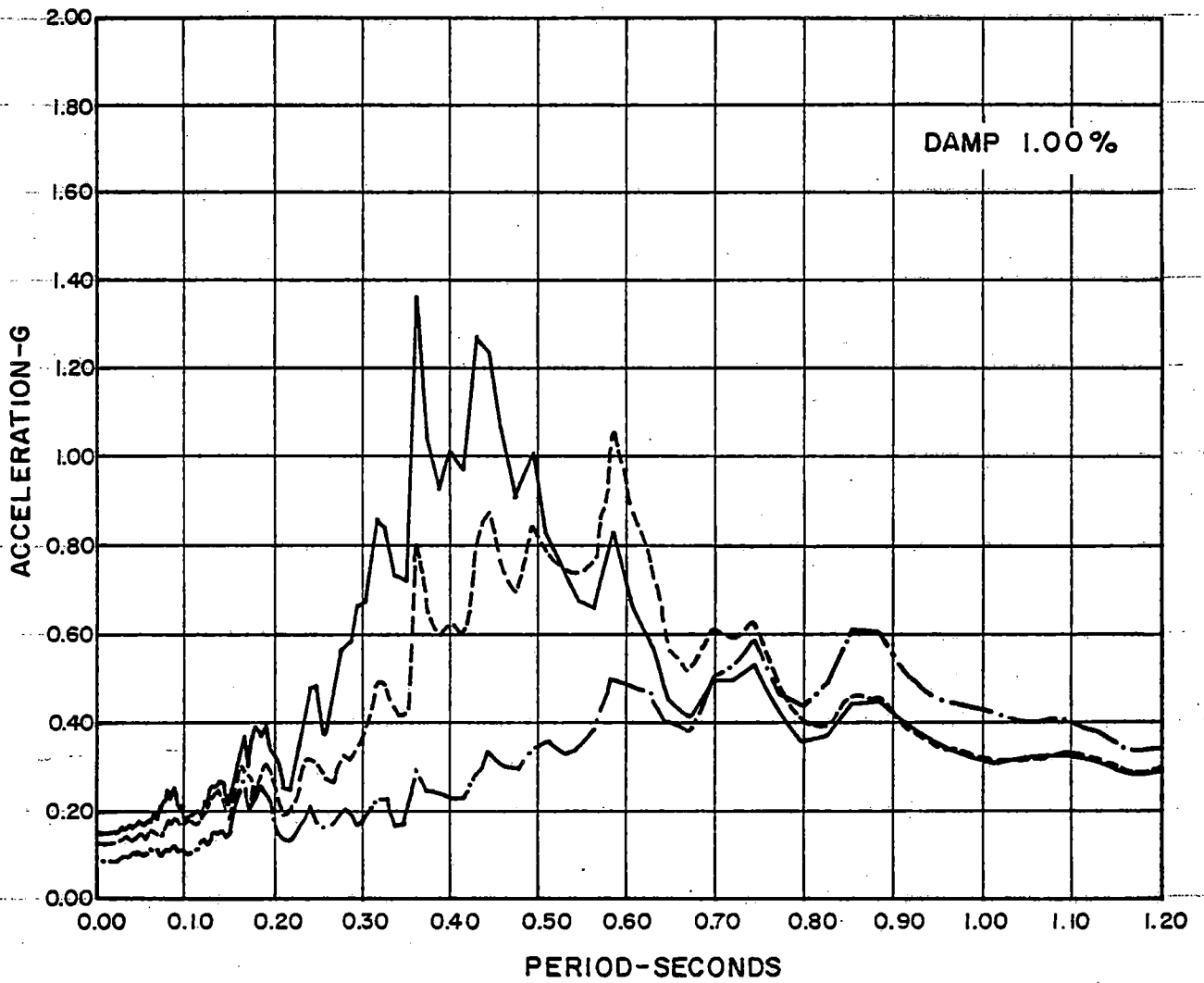
FIGURE 5-21
 COMPARISON OF ARS FOR
 SOIL PARAMETER VARIATIONS
 HORIZONTAL RESPONSE SPECTRUM
 AT OPERATING FLOOR
 SURRY POWER STATION-UNITS 1 AND 2



LEGEND

- LAST ITERATION FROM SHAKE USING $G_{max} + 50\%$
- LAST ITERATION FROM SHAKE USING G_{max}
- · - · - LAST ITERATION FROM SHAKE USING $G_{max} - 50\%$

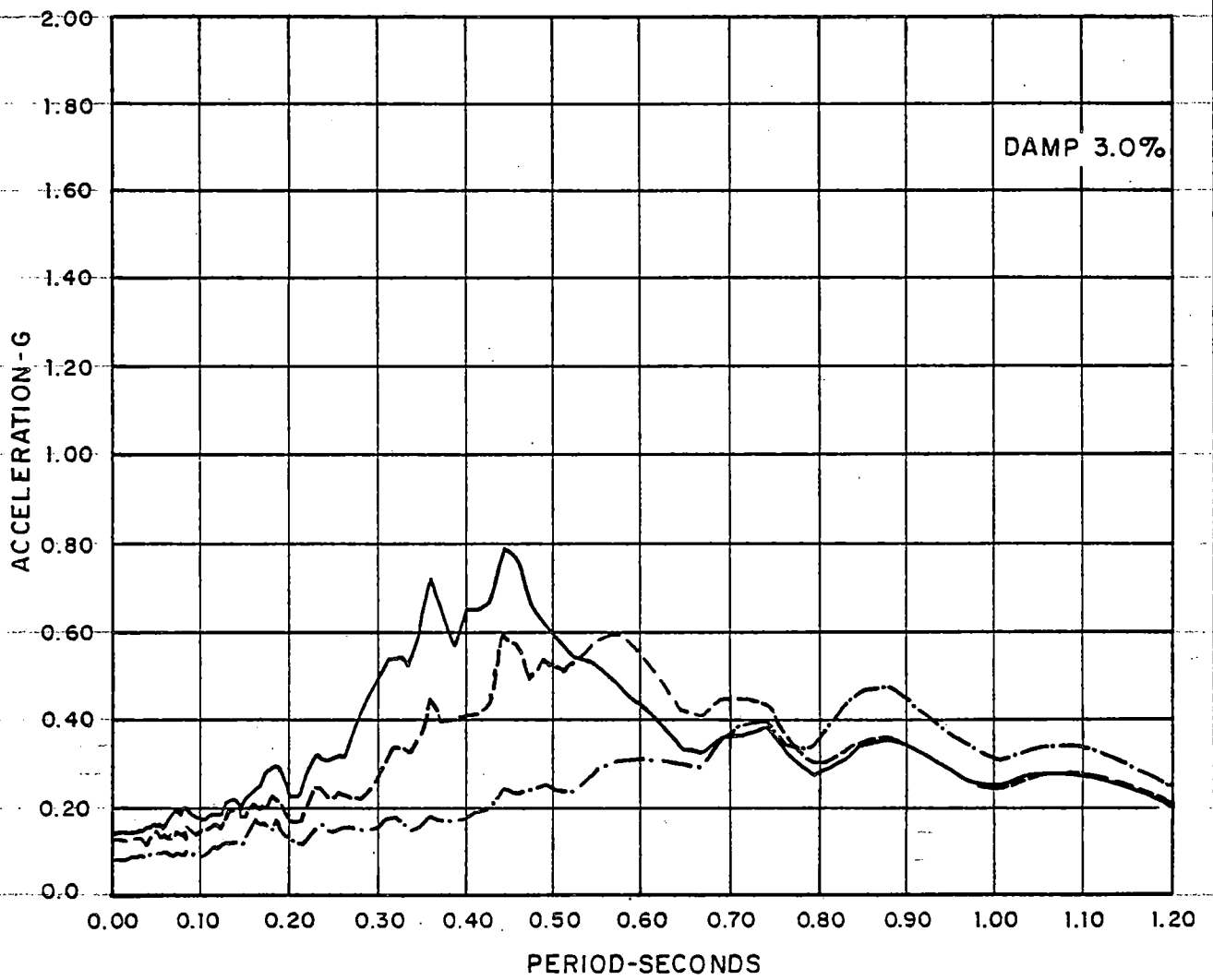
FIGURE 5-22
COMPARISON OF ARS FOR
SOIL PARAMETER VARIATIONS
HORIZONTAL RESPONSE SPECTRUM
AT SPRINGLINE
SURRY POWER STATION-UNITS 1 AND 2



LEGEND

- LAST ITERATION FROM SHAKE USING $G_{max} + 50\%$
- LAST ITERATION FROM SHAKE USING G_{max}
- · - · - LAST ITERATION FROM SHAKE USING $G_{max} - 50\%$

FIGURE 5-23
COMPARISON OF FARs FOR
SOIL PARAMETER VARIATIONS
HORIZONTAL RESPONSE SPECTRUM
AT SPRINGLINE
SURRY POWER STATION-UNITS 1 AND 2



LEGEND

- LAST ITERATION FROM SHAKE USING $G_{max} + 50\%$
- - - - LAST ITERATION FROM SHAKE USING G_{max}
- · - · LAST ITERATION FROM SHAKE USING $G_{max} - 50\%$

FIGURE 5 - 24
COMPARISON OF ARS FOR
SOIL PARAMETER VARIATIONS
 HORIZONTAL RESPONSE SPECTRUM
 AT SPRINGLINE
 SURRY POWER STATION - UNITS 1 AND 2

SURRY POWER STATION, UNITS 1 AND 2

6.0 APPLICATION OF SEISMIC INPUT TO PIPE STRESS ANALYSIS

Seismic input to pipe stress analysis, in general, consists of inertia loads obtained through the application of amplified response spectra and building seismic displacements applied at support points in accordance with the design load combinations for each piping system.

6.1 AMPLIFIED RESPONSE SPECTRA

Amplified response spectra for pipe stress analysis are developed and peak broadened in accordance with methods described in Section 4 of this report. Damping values for piping systems are 0.5 percent for the OBE and 1.0 percent for the DBE.

For piping routed between buildings, or at different elevations within the same building, an enveloped response spectrum curve is developed. This enveloped curve represents the highest acceleration for all periods for either separate buildings or different elevations within the same building.

SURRY POWER STATION, UNITS 1 AND 2

6.2 BUILDING DISPLACEMENTS

Relative seismic structural displacements within a building, as determined from the building seismic analysis, are used as inputs to support motion of piping systems and are considered as static boundary displacements in the piping analysis. For piping running between buildings, the relative support motion includes the effect of each building's motion taken out of phase; this is the most conservative approach.

SURRY POWER STATION, UNITS 1 AND 2

7.0 INVESTIGATION OF THE EFFECTS OF EARTHQUAKES SMALLER THAN THE DBE

Because the soil shear moduli used in the generation of ARS are functions of strain, the ARS are not direct linear functions of maximum ground acceleration. Therefore, it is theoretically possible that at some frequencies the ARS for some smaller earthquake exceed those of the DBE.

The ARS generated for a range of soil moduli provide a basis for estimating the ARS for earthquakes smaller than the DBE. For example, the DBE shear moduli for the first iteration of SHAKE are actually consistent with a smaller earthquake.

For the purpose of this study, an average strain compatible shear modulus for a range of peak horizontal ground accelerations from 0.15 to 0.05 g was determined using SHAKE. The analyses were conducted for the free-field profile using the Taft and El Centro accelerograms and initial Gmax values. The average shear modulus corresponding to each peak horizontal ground acceleration was determined by first averaging the shear moduli from the last iteration of SHAKE for the two accelerograms, then calculating the average value over the profile extending below the containment foundation elevation for a depth of at least 1.5 times the radius of the containment. The variation in average shear modulus versus peak horizontal ground acceleration is given in Figure 7-1.

SURRY POWER STATION, UNITS 1 AND 2

In the course of this study, ARS have been computed for a variety of values of average shear modulus. By referring to Figure 7-1, the peak acceleration can be established that corresponds to each of these values of average shear modulus.

The maximum ground acceleration consistent with the various moduli, divided by 0.15 g, yields a ratio that can be applied to the ARS calculated using the first iteration SHAKE moduli for the DBE. These ratios were used to scale spectra at the operating floor.

Figure 7-2 shows that the resulting family of ARS at the operating floor are enveloped by the DBE spectrum, demonstrating that the effects of the DBE are not exceeded by those of smaller earthquakes. Therefore, it can be concluded that the stresses in piping due to the DBE are not exceeded by those due to smaller earthquakes.

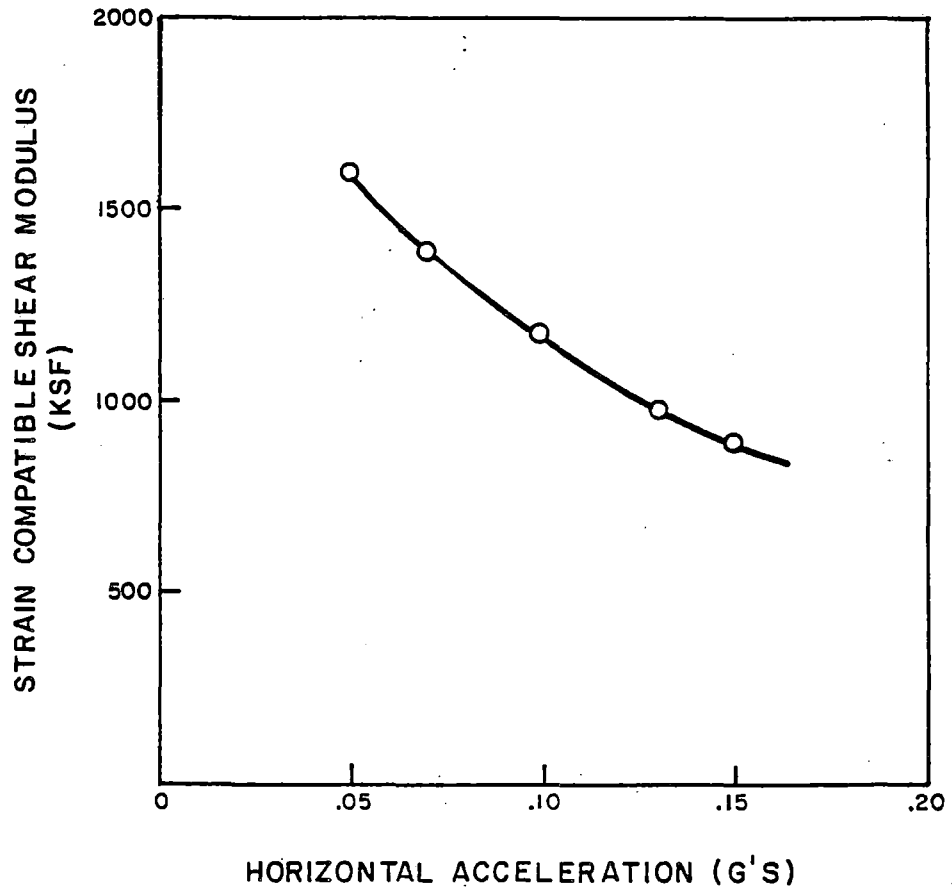
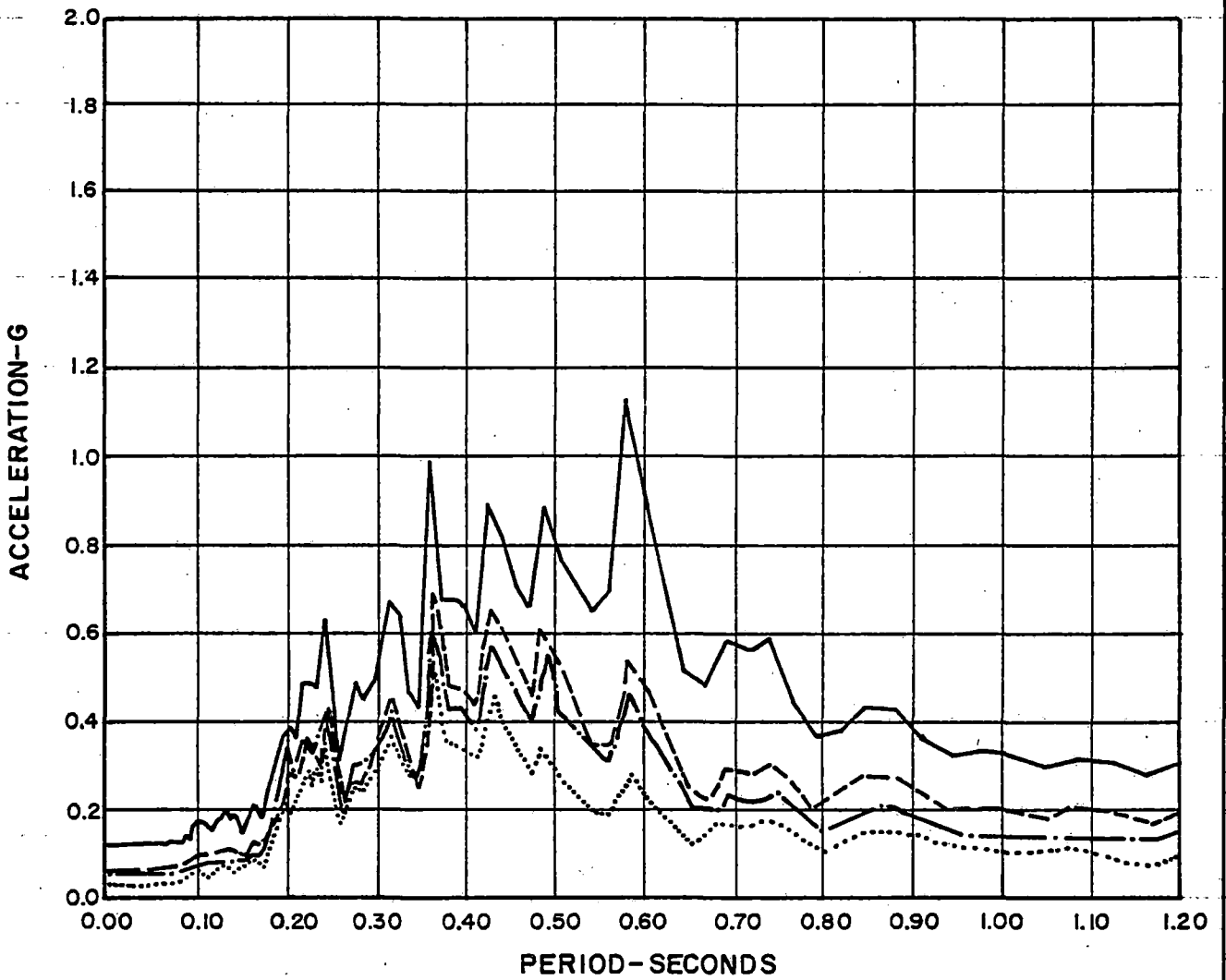


FIGURE 7-1
VARIATION OF SHEAR MODULUS
WITH GROUND ACCELERATION
SURRY POWER STATION - UNITS 1 & 2



LEGEND

- 0.15G
- - - - - 0.082G
- · - · - 0.07G
- 0.05G

FIGURE 7-2
SEISMIC ANALYSIS OF CONTAINMENT FOR
VARIOUS MAXIMUM GROUND ACCELERATIONS
HORIZONTAL RESPONSE SPECTRUM AT
THE OPERATING FLOOR
SURRY POWER STATION-UNITS 1 AND 2

SURRY POWER STATION, UNITS 1 AND 2

8.0 CONCLUSIONS

Based upon the data and studies in this report, the following conclusions can be drawn about the use of soil-structure interaction (SSI) analysis in developing amplified response spectra (ARS) for the Surry Power Station site.

8.1 USE OF SOIL-STRUCTURE INTERACTION

The principles and the methodology of SSI as used herein to develop ARS are applicable to the Surry site and can be used with confidence to conservatively predict the seismic forces on piping systems.

8.2 SOIL PROPERTIES

The soil investigations made at the site to provide information for the licensing and design of Units 1, 2, 3, and 4 are summarized in Section 2 of this report. The data from these investigations provide an adequate basis for the development of strain compatible soil properties for use in the SSI analysis.

Soil shear moduli values derived from in situ measurements at the Surry site are consistent with those obtained from empirical relationships.

SURRY POWER STATION, UNITS 1 AND 2

The use of low strain shear moduli (G_{max}) values for soil is not appropriate in developing ARS because earthquake-induced soil strain levels are approximately 2 orders of magnitude higher than low strain levels.

Using a range of low strain shear moduli values, equal to ± 50 percent of the mean value, to develop the strain compatible free-field soil profile is excessive when compared to a standard deviation on measured values for saturated clays subjected to varying strain levels. A more meaningful range would be a variation of the iterated strain compatible soil shear moduli values by ± 50 percent of the mean value.

8.3 GROUND RESPONSE

Licensed ground response spectra and an enveloping artificial time history as input motion at the ground surface in the free field is appropriate for use in the SSI-ARS analysis.

8.4 AMPLIFIED RESPONSE ANALYSIS

The use of the multi-step analysis procedure described in Section 4 of this report provides an approach that includes conservatism in stating the magnitude of the amplified acceleration values and allows development of the

SURRY POWER STATION, UNITS 1 AND 2

problem in a series of logical steps convenient for an engineering evaluation of results.

8.5 COMPARISON OF RESULTS

The results of comparing the different methodologies, the FSAR earthquake compared with the Regulatory Guide 1.60 earthquake and the effect of varying soil parameters lead to the following conclusions:

1. Comparison of ARS shown in Figures 5-1 through 5-3, calculated using the three-step analysis (REFUND/FRIDAY) and the one-step analysis (PLAXLY), show good agreement at all building levels with respect to frequencies at which peaks occur. The magnitudes of amplified acceleration agree reasonably well at lower levels in the structure. At higher levels, the REFUND/FRIDAY results generally exceed the PLAXLY results. At some frequencies, the ARS calculated for the base mat by REFUND/FRIDAY have amplitudes less than those obtained from PLAXLY. Since the spectral amplitudes involved are small fractions of 1.0 g, there would be no serious consequences in using these spectra in pipe stress analysis. Nevertheless, it is concluded that base mat spectra will not be used in pipe stress analyses.

SURRY POWER STATION, UNITS 1 AND 2

2. Comparisons of ARS made from Regulatory Guides 1.60 ground response spectra and 1.61 damping values and ARS calculated on the basis of the FSAR committed ground response spectra and damping values indicate good agreement in amplitude and frequencies of the peaks.
3. A comparison of ARS for soil parameter variations in Figures 5-7 through 5-15 using low strain shear modulus (G_{max}), first iteration SHAKE, and last iteration SHAKE soil properties shows little variation in frequency of peaks but increasing amplitude of peaks with increasing shear modulus values.
4. Comparisons of ARS for soil parameter variations in Figures 5-16 through 5-24 using strain compatible soil properties from the last iteration of SHAKE based upon (a) the low strain shear modulus (G_{max}) input to SHAKE, (b) $G_{max} + 50$ percent input to SHAKE, and (c) $G_{max} - 50$ percent input to SHAKE show a large variation in amplitude and frequency of the maximum response.
5. Changes in the shear modulus of the soil change the frequencies at which the amplification function has its peaks. This shift in frequency is evident in the general shapes of the response spectra for different values of G . The exact frequencies of the specific individual peaks are influenced by the frequency content of the

SURRY POWER STATION, UNITS 1 AND 2

artificial earthquake, so that each individual peak appears in all spectra. However, the essential phenomenon displayed is a shift in frequency of the amplification function, causing different pre-existing peaks to be selected for amplification.

6. The results show that ARS are not sensitive to torsion in the structure.
7. Studies conducted on three sample pipe stress problems, shown in Tables 5-1, 5-2, and 5-3, compare the results of using ARS based upon Regulatory Guides 1.60 and 1.61 versus FSAR requirements in terms of pipe stresses. Examination of these results shows that neither earthquake produces excessive inertia stress.
8. Spectra calculated using the three-step method, the FSAR Design Basis Earthquake (DBE), the FSAR DBE structure and piping damping values, and the strain compatible free-field soil properties are an adequate basis for analysis of piping systems when peak broadened ± 15 percent. In order to provide additional conservatism encompassing the effects of an exceptionally wide variation in soil properties, the resulting inertia forces on the piping system will be increased by 50 percent in accordance with the NRC position confirmed in a letter dated May 25, 1979.

SURRY POWER STATION, UNITS 1 AND 2

8.6 APPLICATION OF ARS TO PIPE STRESS ANALYSIS

The application of seismic input to pipe stress analysis as defined in Section 6 of this report is conservative and serves as an adequate basis for reevaluation of the designated piping systems.

8.7 EFFECTS OF GROUND ACCELERATION ON ARS

The ARS resulting from the DBE are not exceeded by those of smaller earthquakes. Therefore, the inertial pipe stresses due to the DBE are an adequate basis for qualification of piping.

8.8 COMPUTER PROGRAM VERIFICATION

The computer programs used to generate the SSI ARS have been qualified by (1) comparison of results to those obtained from similar programs which are recognized and widely used; or (2) comparison of program results to those obtained by hand calculations or analytical results published in technical literature. These comparisons are shown for the SHAKE, PLAXLY, REFUND, KINACT, and FRIDAY programs in Section 9 of this report. Reasonable agreement is demonstrated for these computer programs.

SURRY POWER STATION, UNITS 1 AND 2

9.1 SHAKE

SHAKE is a public domain computer program developed at the University of California and described by Schnabel, Lysmer, and Seed.⁽¹⁾ Stone & Webster has made a few changes in the program, principally the addition of plotter capability and improvement of some of the output format, but the program in use for this work is essentially that described by Schnabel, et al.

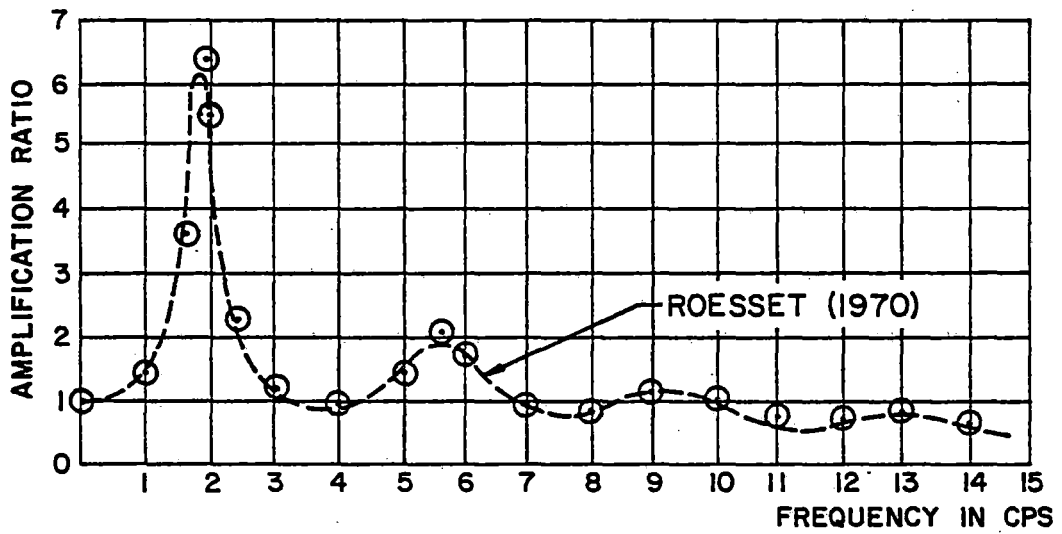
The program solves the problem of vertically propagating shear waves in a layered medium. The values of shear modulus and damping for a particular layer depend on the average shear strain induced in that layer by the earthquake. The program iterates to obtain values of modulus and damping that are compatible with the strains and with curves of modulus and damping versus strain.

Although the program is well known and widely used, Stone & Webster has checked the results computed by the program against those developed independently by Roesset⁽²⁾ and has also checked that the calculations of modulus and damping are internally consistent. For example, Figure 9.1-1 shows the comparison of the amplification functions from SHAKE and Roesset's analysis for the first iteration on the soil profile in Figure 9.1-2.

SURRY POWER STATION, UNITS 1 AND 2

REFERENCES

1. Schnabel, P.B.; Lysmer, J.; and Seed, H.B. SHAKE: A Computer Program for Earthquake Response Analysis of Horizontally Layered Sites, Earthquake Engineering Center, Report No. EERC 72-12, University of California, Berkeley, California, December 1972.
2. Roesset, J.M., Fundamentals of Soil Amplification. In: Seismic Design for Nuclear Power Plants, R.J. Hansen, ed., M.I.T. Press, Cambridge, Mass., 1970, pp 183-244.



⊙ NUMERICAL OUTPUT-SHAKE RUN M7253201

FIGURE 9.1-1
 AMPLIFICATION FUNCTION OF SOIL
 SURRY POWER STATION-UNITS 1 AND 2

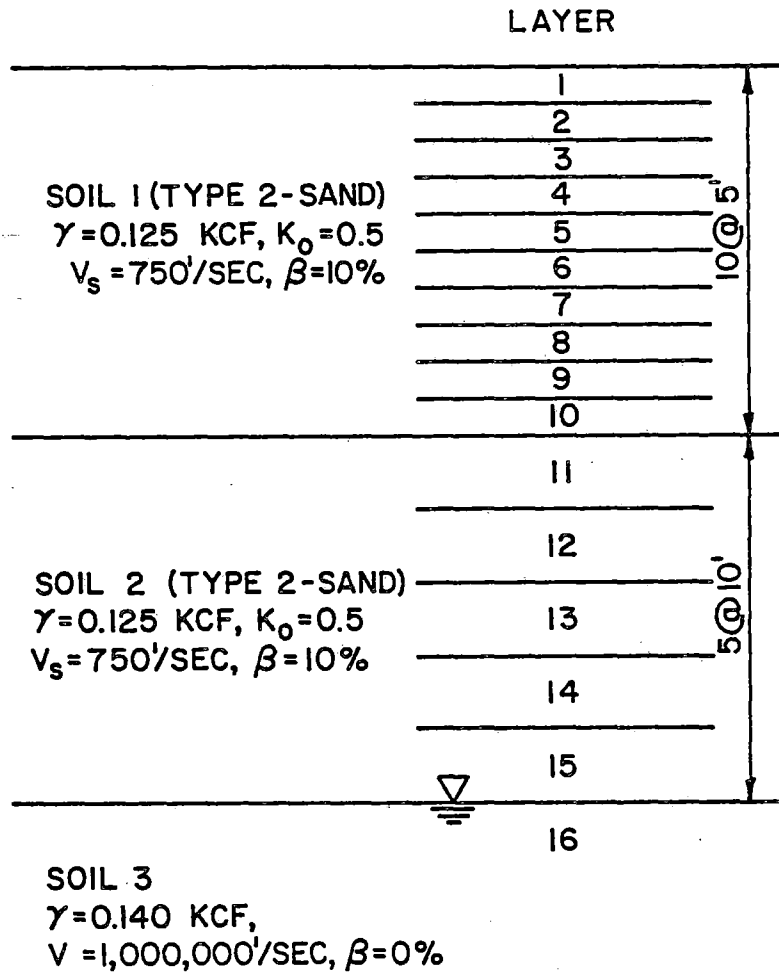


FIGURE 9.1-2
 SOILS PROFILE USED FOR THE
 VERIFICATION OF SHAKE
 SURRY POWER STATION-UNITS 1 AND 2

9.2 PLAXLY

PLAXLY is an isoparametric, plane-strain, finite element computer program used in seismic soil-structure analysis. The equations of motion are solved in the frequency domain.

A primary element in the PLAXLY solution is the consistent transmitting boundary modeling the layered far-field. This boundary avoids the unrealistic reflections associated with more simplistic "free" or "roller" lateral boundary conditions.

The principal limitations upon the program and its application are the following:

1. Geometry and material properties must be such that they can be satisfactorily modeled in two dimensions.
2. Properties of the layered far-field cannot change horizontally.
3. Base rock is assumed to be infinitely stiff.
4. Material properties are isotropic, linearly elastic.

SURRY POWER STATION, UNITS 1 AND 2

For purposes of comparison, the results of PLAXLY and those of a similar program in the public domain, FLUSH (CDC Version 2.2), are shown in Figure 9.2-1. The PLAXLY flow diagram is shown in Figure 9.2-2.

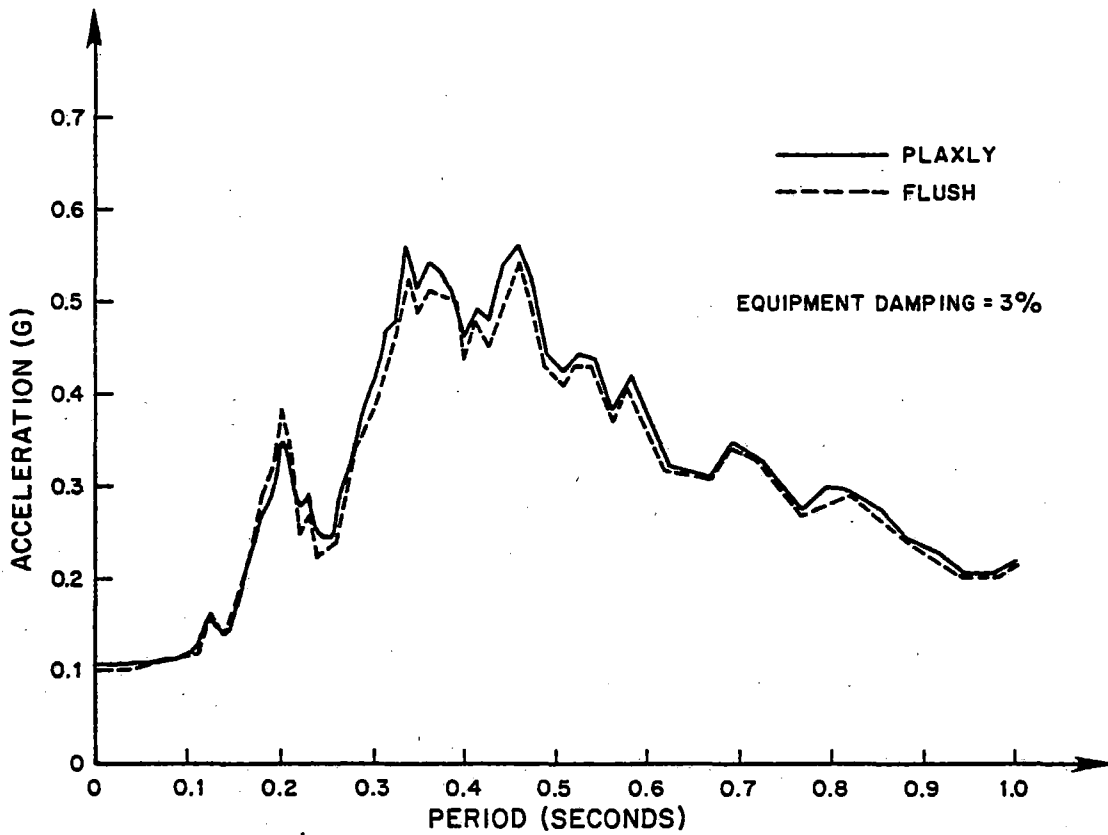


FIGURE 9.2-1
 COMPARISON OF ARS BY PLAXLY
 AND FLUSH AT OPERATING FLOOR
 SURRY POWER STATION-UNITS 1 AND 2

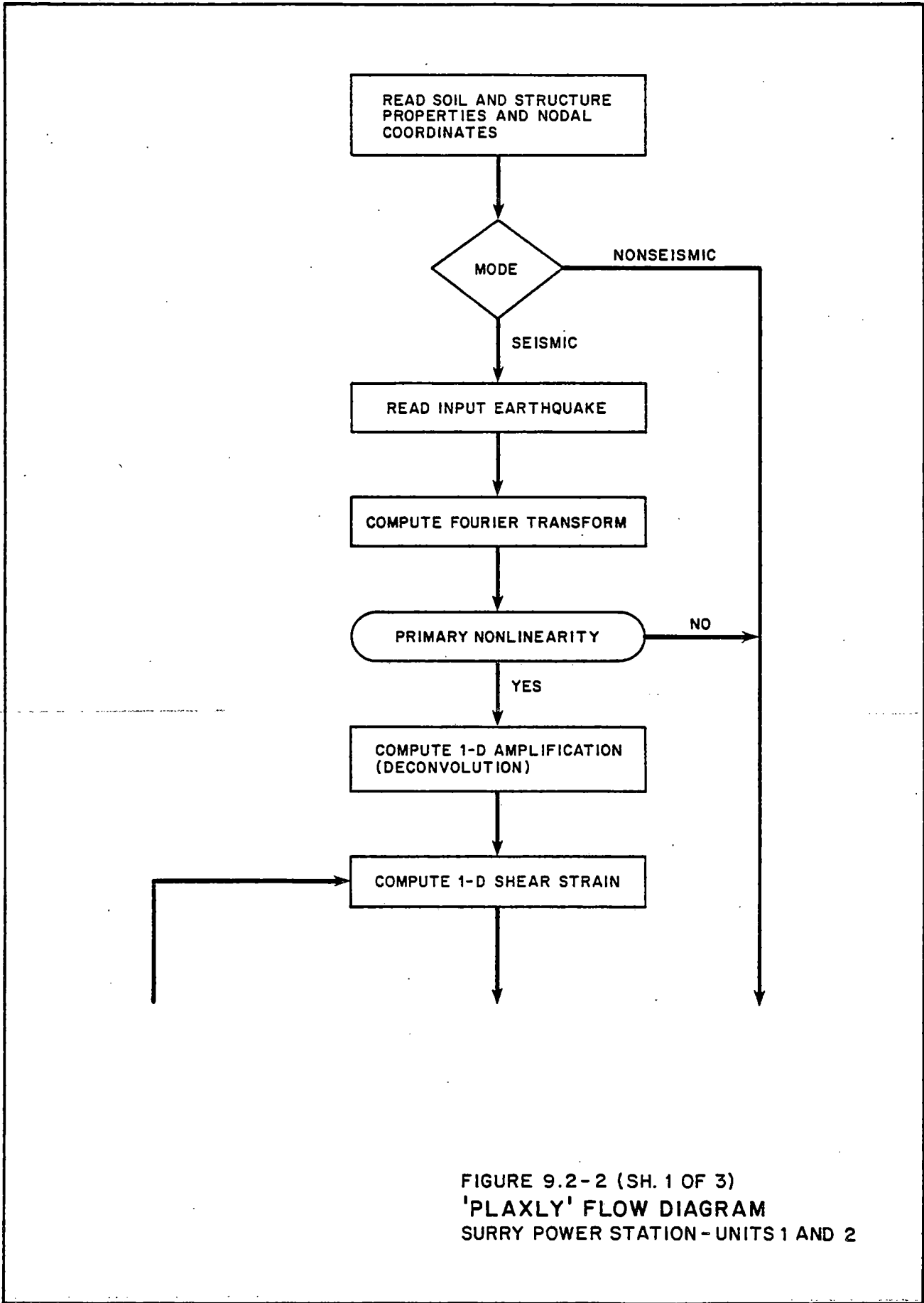


FIGURE 9.2-2 (SH. 1 OF 3)
'PLAXLY' FLOW DIAGRAM
SURRY POWER STATION - UNITS 1 AND 2

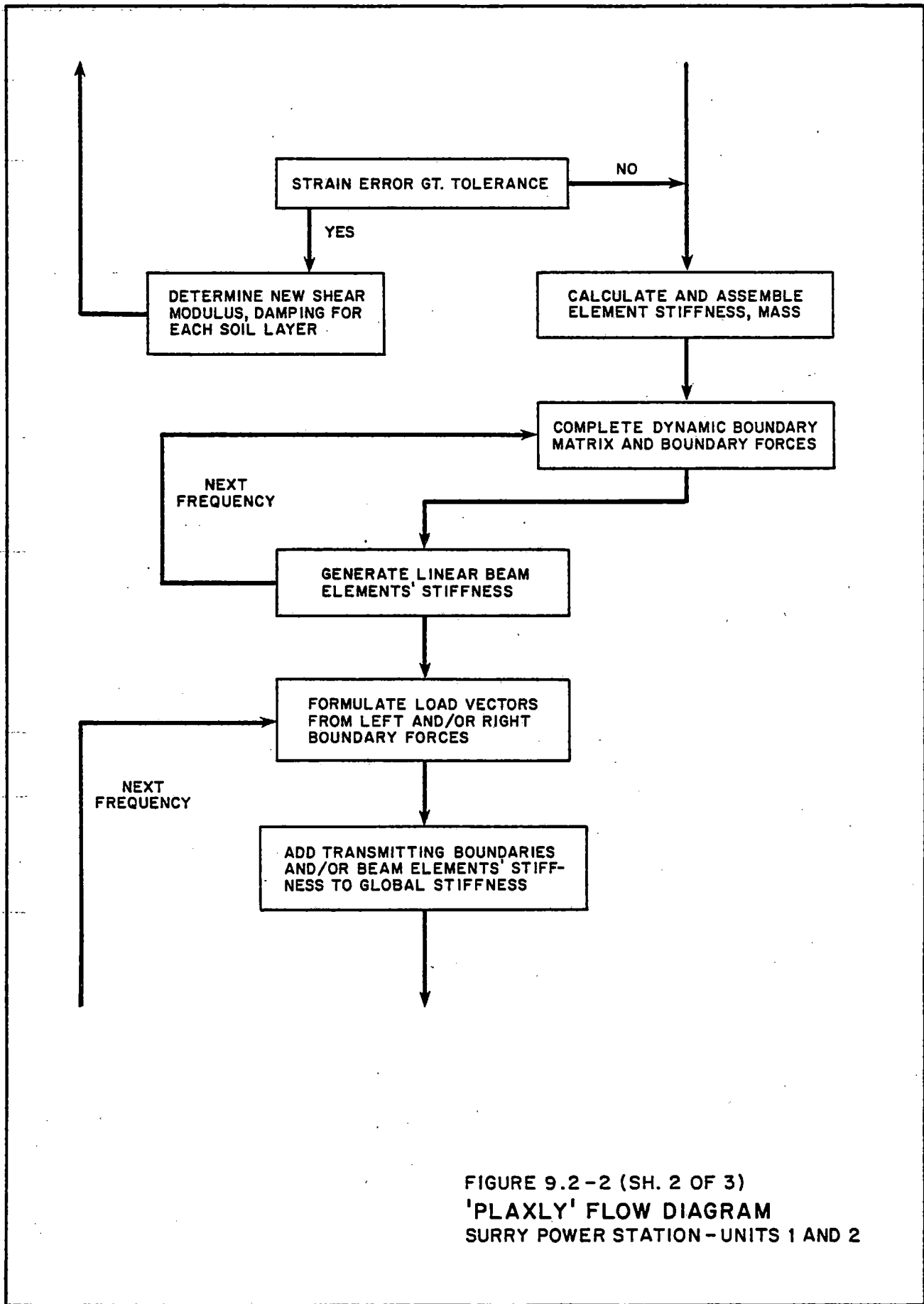


FIGURE 9.2-2 (SH. 2 OF 3)
 'PLAXLY' FLOW DIAGRAM
 SURRY POWER STATION - UNITS 1 AND 2

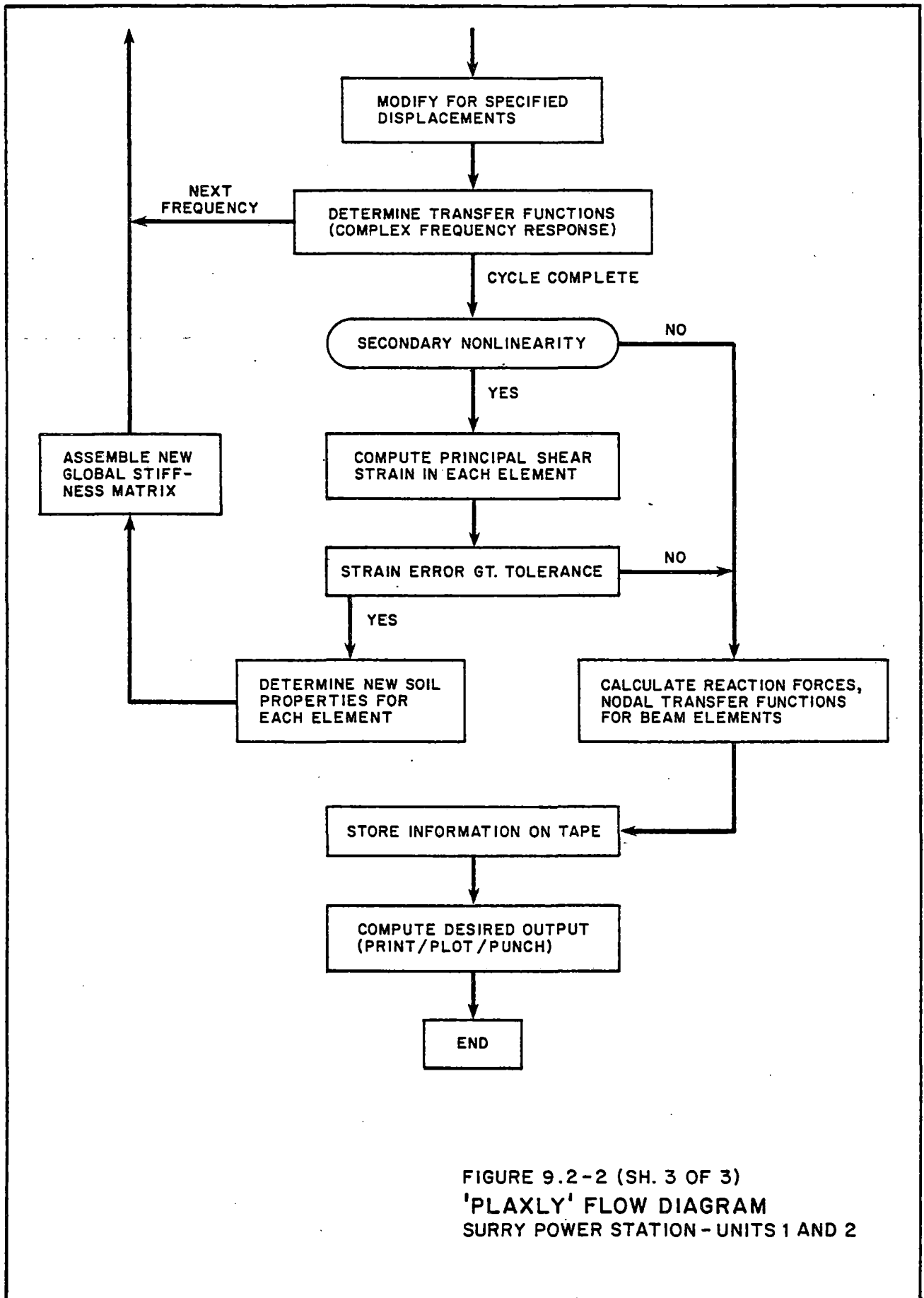


FIGURE 9.2-2 (SH. 3 OF 3)
 'PLAXLY' FLOW DIAGRAM
 SURRY POWER STATION - UNITS 1 AND 2

SURRY POWER STATION, UNITS 1 AND 2

9.3 REFUND AND EMBED

The computer program REFUND is used for computation of the dynamic stiffness functions (impedance functions) of a rigid, massless, rectangular plate welded to the surface of a viscoelastic, layered stratum. The subgrade stiffness matrix is evaluated for all six degrees of freedom for the range of frequencies specified by the user. Embedment effects are applied subsequently by the program EMBED.

The program reads the topology and material properties, assembles the subgrade flexibility matrix, and determines the foundation impedances by inversion. The subgrade flexibility matrix is determined with discrete solutions, to the problems of Cerruti and Boussinesq. A cylindrical column of linear elements is joined to a consistent transmitting boundary, and the flexibility coefficients found by applying unit horizontal and vertical loads at the axis. The rectangular plate is discretized into a number of nodal points, and the global flexibility matrix found using the technique just described. The foundation stiffnesses are then determined solving a set of linear equations which result from imposing unit rigid body translations and rotations to the plate.

Since REFUND is restricted to surface-founded plates, the effects of embedment are included by adjusting the REFUND results with the program EMBED. The

SURRY POWER STATION, UNITS 1 AND 2

theoretical bases of these programs and their application to the solution methodology are described in Section 4.2.

The results of REFUND compare very well with published results. The comparisons shown in Figures 9.3-2 through 9.3-7 are based upon "Impedance Functions for a Rigid Foundation on a Layered Medium", J.E. Luco, Nuclear Engineering and Design, Vol 2, 1974. Of the various solutions presented by Luco, the following was selected for comparison (see Figure 9.3-1):

	<u>Layer 1</u>	<u>Layer 2</u>
Shear wave velocity	1	1.25
Specific weight	1	1.1764
Poisson's ratio	0.25	0.25

The comparisons shown are of the coefficients k and c from which the vertical, translational, and rocking impedances can be expressed:

$$K = K_0 [k + ia_0 c]$$

in which a_0 is a dimensionless measure of frequency and K_0 is a zero-frequency stiffness.

SURRY POWER STATION, UNITS 1 AND 2

The minor differences shown between the REFUND result and Luco's analysis can be attributed to the use of an "equivalent" rectangular plate in the REFUND analysis (Luco's is circular) and differences in boundary conditions at the footing (rough vs. smooth).

The REFUND and EMBED flow diagrams are shown in Figure 9.3-8.

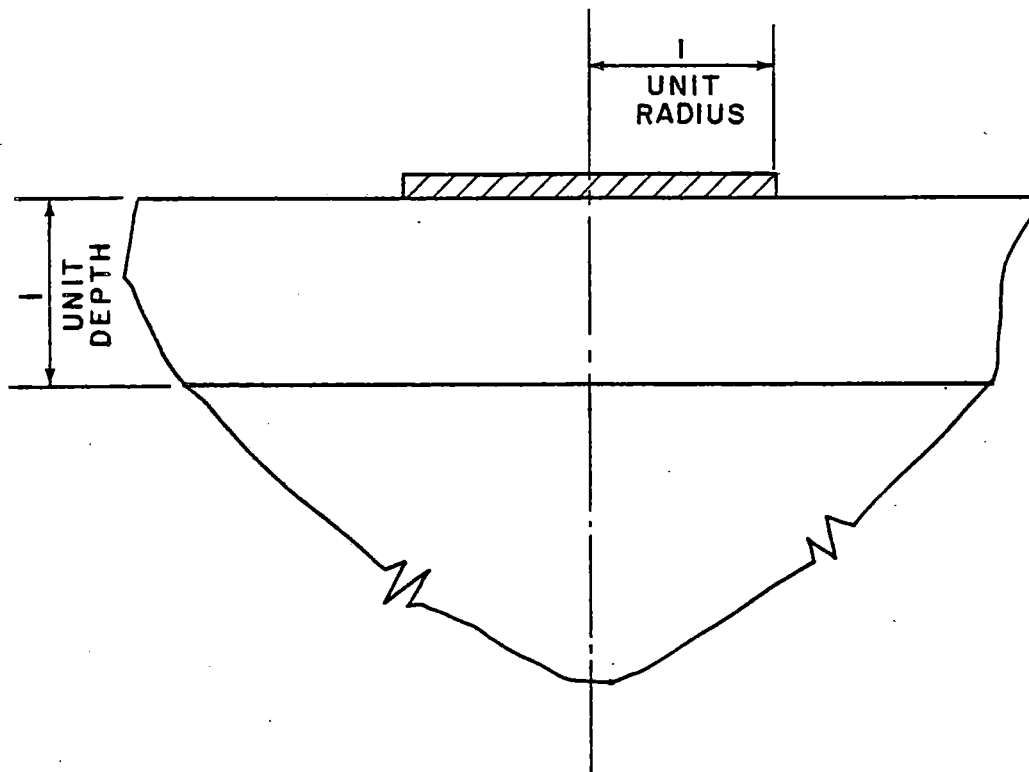


FIGURE 9.3-1
LUCO'S TWO-LAYER PROBLEM
SURRY POWER STATION - UNITS 1 AND 2

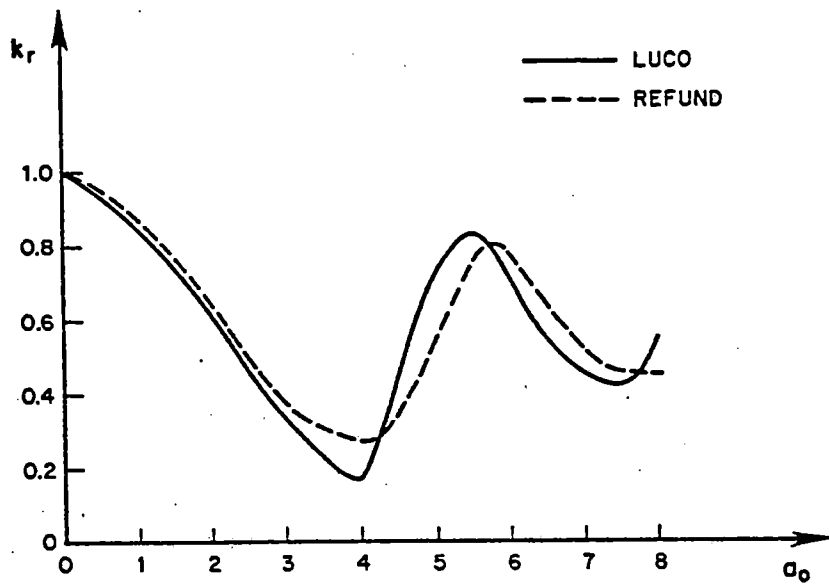


FIGURE 9.3-2
ROCKING STIFFNESS COMPARISON-
REAL PART
SURRY POWER STATION - UNITS 1 AND 2

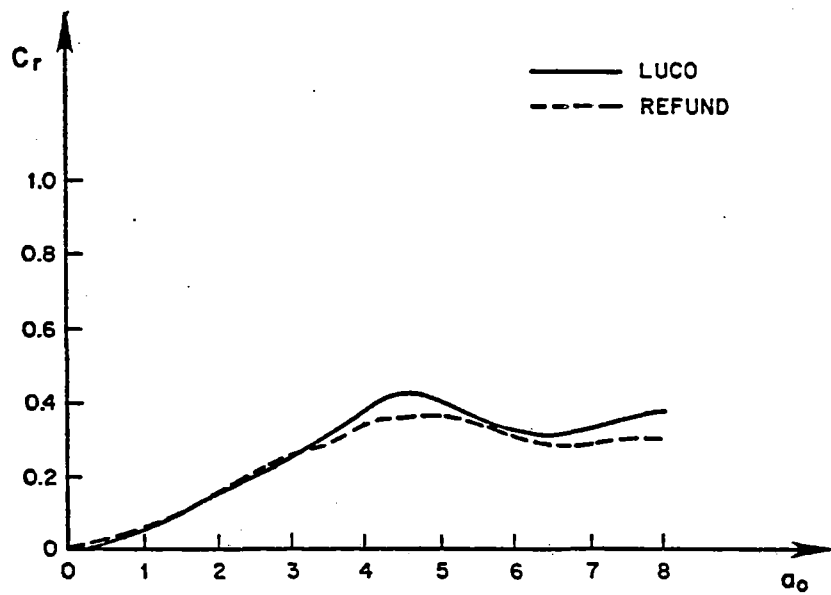


FIGURE 9.3-3
ROCKING STIFFNESS COMPARISON-
IMAGINARY PART
SURRY POWER STATION-UNITS 1 AND 2

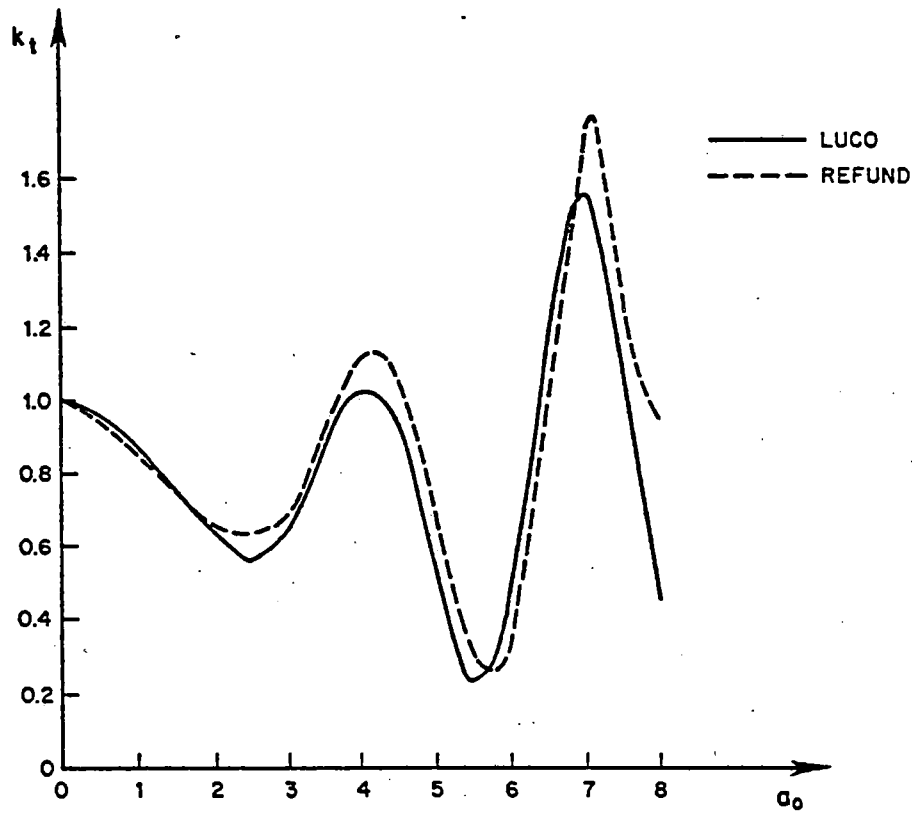


FIGURE 9.3-4
 HORIZONTAL STIFFNESS COMPARISON-
 REAL PART
 SURRY POWER STATION-UNITS 1 AND 2

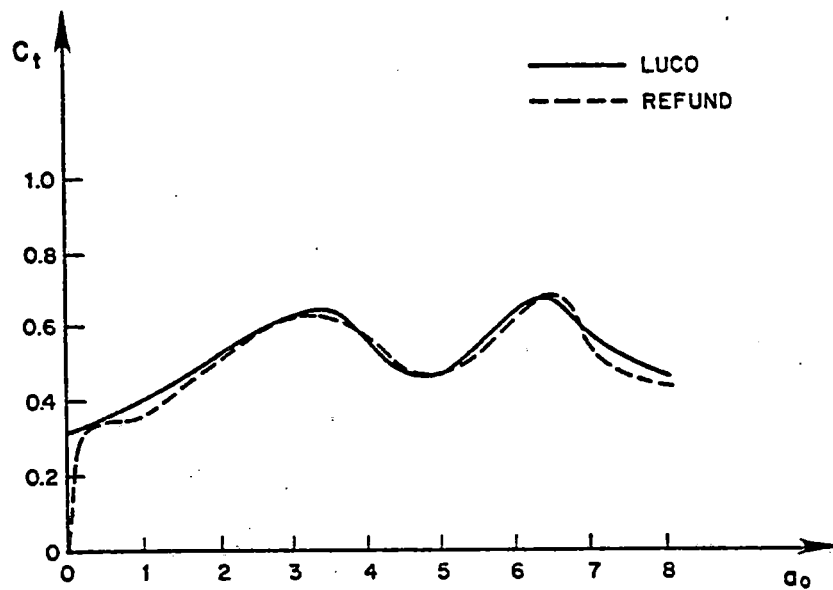


FIGURE 9.3-5
 HORIZONTAL STIFFNESS COMPARISON-
 IMAGINARY PART
 SURRY POWER STATION-UNITS 1 AND 2

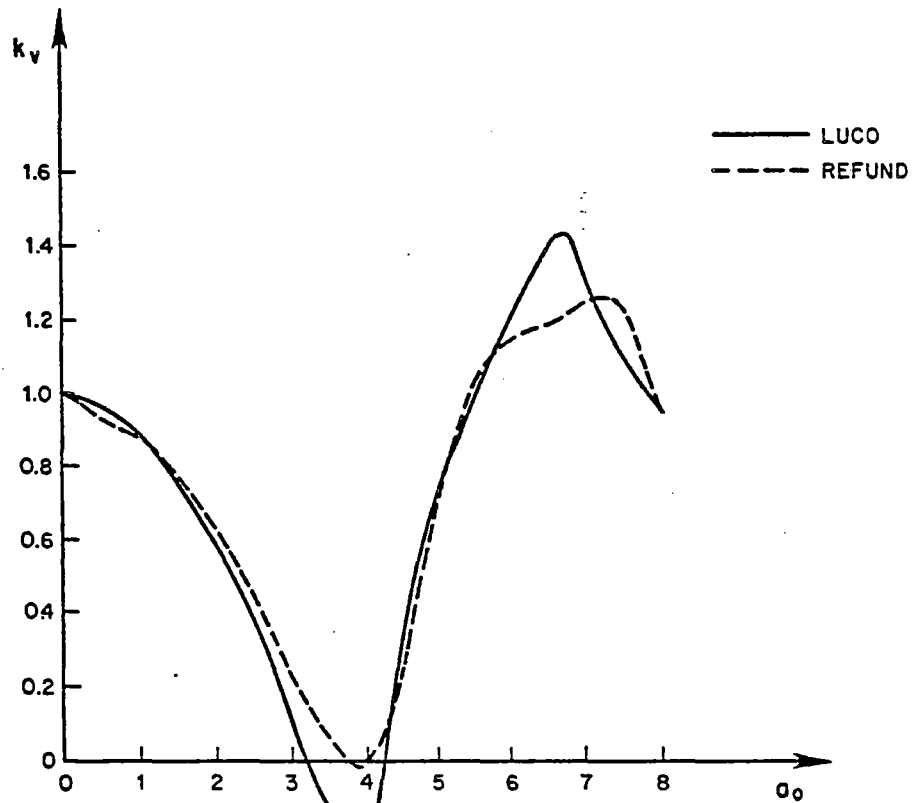


FIGURE 9.3-6
 VERTICAL STIFFNESS COMPARISON-
 REAL PART
 SURRY POWER STATION- UNITS 1 AND 2

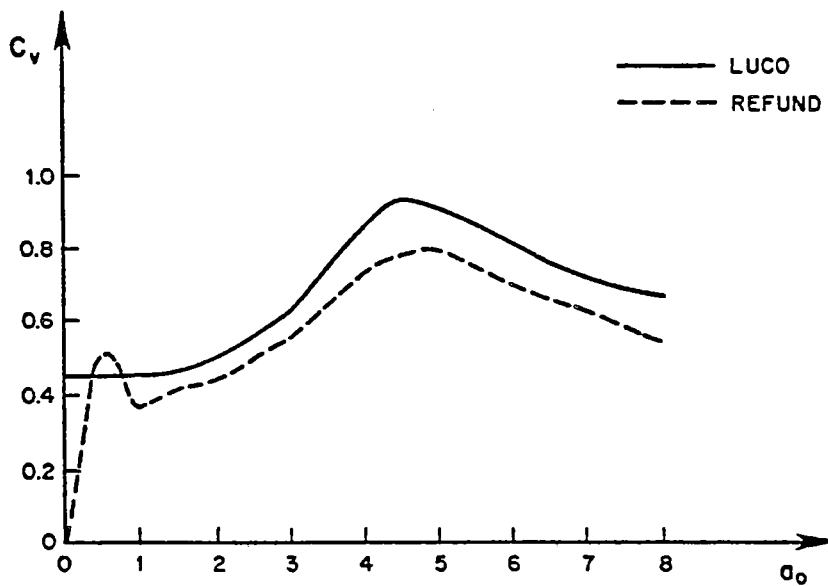


FIGURE 9.3-7
 VERTICAL STIFFNESS COMPARISON-
 IMAGINARY PART
 SURRY POWER STATION-UNITS 1 AND 2

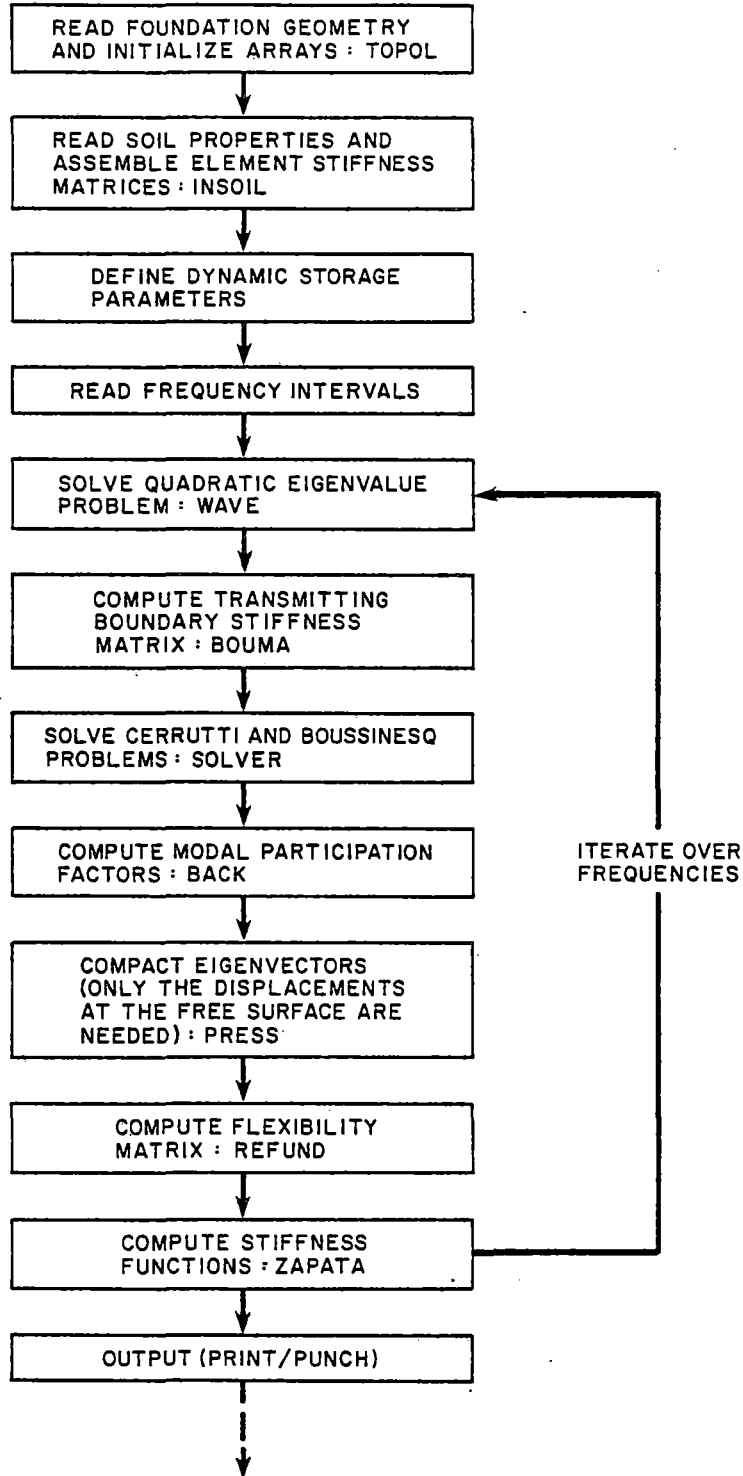


FIGURE 9.3-8 (SH. 1 OF 2)
 'REFUND' AND 'EMBED'
 FLOW DIAGRAMS
 SURRY POWER STATION - UNITS 1 AND 2

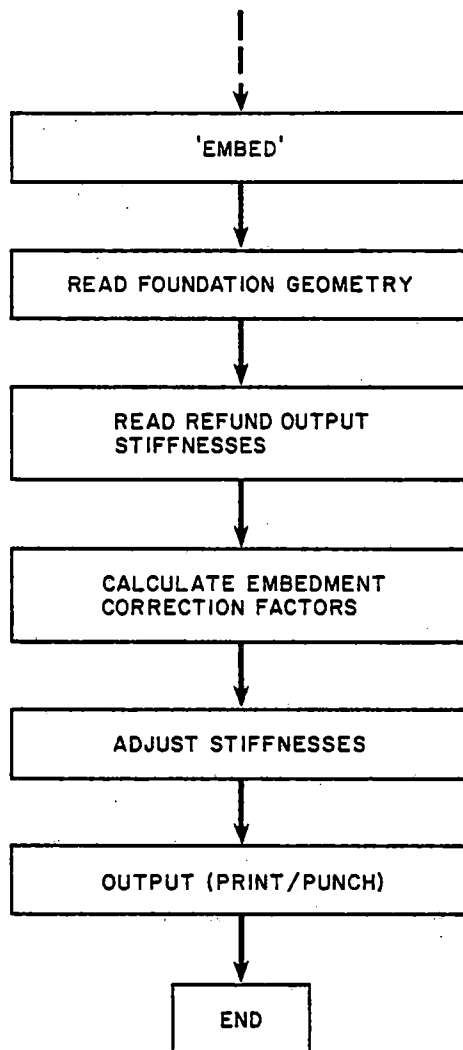


FIGURE 9.3-8 (SH. 2 OF 2)
'REFUND' AND 'EMBED'
FLOW DIAGRAMS
SURRY POWER STATION-UNITS 1 AND 2

9.4 KINACT

KINACT is a computer program used in the three-step solution of soil-structure interaction problems. Briefly, the program modifies the specified translational time history at the surface to translational and rotational time histories at the base of a rigid, massless foundation.

The theoretical basis for the program is derived from wave propagation theory and parametric studies of finite element solutions, described in more detail in Section 4.1.3. Comparisons of the spectra of translational and rotational motion predicted by KINACT and by PLAXLY are shown in Figures 9.4-1 and 9.4-2.

As the figures indicate, KINACT slightly underestimates the translational part of the motion, but significantly overstates the rotational part. This condition results from the dependence of the two variables U and ϕ

$$\ddot{\phi} = C \frac{(\ddot{U}_S - \ddot{U}_B)}{E}$$

SURRY POWER STATION, UNITS 1 AND 2

where

\ddot{U}_S = surface translational acceleration

\ddot{U}_B = translational acceleration of rigid
massless foundation

C = constant

E = embedment

This self-compensating feature of the formulation is insurance against an unconservative result.

The KINACT flow diagram is shown in Figure 9.4-3.

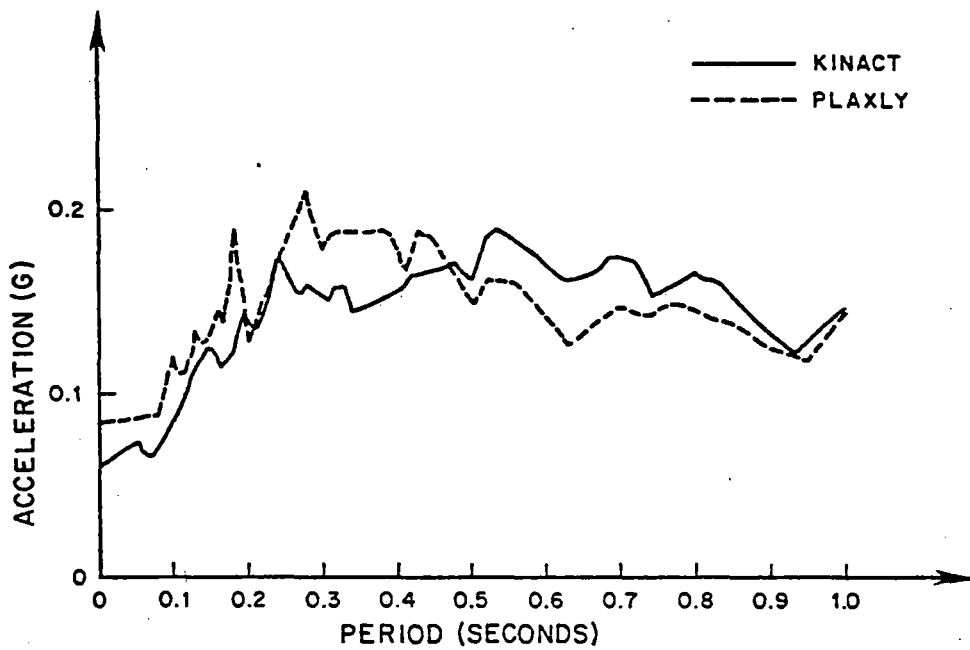


FIGURE 9.4-1
TRANSLATIONAL RESPONSE SPECTRA AT
BASE OF RIGID, MASSLESS FOUNDATION
SURRY POWER STATION-UNITS 1 AND 2

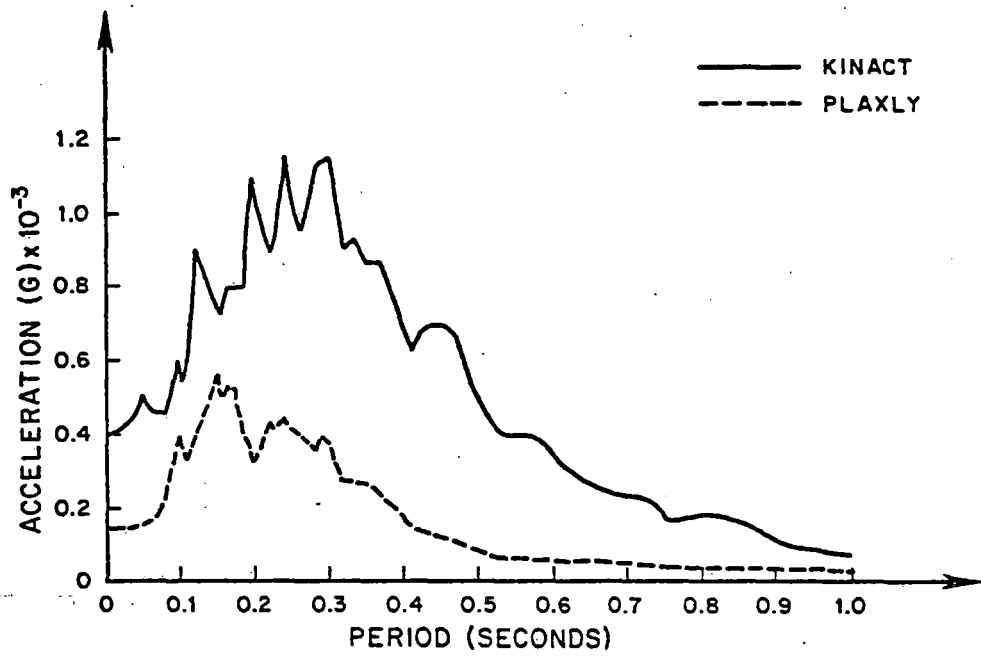


FIGURE 9.4-2
 ROTATIONAL RESPONSE SPECTRUM AT
 BASE OF RIGID, MASSLESS FOUNDATION
 SURRY POWER STATION - UNITS 1 AND 2

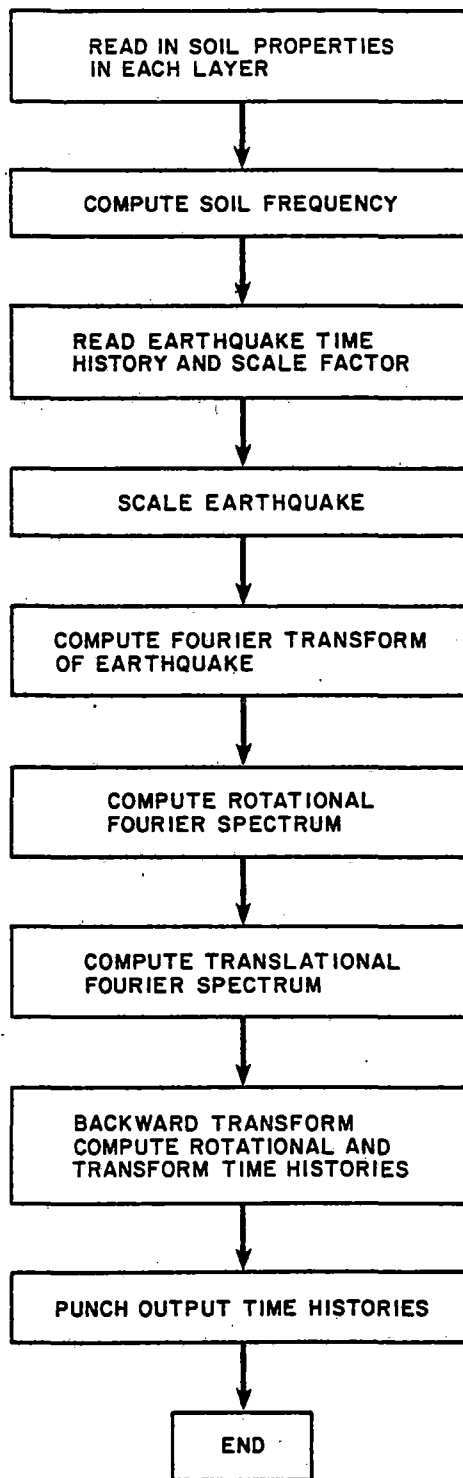


FIGURE 9.4-3
'KINACT' FLOW DIAGRAM
SURRY POWER STATION - UNITS 1 AND 2

SURRY POWER STATION, UNITS 1 AND 2

9.5 FRIDAY

The computer program FRIDAY is used for dynamic analysis of structures subjected to seismic loads, accounting for soil-structure interaction by means of frequency-dependent complex soil springs.

The structure is idealized as a set of lumped masses connected by springs or linear members, and attached to a common support, the mat. The latter is supported by soil springs or impedances, which may or may not be frequency-dependent. Alternatively, the mat may rest on a rigid subgrade. The structure may be three-dimensional, but cannot be interconnected; each structure has to be simply connected. Fourier transform techniques are used to determine time histories; cutoff frequency is prescribed internally to 15 Hz.

The theoretical basis and implementation of the program is described in Section 4.1.4. A comparison of FRIDAY with a public domain program, STARDYNE, for the seismic response of a fixed base, multi-mass, cantilever model is shown in Figure 9.5-1. The model is shown in Figure 9.5-2.

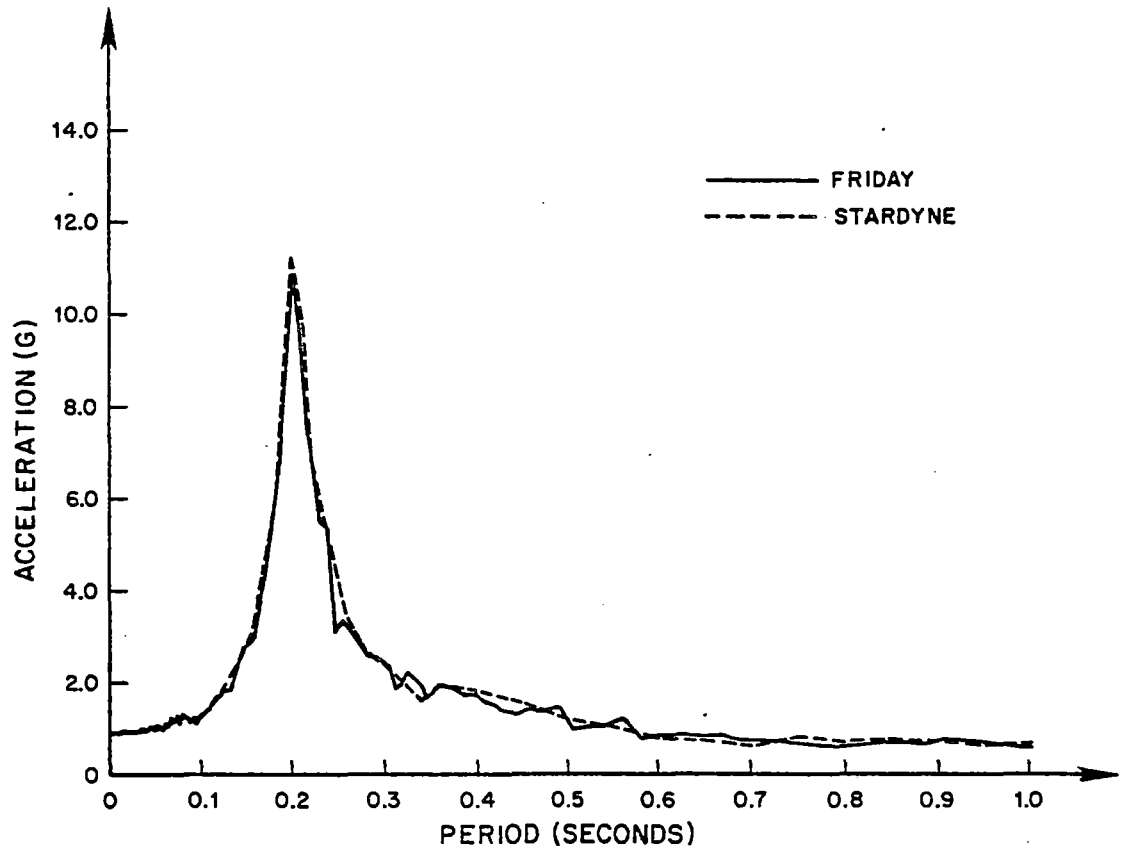


FIGURE 9.5-1
COMPARISON OF 'FRIDAY' AND
'STARDYNE'-ARS AT THE ROOF
SURRY POWER STATION-UNITS 1 AND 2

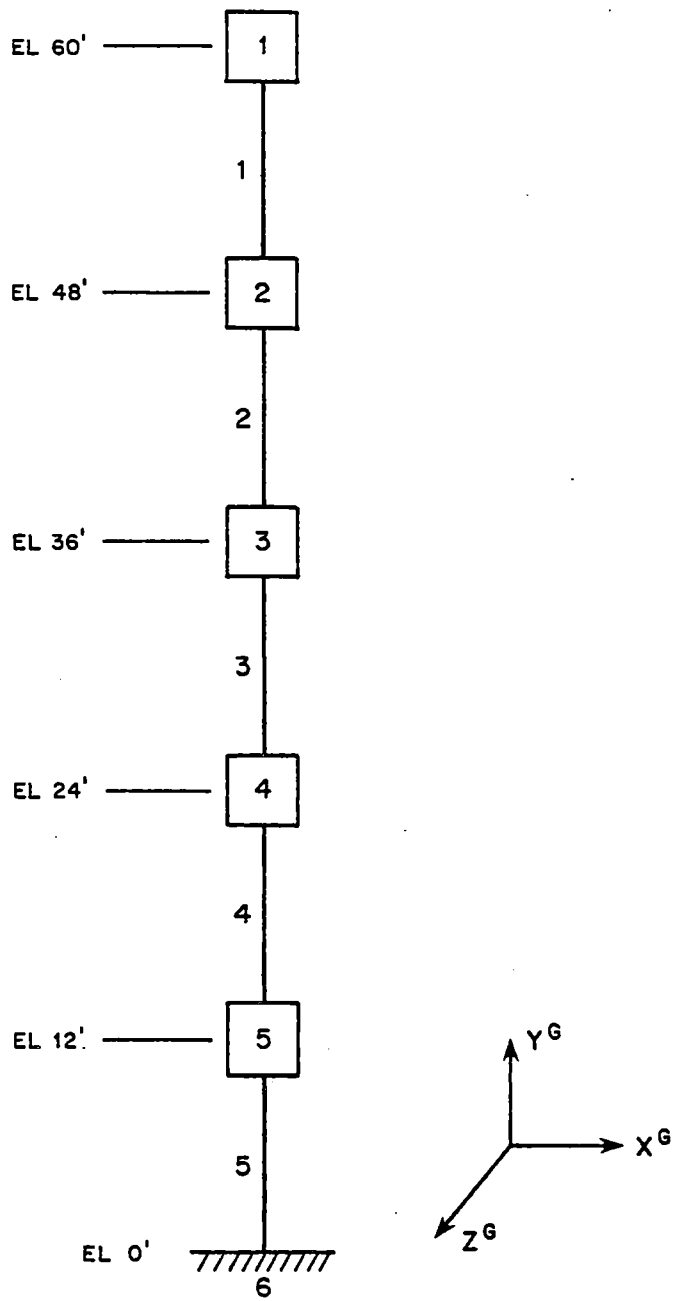


FIGURE 9.5-2
 'STARDYNE' MODEL
 SURRY POWER STATION—UNITS 1 AND 2

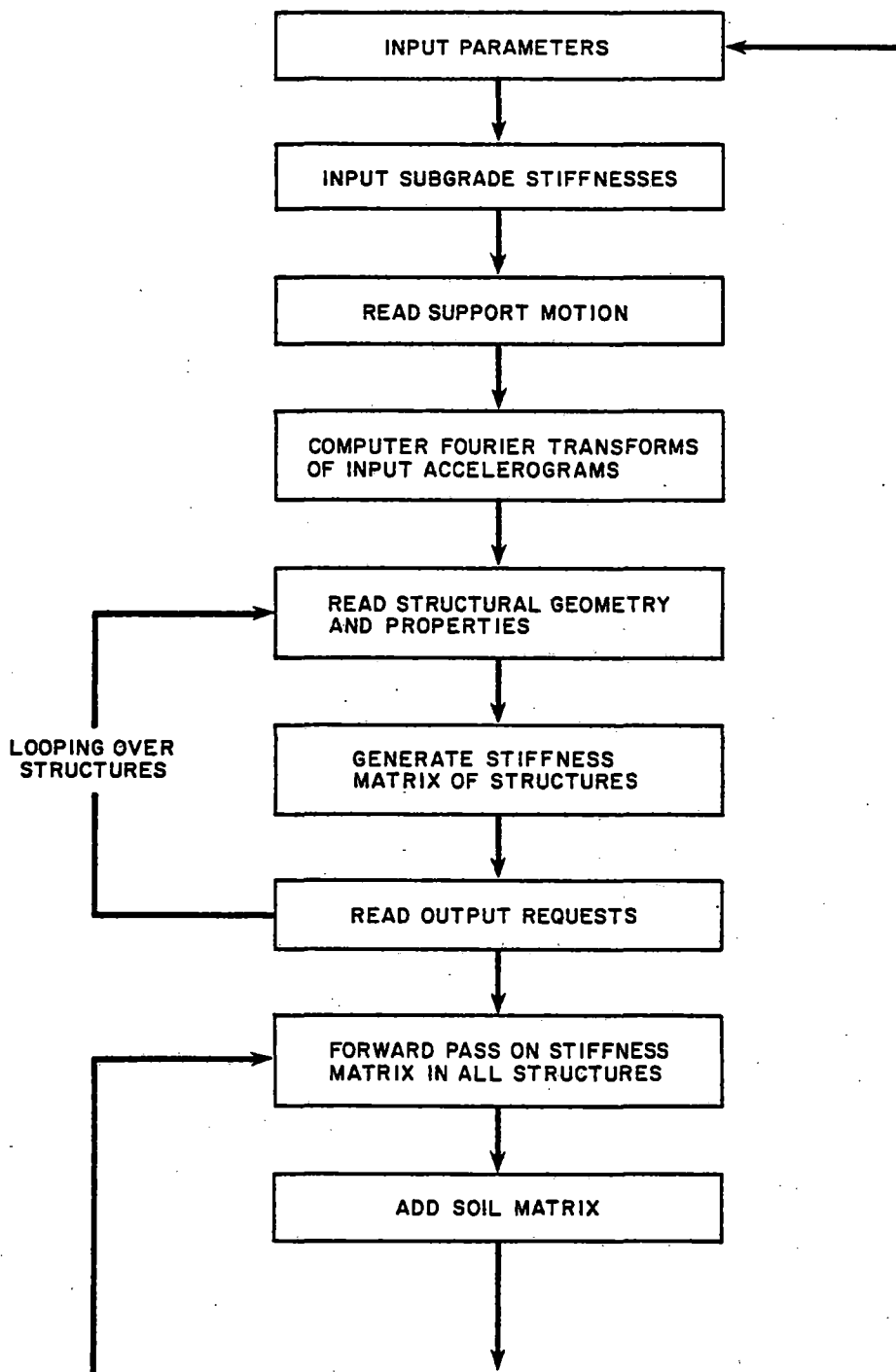


FIGURE 9.5-3 (SH. 1 OF 2)
 'FRIDAY' FLOW DIAGRAM
 SURRY POWER STATION - UNITS 1 AND 2

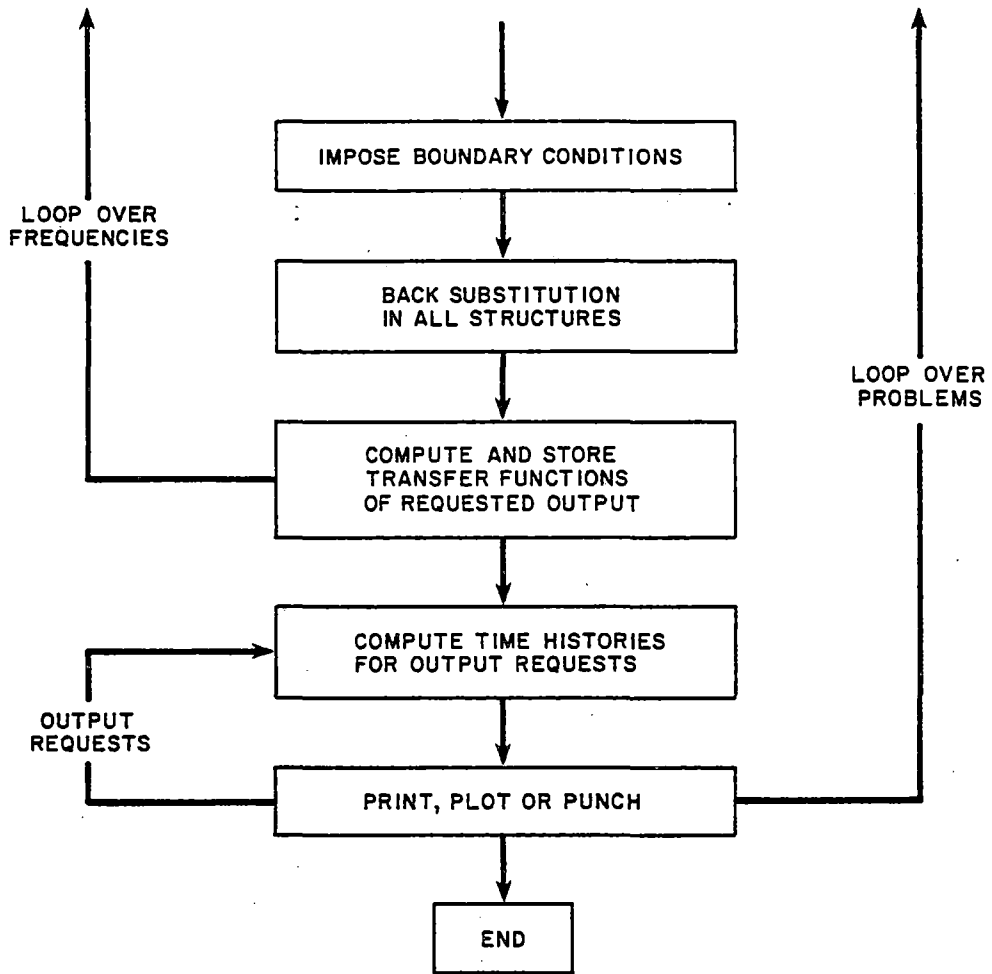


FIGURE 9.5-3 (SH. 2 OF 2)
'FRIDAY' FLOW DIAGRAM
SURRY POWER STATION - UNITS 1 AND 2

SURRY POWER STATION, UNITS 1 AND 2

APPENDIX 9.6

CONSOLIDATION TEST DATA
CONDENSATE POLISHING DEMINERALIZER
SURRY POWER STATION, UNITS 1 AND 2

SURRY POWER STATION, UNITS 1 AND 2

9.6 CONSOLIDATION TEST DATA

Four constant rate of strain consolidation (CRSC) tests, three incrementally loaded consolidation tests, and Atterberg limits were run on samples of Pleistocene clay as part of the foundation investigation for the Surry 1 and 2 condensate polishing demineralizer, located east of the Unit 2 turbine building (see Figure 2-1). These tests were used to obtain additional data for comparison with Pleistocene clays tested at Units 3 and 4 and plotted on Figures 2-7 and 2-8. Enclosed in this appendix are copies of the vertical strain vs effective stress plots for the seven consolidation tests.

STONE & WEBSTER ENGINEERING CORPORATION
 CONSOLIDATION TEST REPORT

PAGE NO. _____
 PRELIMINARY _____
 ITEM _____

CLIENT VEPCO

J.O. NO. 1305810

SUBJECT SURRY - UNITS 1&2

DATE 25 FEB 78 BY D.R.M.

BORING#2

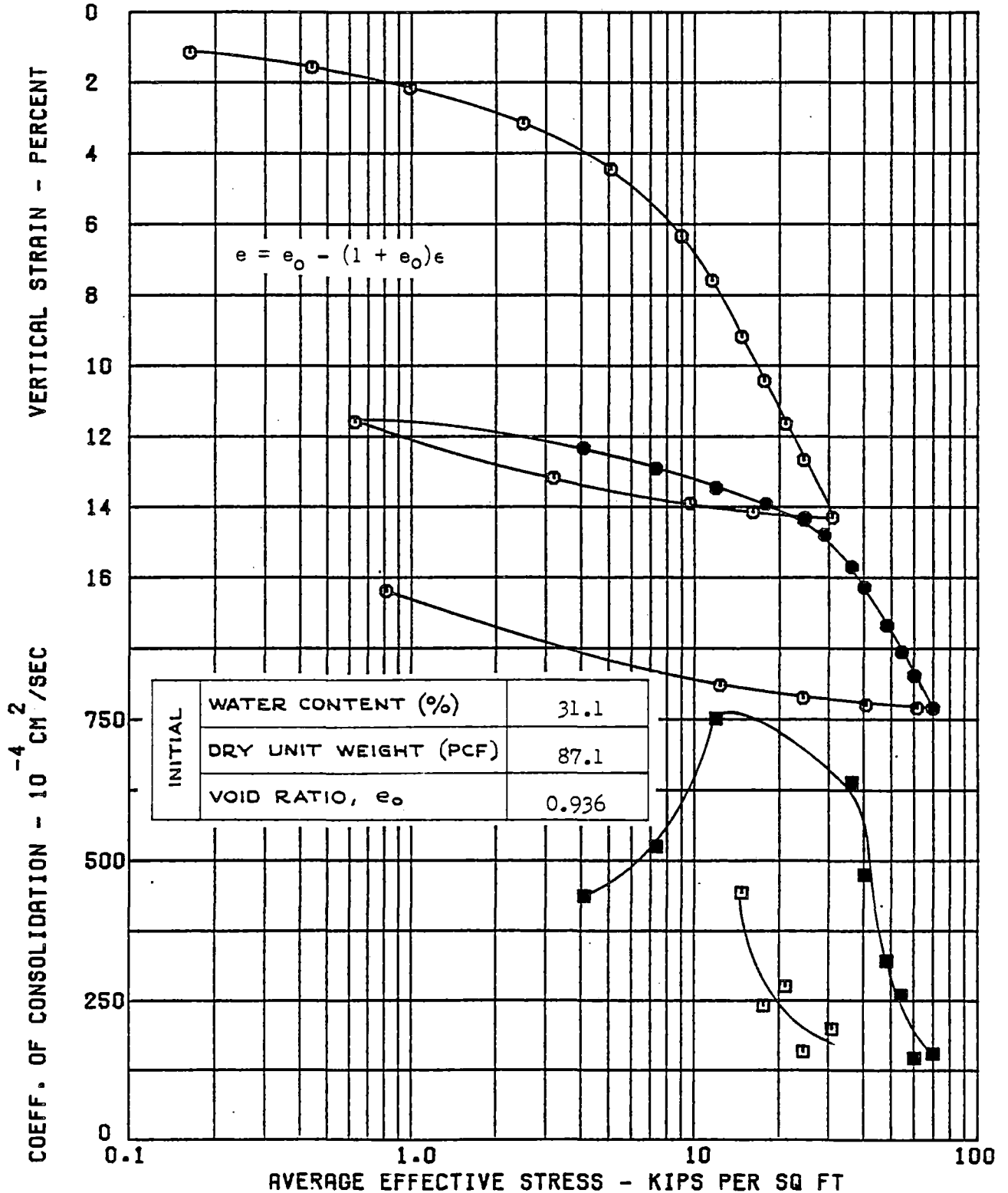
SAMP#B

DEPTH 47.3 FT

CHECKED 27 FEB 78 BY N.J.M.

BASED ON COMP. RUN J8144020 - 02/22/78 14.06.38 REVISED BY
 COMPILED 77.196 12.53.37 VER 2 LEV 0 GT-24 OEDPLOT

CONSTANT RATE OF STRAIN - 0.047 PERCENT PER MINUTE



40 CMDS JOB 1781 02/21/78 10:20

INPUT FROM RUN J8144018 ULICOR.../BT

STONE & WEBSTER ENGINEERING CORPORATION
 CONSOLIDATION TEST REPORT

PAGE NO. _____
 PRELIMINARY _____
 ITEM _____

CLIENT VEPCO

J.O. NO. 13058.10

SUBJECT SURRY UNITS 1&2

DATE 24 FEB 78 BY DRM

BORING C1

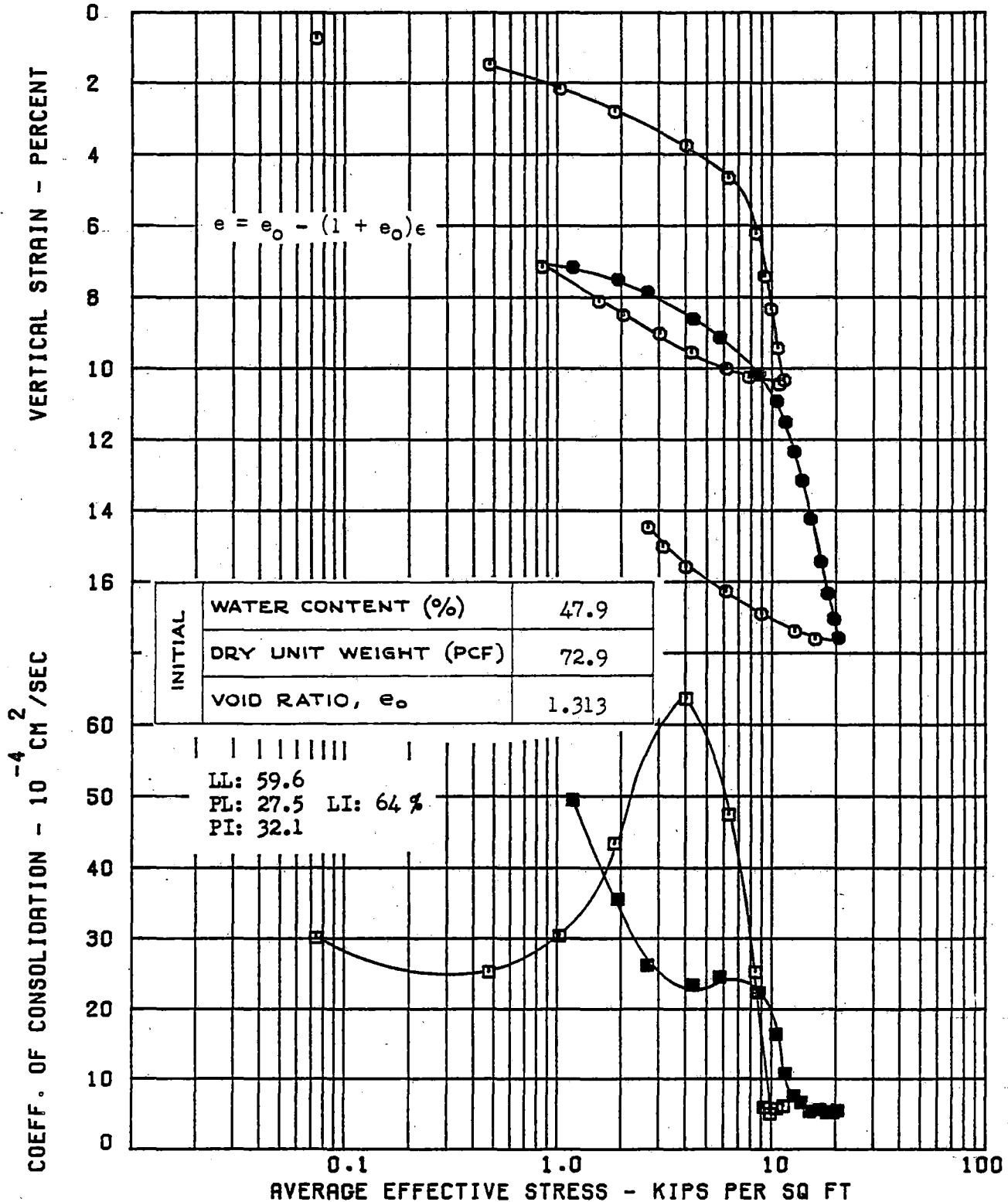
SAMP 11C

DEPTH 44.0 FT

CHECKED 24 FEB 78 BY [Signature]

BASED ON COMP. RUN J8144023 - 02/23/78 15.41.10 REVISED BY
 COMPILED 77.196 12.53.37 VER 2 LEV 0 GT-24 OEDPLOT

CONSTANT RATE OF STRAIN - 0.039 PERCENT PER MINUTE



47 CM008 JOB 000 01/30/78 21:04

INPUT FROM RUN J8144023 ULJCHG.../BT

STONE & WEBSTER ENGINEERING CORPORATION
 CONSOLIDATION TEST REPORT

PAGE NO. _____
 PRELIMINARY _____
 ITEM _____

CLIENT VEPCO

J.O. NO. 13058

SUBJECT SURRY - UNITS 1&2

DATE 24 FEB 78 BY DRM

BORING C3

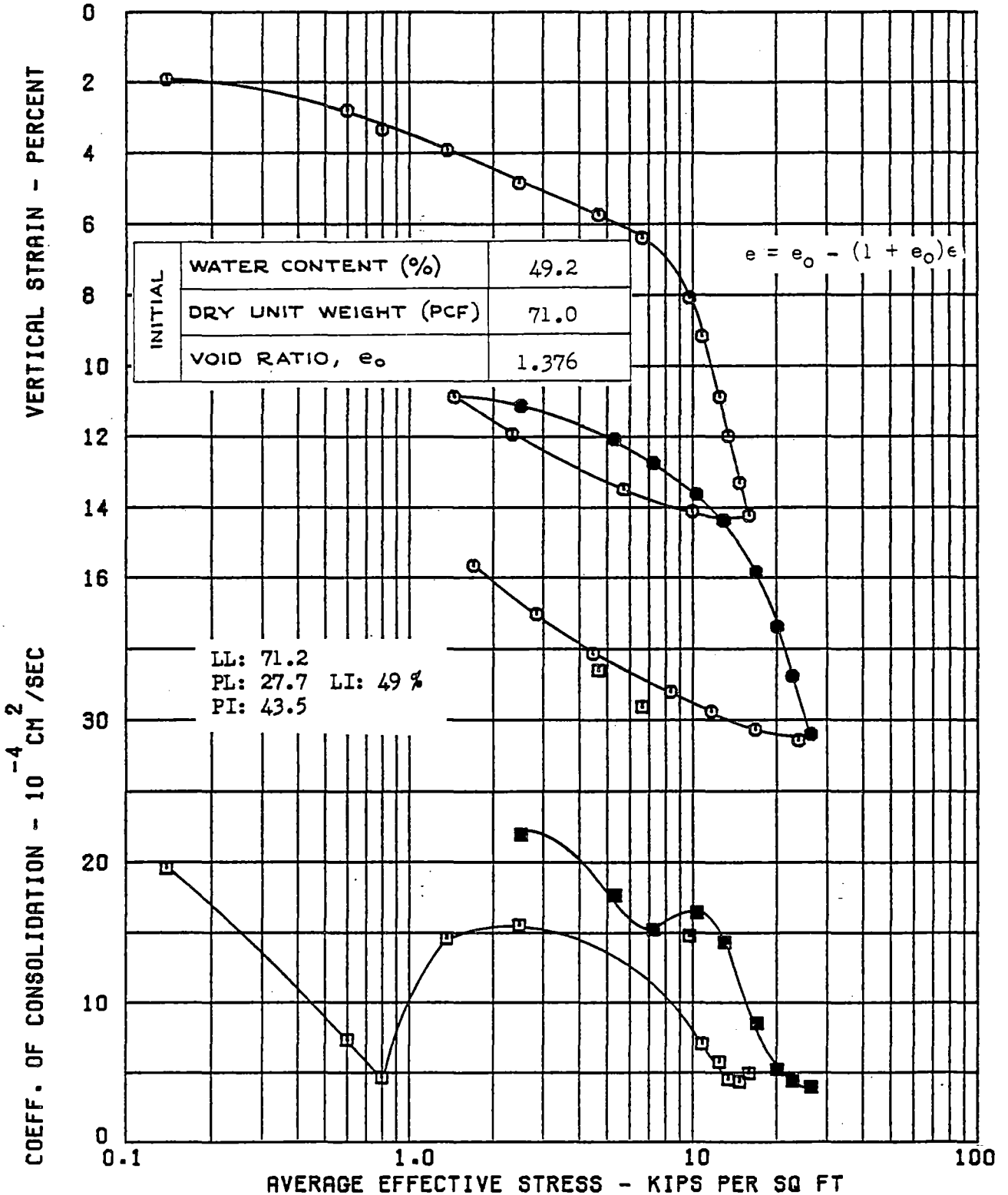
SAMP 12C

DEPTH 40.8 FT

CHECKED 24 Feb 78 BY VMM

BASED ON COMP. RUN J8144021 - 02/22/78 14.07.28 REVISED BY
 COMPILED 77.196 12.53.37 VER 2 LEV 0 GT-24 OEDPLOT

CONSTANT RATE OF STRAIN - 0.037 PERCENT PER MINUTE



41 CERM JOG 1727 02/21/78 10:57

INPUT FROM RUN J8144021 ULTCOR.../BT

STONE & WEBSTER ENGINEERING CORPORATION
 CONSOLIDATION TEST REPORT

PAGE NO. _____
 PRELIMINARY _____
 ITEM _____

CLIENT VEPCO

J.O. NO. 13058.10

SUBJECT SURRY - UNITS 1&2

DATE 23 FEB 78 BY DRM

BORING C1'

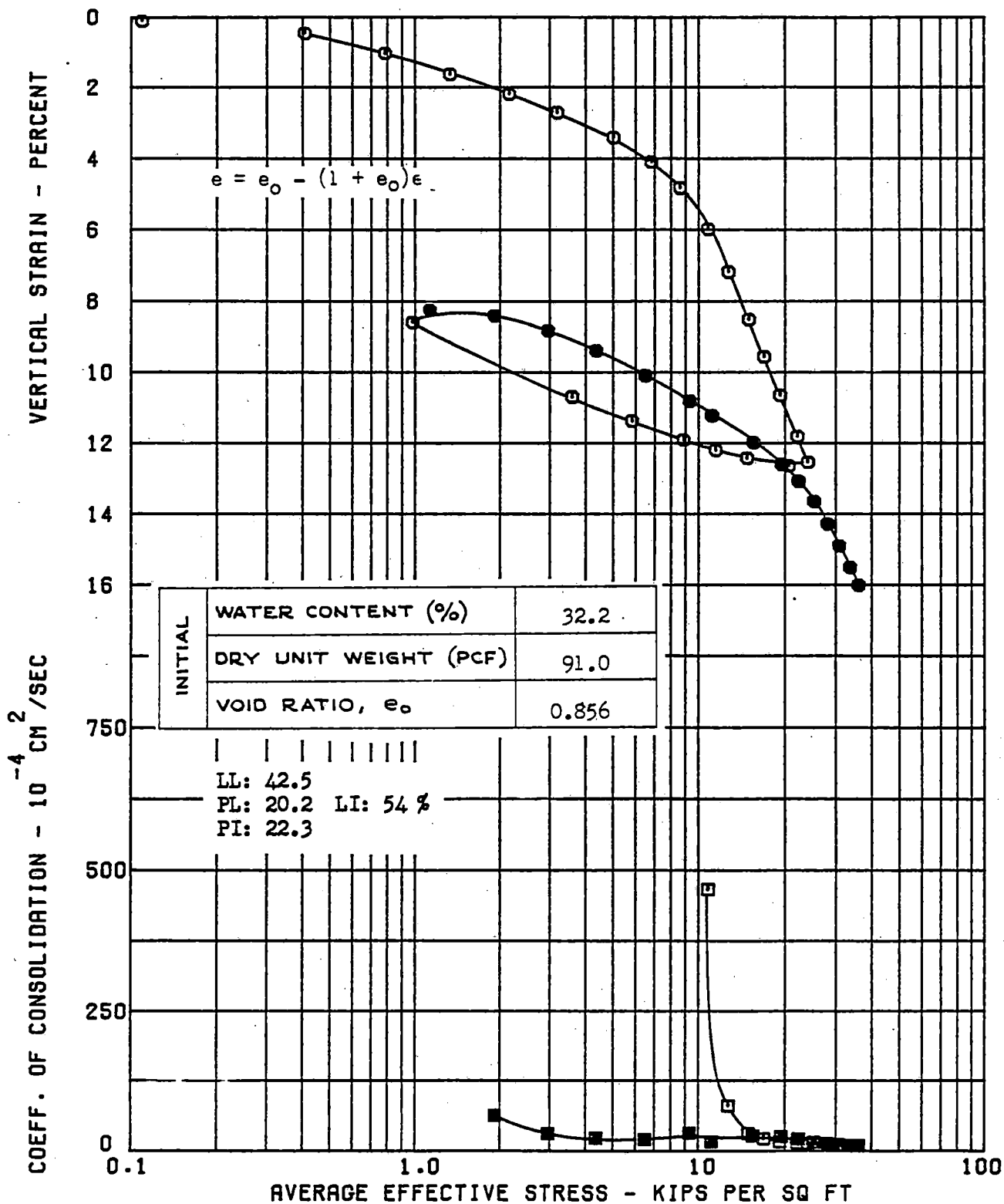
SAMP 150

DEPTH 54.1 FT

CHECKED BY [Signature] BY [Signature]

BASED ON COMP. RUN J8144024 - 02/23/78 15.52.03 REVISED BY
 COMPILED 77.196 12.53.37 VER 2 LEV 0 GT-24 OEDPLOT

CONSTANT RATE OF STRAIN - 0.050 PERCENT PER MINUTE

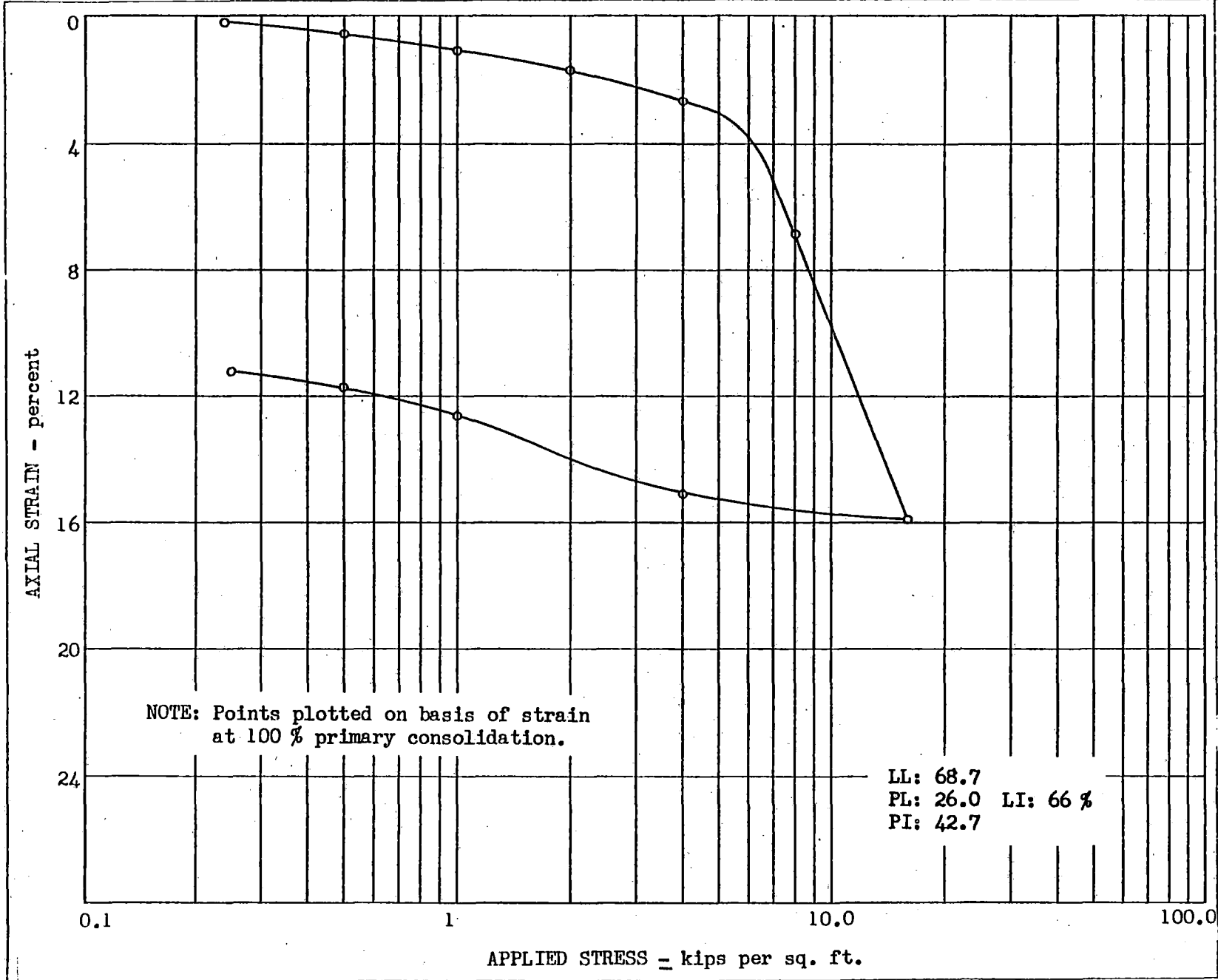


INPUT FROM RUN J8144022 MICHELL.../BT 49 CMB08 JOB 097 02/23/78 12:01

CLIENT
 VIRGINIA ELECTRIC POWER COMPANY
 DATE
 SURRY POWER STATION

J.O. NUMBER
 13058.10
 DATE
 28 JAN 78

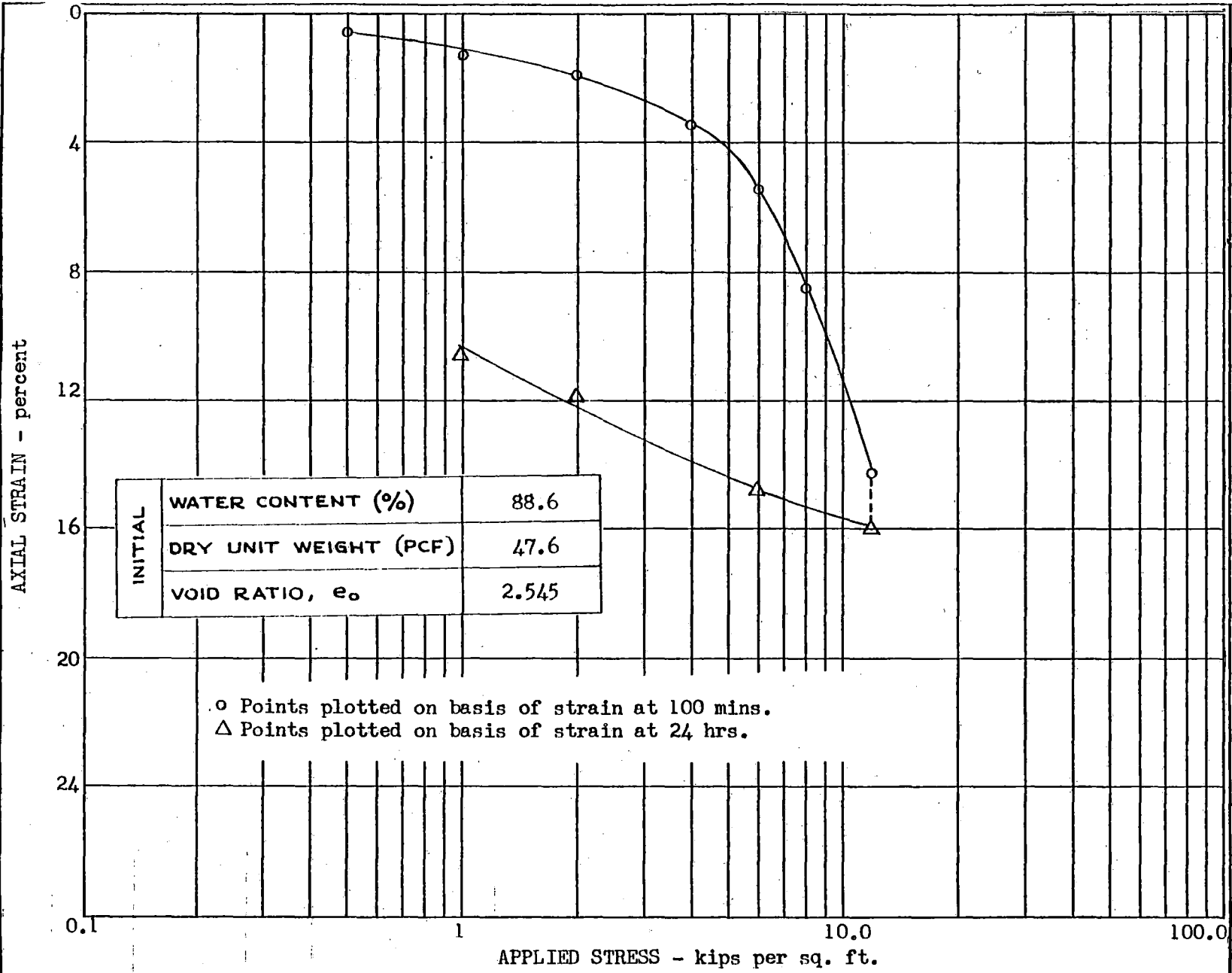
BOREHOLE NUMBER
 C3
 SAMPLE NUMBER
 10E
 DEPTH



CLIENT VIRGINIA ELECTRIC POWER COMPANY
 SITE SURREY POWER STATION

J.O. NUMBER 13058.10
 DATE 7 MAR 78

BORING NUMBER C2
 SAMPLE NUMBER 1E
 DEPTH 38.3



CLIENT	VIRGINIA ELECTRIC POWER COMPANY	J.O. NUMBER	13058.10	BORING NUMBER	03
SITE	SURRY POWER STATION	DATE	28 JAN 78	SAMPLE NUMBER	16E
				DEPTH	56.7 FT.

